ORGANIC GEOCHEMISTRY AND CRUDE OIL SOURCE ROCK CORRELATION OF THE DEVONIAN-MISSISSIPPIAN PETROLEUM SYSTEMS NORTHERN OKLAHOMA

By

IBRAHIM AL ATWAH

Bachelor of Science in Geology

University of Tulsa

Tulsa, OK

2011

Submitted to the Faculty of the
Graduate College of the
Oklahoma State University
in partial fulfillment of
the requirements for
the Degree of
MASTER OF SCIENCE
May, 2015

ORGANIC GEOCHEMISTRY AND CRUDE OIL SOURCE ROCK CORRELATION OF THE DEVONIAN-MISSISSIPPIAN PETROLEUM SYSTEMS NORTHERN OKLAHOMA

Thesis Approved:

Dr. James Puckette

Thesis Adviser

Dr. Jack Pashin

Dr. Tracy Quan

ACKNOWLEDGEMENTS

I cannot express enough thanks to my committee members for their support during my thesis research. Special thanks to my thesis advisor Dr. Jim Puckette for his crucial guidance and encouragement. Also, thanks to Dr. Jack Pashin for helping with organic petrography analysis, and Dr. Tracy Quan for assisting with biomarker interpretation.

I am also grateful for Saudi Aramco for their generous funding of my master's studies in the United States. I am very confident that I was able to develop key skills that will help me succeed in my future career as a research scientist at Saudi Aramco.

Thanks heaps to my mentor and role-model Dr. Khaled Arouri at Saudi Aramco. Even though during my studies we were separated by continents, Dr. Khaled's encouragement and helpful insight played a major role in my research success.

My completion of this project could not have been accomplished without the analysis and interpretation support from Prof. Mike Moldowan, and all his staff members at Biomarker Technology Inc. at Rohnert Park, California. I offer my sincere appreciation for the learning opportunities during my training at BTI.

Name: IBRAHIM AL ATWAH

Date of Degree: MAY, 2015

Title of Study: ORGANIC GEOCHEMISTRY AND CRUDE OIL SOURCE ROCK CORRELATION OF THE DEVONIAN-MISSISSIPPIAN PETROLEUM SYSTEMS NORTHERN OKLAHOMA

Major Field: PETROLEUM GEOCHEMISTRY

Abstract:

The Mississippian limestone in northern Oklahoma and southern Kansas is a major oil play within the southern Midcontinent region. Mississippian carbonate reservoirs are known for their heterogeneity with respect to reservoir quality and produced fluids. Oil and gas from the Mississippian reservoirs are chemically heterogeneous, and cannot be explained solely by a single Woodford Shale source-rock model. New molecular geochemical data from east and west of the Nemaha uplift in north-central Oklahoma provides a new insight into the source of hydrocarbons in the Mississippian play, and attempts to provide a plausible scenario of the hydrocarbon charge history. Organic-rich zones within the Mississippian carbonate section were sampled and screened for total organic carbon (TOC), organic petrography, Rock-Eval pyrolysis and geochemical markers. Additionally, twelve oil samples were analyzed from Mississippian and Woodford producing wells. Rock extracts and oil samples were analyzed using gas-chromatography and gas-chromatography mass-spectrometry techniques for quantitative analysis of diamondoids, saturate and aromatic biomarkers.

Results indicate that the Mississippian source-rock has good generation potential (average 2% TOC) and reached the early oil window (average vitrinite reflectance of 0.74% R_o). Extracted bitumen from Mississippian rocks and related oils show unique biomarker signatures; these include the presence of extended tricyclic terpane, high gammacerane index, and high C_{23} tricyclic terpane relative to hopane, high input of C_{27} relative to C_{28} and C_{29} in regular and rearranged steranes, together with high C_{27} monoaromatic steroids relative to their C_{28} and C_{29} homologues. Moreover, on the basis of diamondoid compound class, the Mississippian samples showed abundance of 4,8- and 4,9-dimethyl dimantanes relative to the 3,4- isomer. The extent of cracking as measured by diamondoids reveals a dramatic change in diamondoid concentration across the Nemaha uplift. A high concentration of diamondoids was observed west of the Nemaha uplift, thus indicating episodic hydrocarbon charge of uncracked oil followed by cracked oil migrating out of the Anadarko Basin, which supports a long-distance migration model. In contrast, the Mississippian samples from east of the Nemaha uplift are depleted in diamondoids, suggesting limited migration and localized hydrocarbon generation under lower thermal stress.

TABLE OF CONTENTS

LIST OF TABLES

Table Page

LIST OF FIGURES

Figure Page

CHAPTER I

INTRODUCTION

1.1 Carbonate vs. Shale Source Rocks

The hydrocarbon generation potential of carbonate rocks has long been recognized by petroleum geochemists and geologists (Palacas, 1984). Carbonate rocks, beyond being global prolific reservoirs, can be hydrocarbon generating sources. It is estimated that one half of the giant oil and gas fields worldwide are contained within carbonate reservoirs (Carmalt and John, 1986). Carbonate source rocks are documented in many basinal settings, such as the Jurassic Smackover Limestone in the southeastern United States, the Cretaceous Austin Chalk in the East Texas Basin and Cretaceous La Luna in the Colombian Magdalena Basin, among many others (Hunt and McNichol, 1984; Oehler, 1984; Zumberge, 1984). Carbonate source rocks can be deposited in a number of depositional environments, including evaporative sabkha, lacustrine, shallow-marine platform and deep-marine environments (Kirkland and Evans, 1981; Malek-Aslani, 1980; Rice, 1984; Tissot et al., 1978). Crude oil generated from organic-rich carbonate rocks has a distinctive chemical fingerprint when compared to oil sourced from shale. Major chemical variations between oil generated from carbonate and shale source rocks are summarized in Table 1 (Palacas, 1988).

An active pod of organic-rich rock that is contained in the correct thermal regime (referred to as hydrocarbon kitchen) is an essential component of both conventional and unconventional petroleum systems. Therefore, elucidating the number of active source rocks within a sedimentary

section determines the number of petroleum systems in a given basin (Magoon and Dow, 1994). This becomes crucial in area such as northern Oklahoma, where two and more potential source rocks exist within close proximity, such as the Devonian-Mississippian Woodford Shale overlain by organic-rich Mississippian carbonate.

Table 1. *Major chemical differences between carbonate and shale derived petroleum(Palacas, 1988).*

Parameter	Carbonate	Shale
CPI, C_{22}-C_{32} *n*-alkanes	≤1	≥1
Pristane/phytane	≤1	≥1
Phytane/*n*-C_{18}	High (0.3-1.5)	Low ≤ 0.4
Steranes+triterpanes/*n*-alkanes	High-medium	Low-medium
Diasteranes	Low-medium	Medium-high
Hopane/C_{27}-C_{29} steranes	>20	<20
C_{35}/C_{34} extended hopanes	≥1	≤1
C_{24} tetracyclic/C_{26} tricyclic	High-medium	Medium-low
Thiophenic sulfur	High in benzothiophenes	Low in benzothiophenes

1.2 The Mississippian Oil Play

Mississippian carbonate rocks in northern Oklahoma and southern Kansas have been recognized as prolific petroleum reservoirs, especially since the onset of horizontal drilling and multi-stage hydraulic fracturing technology (Boyd, 2012). Oil and gas fields producing from chert-bearing Mississippian carbonate reservoirs (pre-Chesterian) extend across a large area of Oklahoma and Kansas (Fig. 1). Informally, the oil and gas producing Mississippian carbonates are known as the Mississippian play, and specific reservoir intervals are known as “Miss chat”, “Miss chert” or “Miss Lime”. Mississippian producing intervals within the Miss chat have been generally characterized as having dual matrix and fractured porosity types, with porosity averaging between 25-30%, and permeability ranging from 0.1 to 50 millidarcy (mD). In these reservoirs, produced oil is typically associated with salt water production (Boyd, 2008, 2012; Rogers, 2001). Mississippian reservoirs are characterized as self-sealed by change from porous to tight carbonate facies, and are trapped by a combination of structural and stratigraphic mechanisms (Adler et al., 1987).

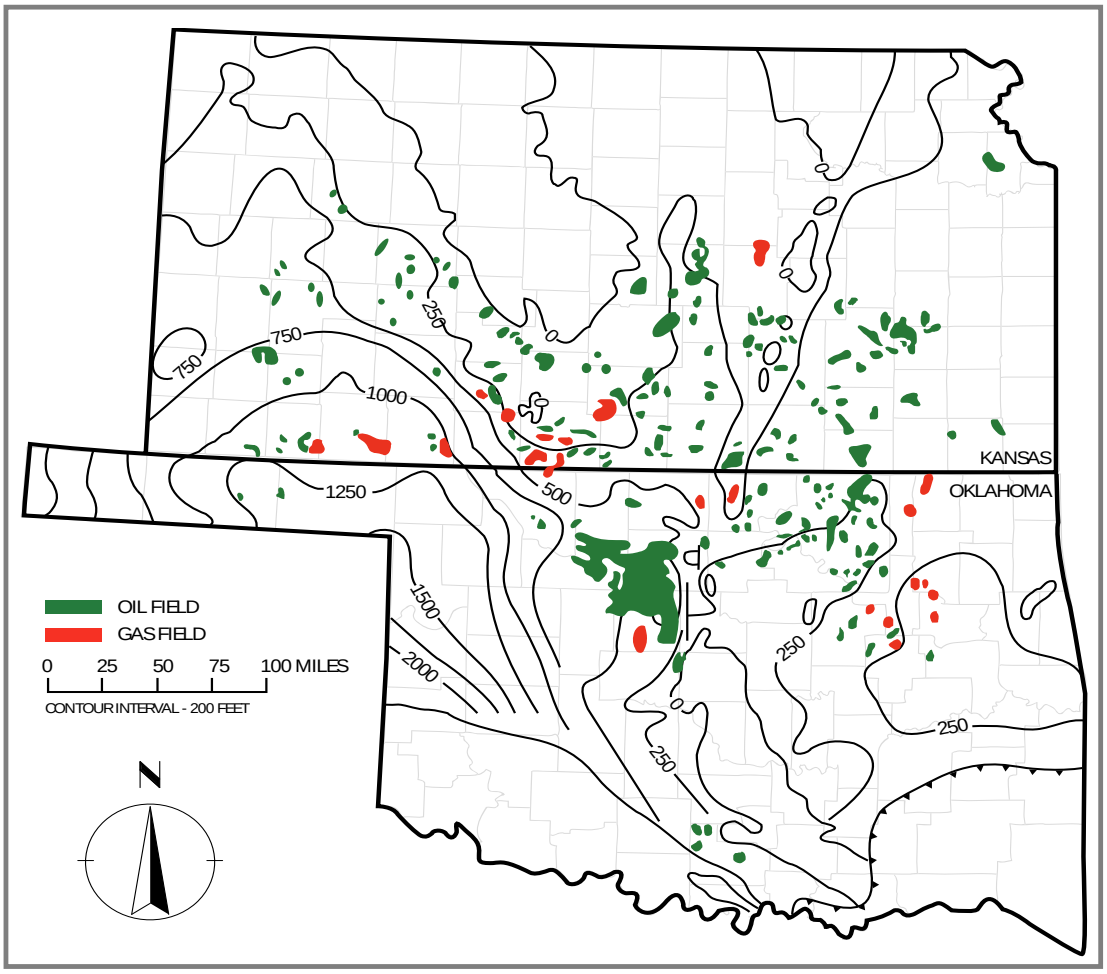

Figure 1. Major Mississippian oil and gas fields across Oklahoma and Kansas. Contour lines represent Mississippian (pre-Chester) thickness. Modified from Adler et al. (1987).

1.3 Study Motivation

Because the Mississippian carbonate reservoirs are stratigraphically adjacent to the organic-rich Woodford Shale, regional studies have assumed that the Woodford is a regionally extensive source rock interval that must have charged Mississippian reservoirs (Burruss and Hatch, 1989; Dolton and Finn, 1989). However, Mississippian carbonate reservoirs are known for their heterogeneity with respect to reservoir quality as well as the composition of produced fluids. Hence,

hydrocarbons from the Mississippian reservoirs are chemically heterogeneous, and cannot be explained solely by a single Woodford Shale source-rock model (Da Wang and Philp, 1997). Several geochemical studies of oils and related source rocks within Oklahoma have been very broad in terms of petroleum systems analysis. To date, however, there has not been a sufficient geochemical investigation that examines the relationships between organic-rich Mississippian carbonate intervals and produced oils in north-central Oklahoma. In addition, there are no studies comparing and contrasting produced Mississippian oil from each side of the Nemaha uplift, which is a north-south elongate uplift that may have formed a significant hydrodynamic barrier.

1.4 Aim and Scope

The aim of this study is to evaluate the hydrocarbon generation and the thermal maturity of the organic-rich facies in the Mississippian limestone in north-central Oklahoma (Fig. 5) and to investigate the origin of produced crude oil from the Mississippian and Woodford intervals. A set of Mississippian limestone and Woodford Shale samples was assessed for total organic carbon (TOC), total inorganic carbon (TIC), kerogen composition, vitrinite reflectance (R_o%) and Rock-Eval pyrolysis. Potential source rocks were then analyzed along with crude-oil samples for aromatic biomarkers, saturate biomarkers and diamondoids. Geochemical assessment based on thermal maturity of crude oil samples was compared to regional depositional and structural patterns, with the aim to better understand the dynamics of hydrocarbon charging to the Woodford and Mississippian reservoirs.

1.5 Study Significance

Petroleum geochemistry plays a significant role in hydrocarbon exploration and production by identifying active source rocks, determining thermal history, and correlating crude oil to their source rocks. Petroleum geochemistry, when coupled with other geological and geophysical information, provides an important tool for exploring and developing hydrocarbon resources. Elucidating the origin of petroleum is a critical factor in hydrocarbon resource plays, as it facilitates resource assessment, reduces exploration risk, and increases exploration and production efficiencies (Peters and Fowler, 2002). Figure 2 illustrates the value that petroleum geochemistry adds to exploration and production efficiencies. Without incorporating petroleum geochemical techniques, depending on trap structure and reservoir quality, the forecasting efficiency in finding hydrocarbons are estimated to be 28%. On the other hand, when combining geochemical and geophysical methods, the forecasting efficiency of petroleum discoveries increases to 63% (Peters and Fowler, 2002).

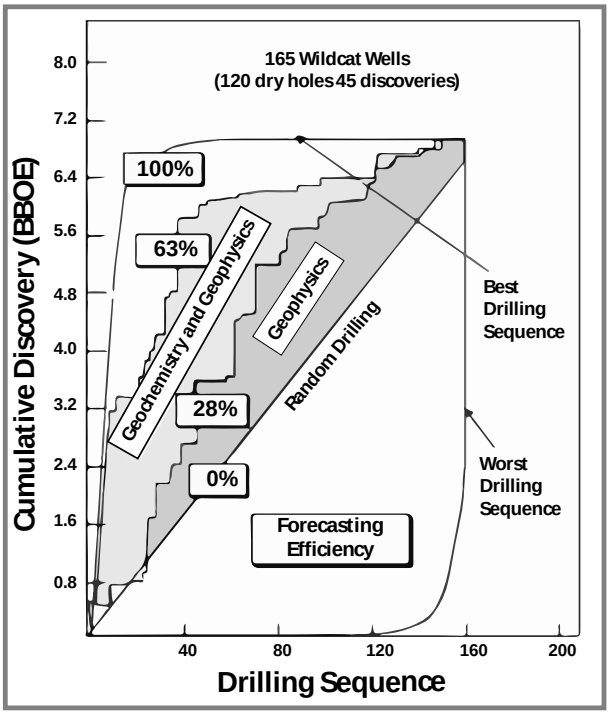

Figure 2 Prediction of petroleum geochemistry impact in exploration; the forecasting data is a result of 165 wildcat wells before drilling. Vertical axis is cumulative discovered volume in Barrel of Oil Equivalent (BBOE), and the x axis is the well sequence number(Peters and Fowler, 2002).

The significance of this study is advancing the knowledge of petroleum and source rock geochemistry in northern-central Oklahoma's Devonian-Mississippian petroleum systems. This knowledge advancement has implications for both exploration and production. For instance, the geochemical signatures established in this study will provide a foundation for future source rock-oil or oil-oil correlation efforts in the Devonian-Mississippian petroleum systems. In addition, this

study provides valuable data that can be used to refine and calibrate basin models. For example, adding source rock intervals to the Mississippian petroleum systems that were previously overlooked, provides additional sources of oil and gas to augment the Woodford source.

1.6 Thesis Structure

In addition to the introduction, this thesis consists of four further chapters within two main parts. Part I (Chapters 2 and 3) provides a literature review and an overview of the analytical techniques used in this study. Chapter 2 synthesizes previously published literature on the regional geology, primarily covering tectonics and paleodepositional settings of the USA Midcontinent region during the Mississippian Period. This is followed by a review of more detailed organic geochemical studies of Oklahoma's Anadarko Basin. Chapter 3 describes the research methodology, particularly the instrumentation and analyses used in the research, including: total organic and inorganic carbon analysis (TOC & TIC), organic petrology, vitrinite reflectance (R_o %), gas-chromatography (GC-FID), gas-chromatography mass-spectroscopy (GC-MS) and gas-chromatography equipped with triple quadrupole Mass spectrometer (GC-MS-MS).

Part II (Chapters 4 and 5) of this thesis covers major findings of the geochemical experiments, discussion, conclusions and future work. In Chapter 4, results are organized based on the analysis conducted accordingly. Chapter 4 contains the results and discussion section, which is divided into a series of subsections. The discussion subsections start with the source rock evaluation within the Mississippian interval, then source rock geochemistry, oil geochemistry and source to crude oil chemical correlation, and concludes with regional thermal maturation and charge history discussion. The conclusion section of Chapter 5 represents a reflective evaluation of the study and offers suggestions for future research. Appendices I-IV contain the basic data generated in this

study, which include carbon analysis, Rock-Eval pyrograms, vitrinite reflectance analysis reports, gas-chromatograms and mass-chromatograms.

CHAPTER II

GEOLOGICAL SETTING

2.1. Regional Geology

The tectonic setting of the North American continent during the Early Mississippian featured active and passive shelf continental margins (Gutschick and Sandberg, 1983). The southern margin of the Laurussian plate was dominated by a carbonate shelf setting along the passive margin of the Ouachita embayment, bounded by three extended foreland depressions formed by Neo-Acadian, Ellesmerian, and Antler orogenesis (Gutschick and Sandberg, 1983; Lane and De Keyser, 1980). Tectonically active edges bordering the foreland basins were accompanied by convergence in the west with the Pacific plate, to the east by Africa and Europe, and to the south by the South American plate (Gutschick and Sandberg, 1983). The convergence and associated compressional stresses, resulted in a series of orogenies, namely Acadian orogeny (East), Antler Orogeny (West) and the Proto-Ouachita Orogeny ((Gutschick and Sandberg, 1983) and references therein). By Late Mississippian time, collision between Gondwana and Euramerica resulted in uplift of the subducted complex and an increased relief on the Ouachita orogeny, which increased the supply of siliciclastic sediments to the cratonic basins (Curtis and Champlin, 1959; Walper, 1977).

During Early to mid-Mississippian time, Oklahoma and most of the southern margin of North America continent was covered with a wide carbonate platform (Fig. 4) (Gutschick and Sandberg, 1983). The wide carbonate shelf ranged from shallow to intermediate water depth and

was warm as a result of its subtropical setting (Curtis and Champlin, 1959; Gutschick, 1983). More specifically, present Oklahoma was close to the equator around 15° south latitude (Fig. 3). Based on the regional tectonic settings and paleogeography during the Mississippian time, the southwest-

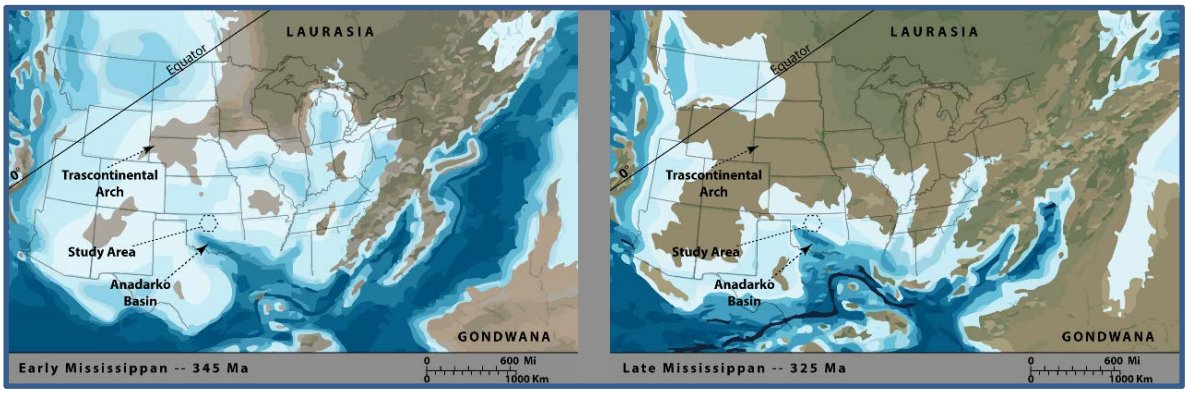

Figure 3 Paleogeographic maps of during Early Mississippian (Left) and Late Mississippian (Right), Modified from(Blakey, 2011).

northeast trending Transcontinental Arch was bounded by a subparallel oriented carbonate shelf, starved basins and orogenic highlands respectively (Fig. 4) (Gutschick and Sandberg, 1983; Lane and De Keyser, 1980; Noble, 1993). More recent interpretation highlights the influence of local

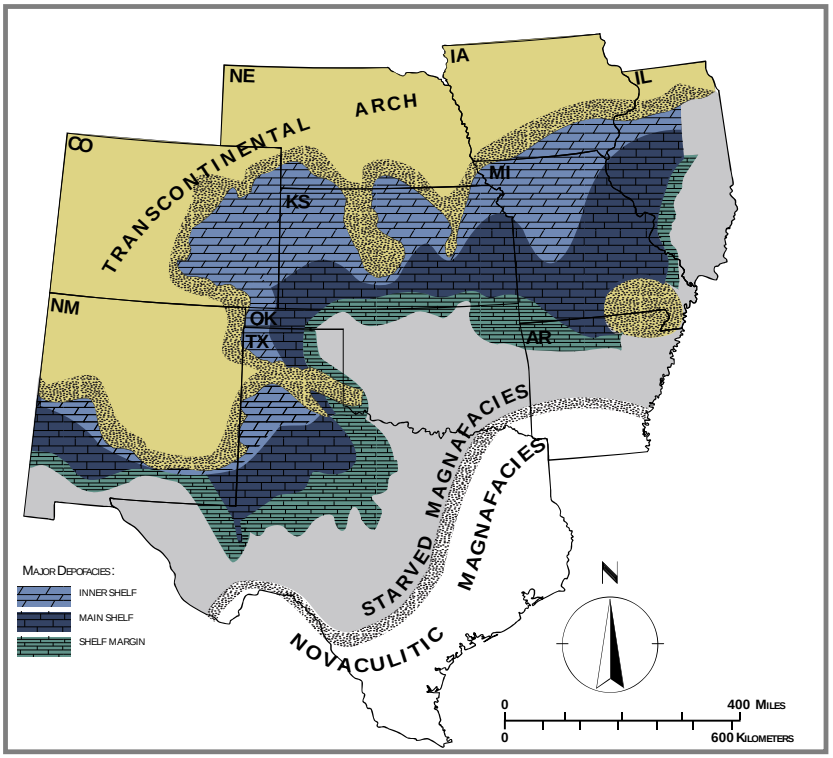

Figure 4. Generalized lithology model of Early Mississippian depositional settings, modified from (Lane and De Keyser, 1980)

tectonics on depositional features and proposes a carbonate ramp setting during the Early Mississippian (Boardman et al., 2013; Mazzullo et al., 2013; Mazzullo et al., 2011).

The discussed paleogeographic and paleobathymetric settings during Mississippian time favored development of petroleum source rocks. Moreover, both isotopic and petrographic data suggest that Lower Mississippian carbonates in Oklahoma were deposited within low-energy outer-ramp settings (Koch et al., 2014). Carbonate source rocks during the Mississippian time occurred in other basins (e.g. Mississippian Lodgepole carbonate source rock, Williston basin) (Jiang et al., 2001).

2.2 Structural Framework

The Anadarko and Arkoma basins are major oil and gas producing provinces, and hydrocarbon kitchen areas in the southern Midcontinent. The Anadarko Basin extends from western Oklahoma into the Texas Panhandle (Fig 5), and has a broad northern slope that connects with the Hugoton embayment of western Kansas. The Anadarko basin is bounded to the east by the Nemaha uplift, the west by the Cimarron Arch, the south by the Wichita and Amarillo uplifts (Fig. 5). Structurally, the Anadarko Basin has a polyphase history, beginning as cratonic basin, and evolving later into a foreland basin which subsided and disjointed during Pennsylvanian tectonic compression (Gilbert, 1992; Johnson, 1989). The Woodford Shale in the southern and deepest region of the Anadarko basin is currently within the dry-gas window as indicated by vitrinite reflectance (Fig. 5) (Cardott and Lambert, 1985), with the modeled onset of petroleum generation at 330 Ma, and peak oil generation from 300 to 220 Ma (Higley, 2013). Overlying the Woodford Shale is the Mississippian limestone, which is predominantly relatively clean carbonate that reache thickness exceeding 1,650 feet near the basin axis and is continuous northward over the Anadarko Shelf (Jordan and Rowland, 1959).

The Arkoma Basin is a foreland basin which extends across southeastern Oklahoma and west-central Arkansas. To the north and northeast, the Arkoma Basin is bounded by the Ozark uplift and the Oklahoma/Cherokee Platform, respectively. To the west the basin is bounded by the Arbuckle Mountains and to the south by Ouachita uplift. The Arkoma Basin is classified as a peripheral foreland basin associated with the Ouachita fold-and-thrust belt, and characterized by down-to the south normal faults influencing Pennsylvanian and older strata (Perry, 1995; Suneson, 2012). The Woodford Shale within the Arkoma Basin exhibits elevated thermal maturity compared to the Woodford in the Anadarko Basin. Woodford vitrinite reflectance values from the Arkoma Basin indicate that the basin passed the oil window and currently is within the wet and dry gas windows (Cardott, 2012). In eastern Oklahoma, south of approximately 35º 30', the Woodford Shale is overlain by Mississippian argillaceous carbonate and siltstone known as the Caney Shale. The Caney reaches a maximum thickness of approximately 480 feet, and is widely distributed east of the Arbuckle Uplift, where it essentially represents the entire Mississippian section (Jordan and

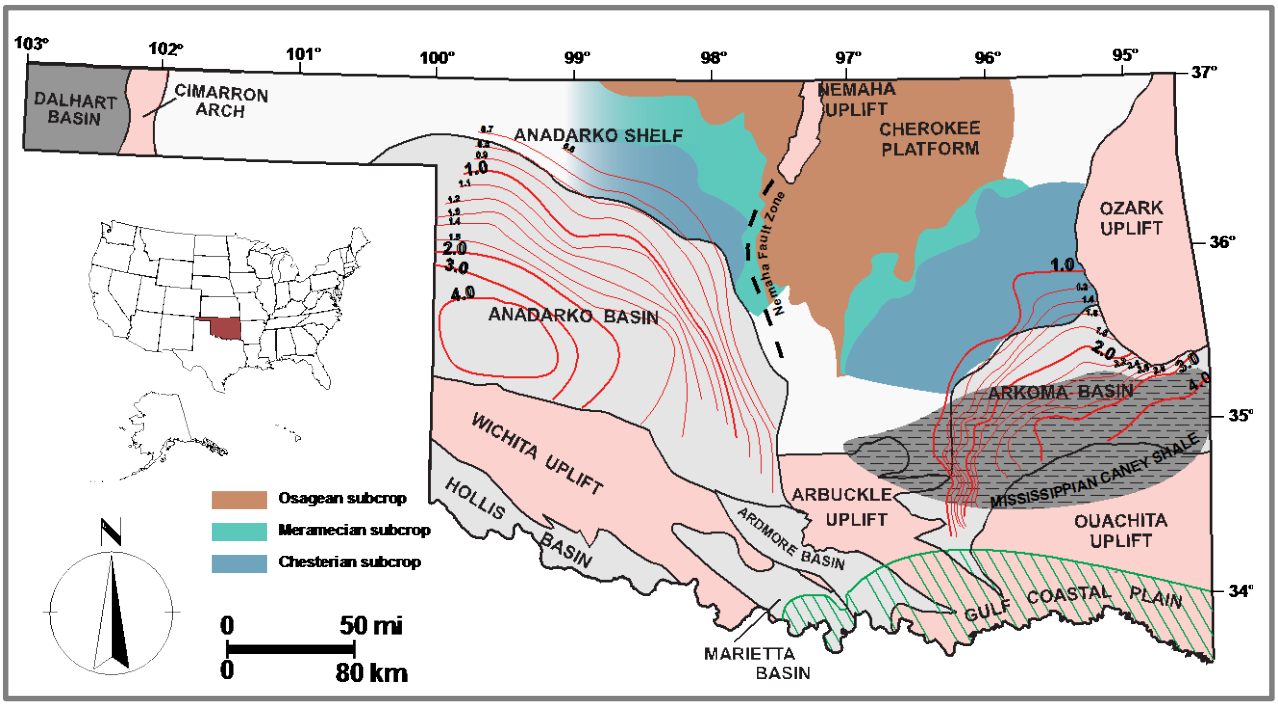

Figure 5. Regional map depicting major structural features within Oklahoma and generalized distribution of different Mississippian subcroup sections from (Jordan and Rowland, 1959; Sutherland, 1988), marked in red contours are isoreflectance values from (Cardott, 2012; Cardott and Lambert, 1985).

Rowland, 1959). North of approximately 35º 30' the lithology of the Mississippian section changes from argillaceous to clean carbonate (Fig. 5) (Sutherland, 1988).

The Nemaha uplift, which is a major structural feature within Midcontinent region, extends from southeastern Nebraska to central Oklahoma, and is approximately 415 miles in length and 12-14 miles in width (Burchett et al., 1983). The Nemaha uplift separates the Cherokee Platform in northeastern Oklahoma from the Anadarko shelf and basin to the west (Dolton and Finn, 1989). Moreover, to the south the uplift extends obliquely over the platform separating Arkoma and Anadarko basins, and forms the eastern boundary of the Anadarko Basin. Structurally, the uplift is composite and complex, featuring different structural elements such as high-angle normal and reverse faults (Carlson, 1971; Cronenwett, 1956). The origin of the Nemaha uplift is believed to result from a narrow transpressional (left-lateral strike-slip) fault system during Ordovician or before (Amsden, 1975; McBee, 2003)

2.3. Previous Work

Geochemical studies of oil and related source rocks within Oklahoma are very broad from the standpoint of defining petroleum systems. Mississippian and Devonian oils and organic-rich rocks were initially studied geochemically as one petroleum system and compared with either older or younger geological successions, such as the Silurian and Pennsylvanian petroleum systems (Burruss and Hatch, 1989; Jones and Philp, 1990). However, Wang and Philp (1997) noted chemical variations between the produced oil and rock samples from the lower Mississippian limestone (Osagean) in comparison with Woodford Shale. Moreover, they identified the most distinctive biomarker characteristic of Lower Mississippian samples, which is high abundance of extended tricyclic terpanes that reach up to C_{45} (Da Wang and Philp, 1997). In a subsequent study, the presence of extended tricyclic terpanes within the organic-rich Lower Mississippian intervals was investigated (Kim and Philp, 2001). This work focused more on identifying the biological

precursor that gave rise to the extended tricyclic terpane, rather than evaluating the petroleum generation potential within the Lower Mississippian beds. Based on petrographic examination at facies scale combined with geochemical analysis of each facies, the authors attributed the dominance of tricyclic terpane biomarkers to a marine algal origin, and speculated the possibility of algal bloom events that occurred during Early Mississippian time (Kim and Philp, 2001). Table 2 summarizes the major biomarker ratio differences between the oil and source rock of the Lower Mississippian compared to the Woodford Shale.

Table 2. Comparison of the main biomarker characteristics between the Lower Mississippian limestone and the Woodford Shale (Jones and Philp, 1990; Kim and Philp, 2001).

Biomarkers Ratios	Lower Mississippian Lime.	Woodford Shale
C_{27} Diasterane/C_{27} Sterane	(2.40 - 6.92) avg.= 3.22	(1.16 - 1.57) avg.=1.35
C23 Tricyclic terpane/C_{30} Hopane	(2.21 - 8.90) avg.= 5.23	(0.73 - 4.29) avg.=1.83
C_{24}Tetracyclic terpane/C_{30} Hopane	(0.21 - 0.84) avg.= 0.60	(0.13 - 0.43) avg.=0.21
Ts/Tm	(1.52 – 24.0) avg.= 7.31	(0.91 - 2.08) avg. =1.59
Extended Tricyclic terpanes	Up to C_{45}	Up to C_{30}

CHAPTER III

METHODOLOGY

3.1 Study Area and Sampling

The study area of this project was focused on north-central Oklahoma and includes Payne and Logan counties on the east side of the Nemaha uplift, and Alfalfa and Woods counties west of the Nemaha uplift on the northern shelf of the Anadarko basin. Rock and oil samples were obtained from Payne and Logan counties, whereas oil samples only were obtained from Woods and Alfalfa counties (Fig. 5). Mississippian rock samples were collected from three wells Ad-Lo, El-Py and Wi-Py, and Woodford rock samples were collected from Wd-Py (Table 3) with a total of 61 rock samples screened in this study. Additionally, crude oil samples were taken from the Lower Mississippian

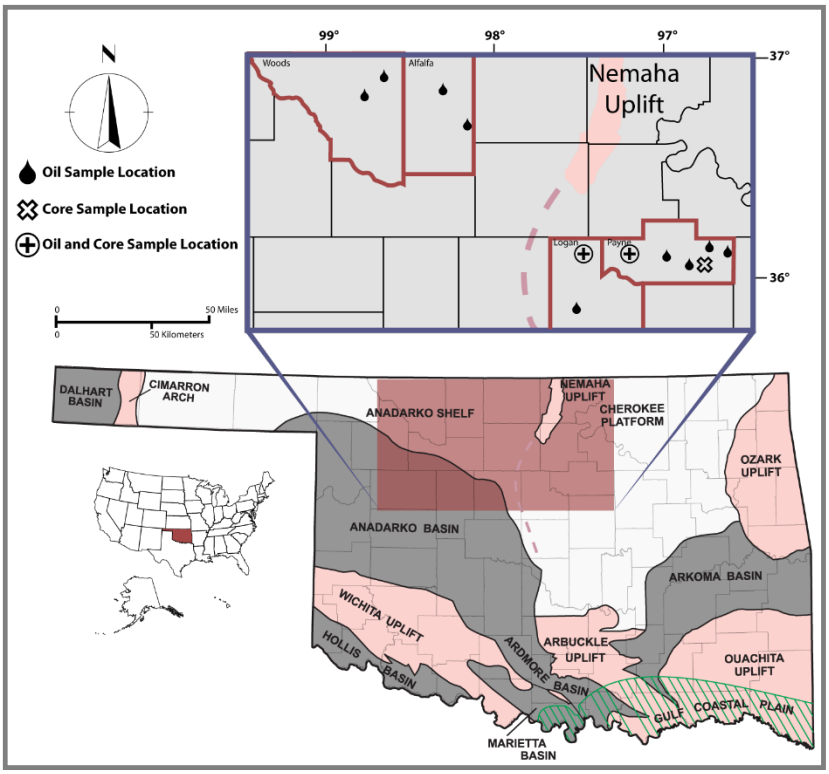

Figure 6. Study area map showing approximate location of sampled crude oil and rocks, including Payne and Logan counties east of the Nemaha uplift and Woods and Alfalfa counties to the west of the uplift.

.

and Woodford reservoirs, Mississippian oils were collected from wells: Ad-Lo, Da-Wo, El-Py, Je-Py, Ka-Al, Ri-Wo, St-Al, To-Py, and Wh-Lo. Woodford oil samples were obtained from wells Me-Py, Wh-Lo Wd-Py and Wi-Py (Table 3)(Fig. 6).

Table 3 Location information for both rock and oil samples examined in this study.

Sample ID	Type	County	Latitude	Longitude	Formation	Depth (ft)
Ad-Lo-1	Core Sample	Logan	36.04	-97.31	Lower Mississippian	5570
Ad-Lo-2	Core Sample	Logan	36.04	-97.31	Lower Mississippian	5589
Ad-Lo-3	Core Sample	Logan	36.04	-97.31	Lower Mississippian	5633
Ad-Lo-4	Core Sample	Logan	36.04	-97.31	Lower Mississippian	5701
Ad-Lo-5	Core Sample	Logan	36.04	-97.31	Lower Mississippian	5820
Ad-Lo-6	Oil Sample	Logan	36.04	-97.31	Lower Mississippian	6250
Da-Wo-1	Oil Sample	Woods	36.83	-98.73	Mississippian (Meramec)	5565
El-Py-1	Core Sample	Payne	36.03	-97.02	Lower Mississippian	4365
El-Py-2	Core Sample	Payne	36.03	-97.02	Lower Mississippian	4462
El-Py-3	Oil Sample	Payne	36.03	-97.02	Lower Mississippian	4829
Je-Py-1	Oil Sample	Payne	36.09	-96.65	Lower Mississippian	3280
Ka-Al-1	Oil Sample	Alfalfa	36.81	-98.33	Mississippian (Meramec)	5924
Me-Py-1	Oil Sample	Payne	36.11	-96.72	Woodford Shale	3450
Ri-Wo-1	Oil Sample	Woods	36.90	-98.64	Mississippian (Osage)	5307
St-Al-1	Oil Sample	Alfalfa	36.68	-98.12	Middle Mississippian	5670
To-Py-1	Oil Sample	Payne	35.99	-96.89	Lower Mississippian	3900
Wd-Py-1	Core Sample	Payne	n.a.	n.a.	Woodford Shale	3367
Wd-Py-2	Core Sample	Payne	n.a.	n.a.	Woodford Shale	3381
Wh-Lo-1	Oil Sample	Logan	35.88	-97.50	Lower Mississippian	5632
Wh-Lo-2	Oil Sample	Logan	35.88	-97.50	Woodford Shale	5785
Wi-Py-1	Core Sample	Payne	36.03	-97.19	Lower Mississippian	5144
Wi-Py-2	Core Sample	Payne	36.03	-97.19	Lower Mississippian	5157
Wi-Py-3	Core Sample	Payne	36.03	-97.19	Lower Mississippian	5162
Wi-Py-4	Core Sample	Payne	36.03	-97.19	Lower Mississippian	5185
Wi-Py-5	Core Sample	Payne	36.03	-97.19	Lower Mississippian	5281
Wi-Py-6	Oil Sample	Payne	36.03	-97.19	Woodford Shale	5656

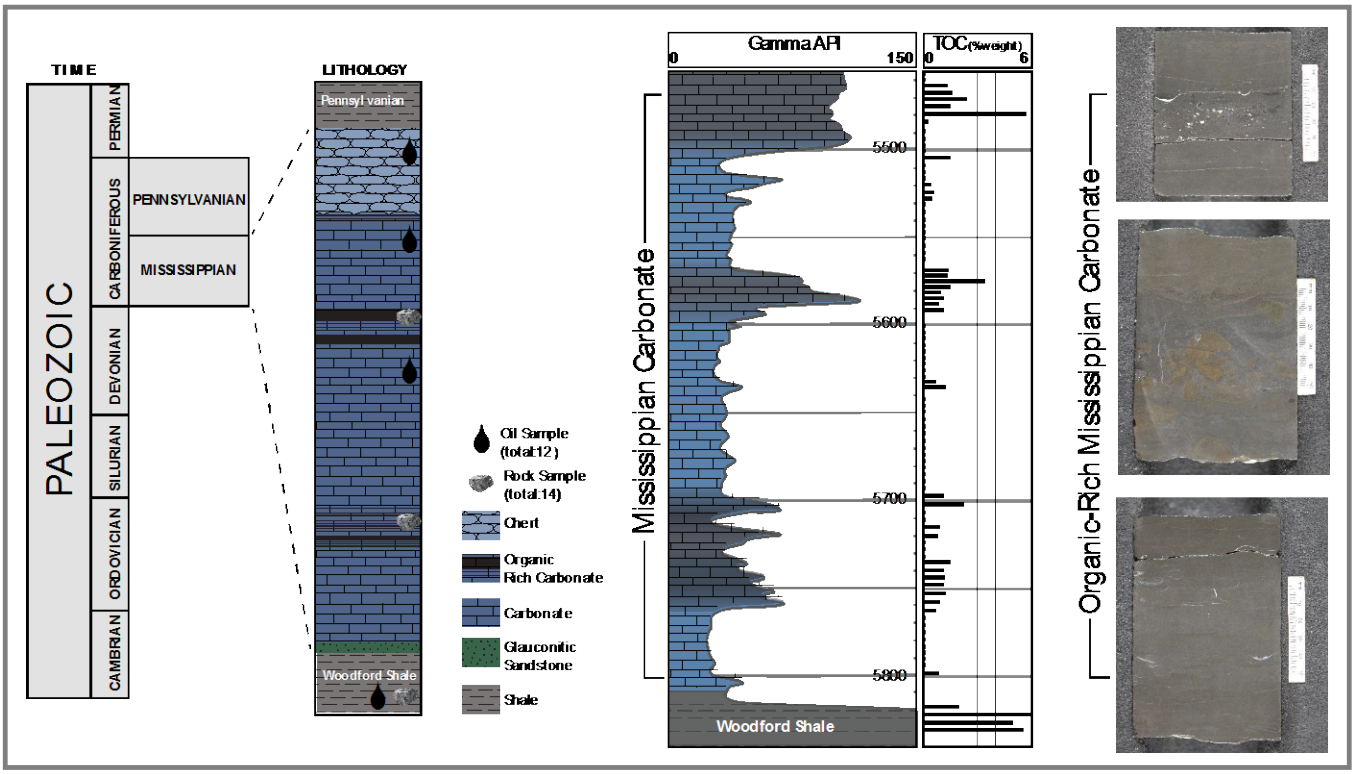

Figure 7. Generalized stratigraphy of northern Oklahoma showing oil and source rock sampling intervals, gamma ray and TOC logs of one of the sampled wells, also core images of sampled organic-rich Mississippian facies.

Core samples were laid out and carefully inspected. Dark-colored intervals were selectively scanned with a portable short-wave ultraviolet light to rapidly evaluate the presence of hydrocarbons. Samples that were visually clean of mud additives were handpicked for chemical analysis to ensure minimal contamination (Fig. 6). Crude oil samples were collected at the wellsite to ensure sample integrity and provenance. Oil samples were stored in 60ml glass bottles and refrigerated. Rock samples were analyzed at OSU for total organic carbon (TOC) content. Out of the 61 rock samples, 14 samples with higher TOC (>1% TOC by weight) were selected and sent to GeoMark for Rock-Eval pyrolysis analysis. Both organic-rich rock and crude oil samples then were shipped to Biomarker Technologies, Inc. (BTI), for further molecular analysis. Figure 7 summarizes the lab analysis that was performed on both rock and oil samples.

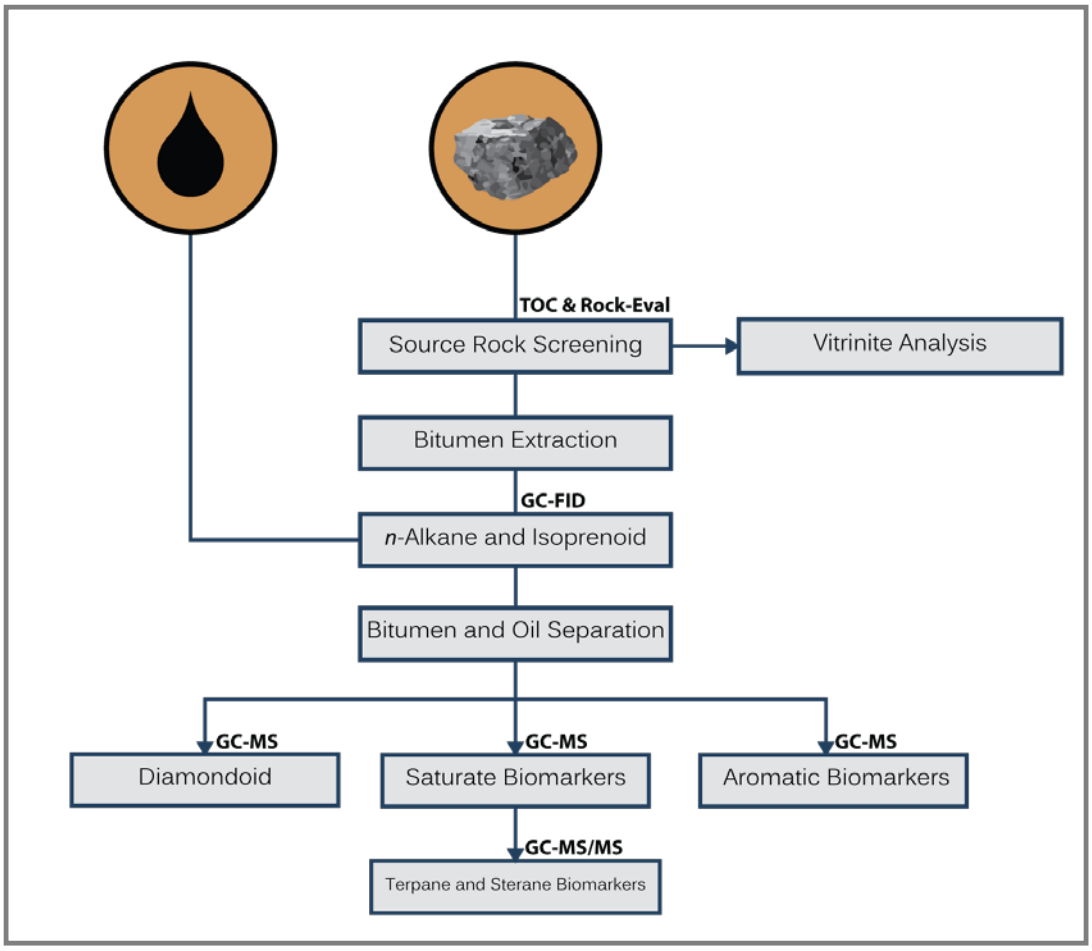

Figure 8. Schematic workflow of the laboratory analysis. TOC= total organic carbon; GC-FID= gas-chromatography flame ionization detector; GC-MS= gas-chromatography mass-spectrometry; GC-MS/MS= gas-chromatography equipped with two dimensional mass-spectrometer.

3.2 Organic and Inorganic Carbon Analysis

Sixty one (61) rock samples were analyzed using the UIC, Inc. CM 5014 coulometer to rapidly screen for potential source rock intervals. The CM 5014 coulometer is equipped with a furnace and CM5130 acidification module for organic and inorganic carbon measurement. Rock samples were crushed to powder, then approximately 100mg of sample powder was placed in the furnace module. The carbon in each sample was combusted at a temperature of 950 °C. Total carbon was then transferred using an oxygen gas carrier to the coulometer for carbon quantification by coulometric titration principles. Inorganic carbon was then measured using the same process; except that, sample powder was introduced to an acidification module with 2 N HCl, to release

inorganic carbon to the coulometer for quantification. TOC was calculated by subtracting the inorganic carbon from total carbon. A pure calcium carbonate ($CaCO_3$) standard was used systemically throughout the analysis, with standard deviation values ranging between (0.3-0.1 %wt.). Coulometer results are listed in Appendix I.

3.3 Pyrolysis Analysis (Rock-Eval II)

Approximately 50-60 mg of powdered rock sample was analyzed using Rock-Eval II running on the TOC mode. Free hydrocarbons (S1 peak) were obtained by pyrolysing the sample at 300 ^{0}C for three minutes. This was followed by programmed pyrolysis at rate of 25^0 C/min to 550^0 C to acquire the thermally cracked hydrocarbons (peak S2). Both of S1 and S2 are measured in milligrams of hydrocarbons generated from one gram of rock sample and detected using a flame ionization detector (FID). The amount of oxygen in the sample is derived from peak S3, which represents carbon dioxide generated per gram of rock sample at temperature up to 390^0 C, and detected using a thermal conductivity detector (TCD) (Peters, 1986). TOC and pyrolysis parameters were determined, and high potential source rock intervals were identified. Rock-Eval results are listed in Appendix II.

3.4 Organic Petrology and Vitrinite Reflectance Analysis

Potential source rock samples with high TOC were prepared for microscopic examination and vitrinite reflectance analysis. Rock samples were reduced to small chips between 5 and 10 mm in size. Sample chips were then mounted in 1-inch epoxy pellets, and polished using coarse, medium and fine silicon carbide grit powder. Polished plugs were examined with a Nikon optical microscope equipped with CRAIC MP-2™ Microscope Photometer and UV light source. Vitrinite was identified, and reflectance (R_o) measurements were made on a random-mean basis. Solid bitumen reflectance was measured and then corrected to vitrinite reflectance equivalence using the

calibration algorithm of Landis and Castano, (1994). Vitrinite reflectance analysis results are listed in Appendix III.

3.5 Molecular Organic Geochemistry Analysis

Rock samples were finely powdered and bitumen was extracted using dichloromethane solvent. Rock extracts and oil samples were analyzed using a gas chromatograph equipped with flame ionization detector (GC-FID). Samples were then fractionated into saturate and aromatic hydrocarbons using silica-gel column chromatography. Afterward, the saturate fraction was spiked with internal standard (5β-cholane), and the normal alkanes were removed from the saturate fraction using silicalite (zeolite). Saturate and aromatic fractions were run on GC-MS and GC-MS-MS instruments to obtain biomarker and diamondoid concentrations. Data were processed using both MassHunter and ChemStation software. Concentrations were derived from targeted-markers' peak area or height, and then compared with internal standard (5β-cholane) and external standard (Stanford-1). In this study, biomarkers and diamondoids are either reported as concentrations (ppm) or normalized ratios. Both gas chromatograms and mass chromatograms data are listed in Appendix IV.

To obtain the overall n-alkane and isoprenoids distribution profile, samples were analyzed using an Agilent HP 6890 GC-FID, equipped with a DB-1 fused silica column 30 m×0.25 mm× 0.25 µm, with hydrogen as a carrier gas, and oven programmed at initial temperature 50 °C for 1 min with rate of 10 °C/min to maximum temperature of 320 °C and held for 15 min. Analysis of biomarkers and diamondoids of the saturate and aromatic fractions were obtained using the Agilent 7890 gas chromatograph interfaced to an Agilent 5975C mass selective detector (GC-MS), with a DB-1 fused silica column (60 m×0.25 mm× 0.25 µm column), and helium as a carrier gas. Moreover, the GC-MS oven was programmed at an initial temperature of 35 °C for 2 min with a rate of 2 °C/min to 80 °C then 3 °C/min from 80 °C to 320 °C, followed by 15 min at 320 °C.

Sterane biomarkers were further analyzed using an Agilent 7890-7000B triple quadruple (GC–MS–MS), equipped with DB-1 fused silica column (60 m×0.25 mm× 0.25 µm column), and oven programmed at initial temperature of 80 °C for one minute then 2 °C/min to 320 °C, followed by 5 min at 320 °C. Helium was used as a carrier gas with flow rate of 2.25mL/min, and in the second quadruple nitrogen was used as collision gas. The GC-MS-MS was run in parent-daughter mode monitoring transitions from C_{26} up to C_{30} of regular and rearranged steranes (i.e. m/z 358 → 217, 372 → 217, 386 → 217, 400 → 217, and 414 → 217).

CHAPTER IV

RESULTS AND DISCUSSION

4.1 Source Rock Potential

Bulk geochemical parameters are summarized in Table 4. Dark mudrock intervals within the Mississippian carbonate have TOC values ranging from 0.83 wt% (Wi-Py-4) up to 2.58 wt% (Ad-Lo-5), and average TOC of 1.39 wt%. Woodford Shale samples are notably richer in organic carbon than Mississppian samples, with the Woodford TOC averaging at 7.88 wt% (Table 4). Similarly, free hydrocarbons as measured by the Rock-Eval S1 peak are generally lower in Mississippian samples (average 0.77 mg HC/g), and higher in Woodford Shale samples

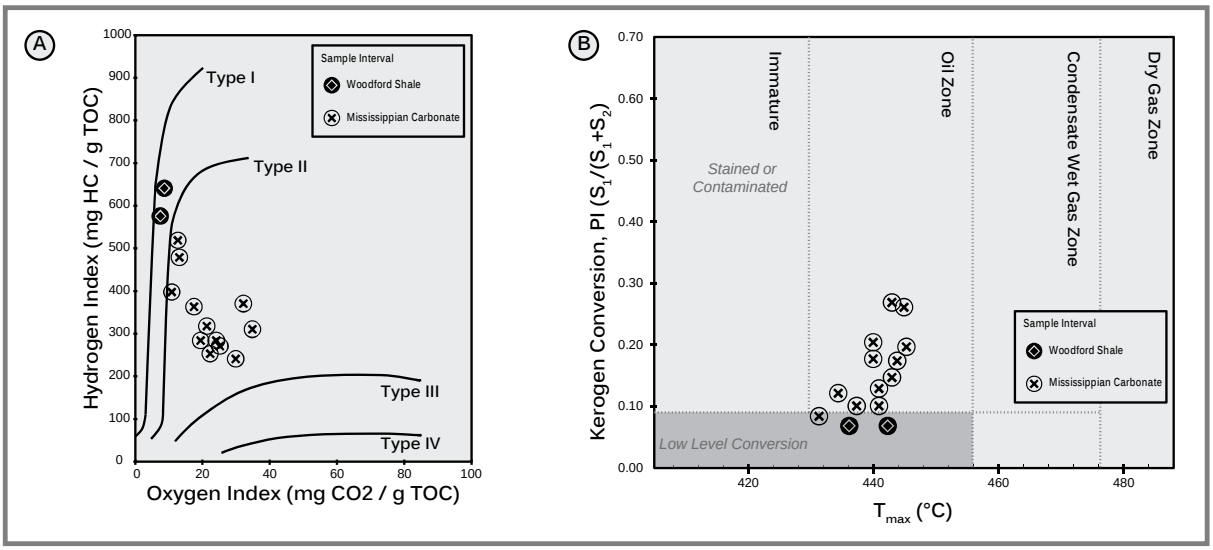

Figure 9. (A) Modified Van Krevelen diagram showing kerogen type of potential Mississippian source rock and Woodford Shale samples.(B) Kerogen conversation measured by plotting Rock-Eval parameters (i.e. production index (S1/(S1+S2)) versus Tmax).

Table 4. Carbon analysis, Rock-Eval pyrolysis and vitrinite reflectance data of rock samples.

Sample ID	Percent Carbonate (wt%)	TOC (wt%)	S1 (mg HC/g)	S2 (mg HC/g)	Tmax (°C)	Measured %Ro[a]	Calculated %Ro	Hydrogen Index (S2×100/TOC)	Oxygen Index (S3×100/TOC)	Production Index (S1/(S1+S2)
Ad-Lo-1	34.06	1.33	1.15	3.06	443	0.77	0.81	230	38	0.27
Ad-Lo-2	42.42	0.99	0.58	2.46	445	0.84	0.85	249	42	0.19
Ad-Lo-3	36.59	1.17	1.09	2.97	444	0.81	0.83	254	40	0.27
Ad-Lo-4	39.50	1.29	0.82	3.27	440	0.82	0.76	253	33	0.20
Ad-Lo-5	38.04	2.58	1.27	11.73	441	0.86	0.78	455	22	0.10
El-Py-1	44.50	2.07	0.83	10.23	431	0.75	0.60	494	22	0.08
El-Py-2	55.07	0.87	0.67	3.01	440	0.81	0.76	348	53	0.18
Wd-Py-1	3.85	7.41	3.97	44.45	442	0.82	0.80	600	6	0.08
Wd-Py-2	6.30	8.34	3.23	42.46	436	0.81	0.69	509	5	0.07
Wi-Py-1	22.14	1.93	0.71	7.30	437	0.74	0.71	378	18	0.09
Wi-Py-2	46.06	1.25	0.59	4.19	442	0.78	0.80	335	30	0.12
Wi-Py-3	21.36	1.03	0.29	2.16	435	0.73	0.67	210	49	0.12
Wi-Py-4	35.89	0.83	0.43	2.39	443	0.79	0.81	287	58	0.15
Wi-Py-5	40.21	1.30	0.77	3.85	444	0.82	0.83	296	36	0.17

[a] This represent both vitrinite reflectance and corrected solid bitumen reflectance using Landis and Castaño (1995) calibration.

(average 3.6 mg HC/g). Using a modified Van Krevelen digram derived from pyrolysis parameters (HI and OI), Mississippian samples plot within Type-II kerogen, whereas Woodford samples are marked as Type-I kerogen (Fig. 8).

Thermal maturity was assessed on both kerogen and extracted bitumen of the rocks. Both Mississippian and Woodford samples have reached the early oil window with vitrinite reflectance ranging from 0.73 to 0.87 R_o%, and T_{max} ranging from 431°C to 445 °C (Table 2). Similarly, molecular maturity indicators of extracted bitumen suggest that these fluids have reached the early

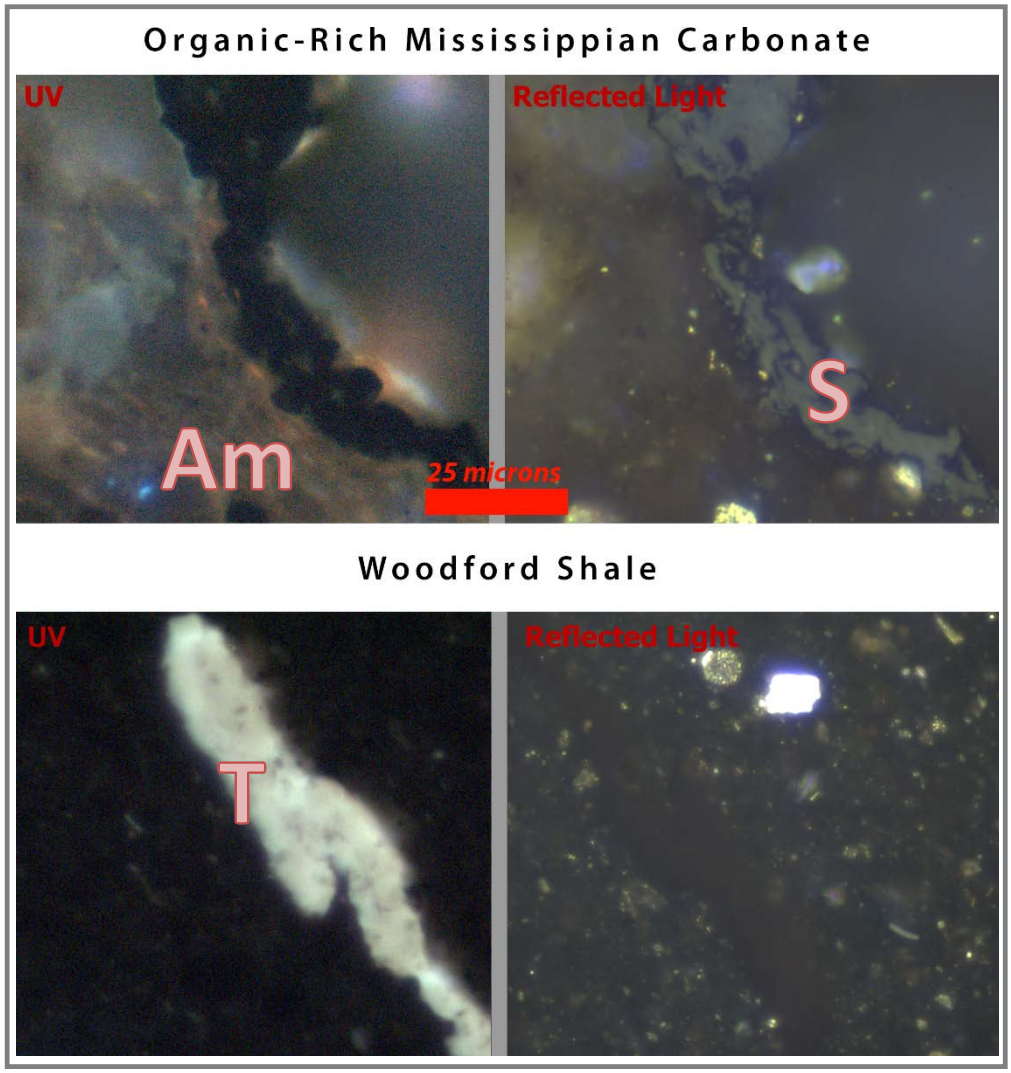

Figure 10. Photomicrographs of macerals within the Lower Mississippian carbonate and Woodford Shale, under reflected white light and fluorescence light, oil immersion; scale bar (25 um). (Am) Amorphous organic matter fused within the rock matrix (S) Solid bitumen filling microfractures (T) telalginite (tasminites) structure found in majority of Woodford Shale samples.

oil window, with the triaromatic and monoaromatic steroids ratios averaging at 0.48 and 0.21, respectively (Table 4). Moreover, petrographic examination reveals that Mississippian kerogen are dominantly amorphous organics lacking identifiable organic structures. Conversely, Woodford Shale kerogen is largely alginite macerals with some preserved structures of telalginite (i.e.*Tasminites*). However, both sets of samples are to a great extent similar in their content of solidified bitumen, with solid bitumen in the Mississippian samples filling elongated microfractures, and solid bitumen in the Woodford occurring as wispy and isolated clasts.

Carbonate source rocks exhibit generally lower TOC (1-5 wt%) when compared with shale source rocks (Hunt, 1996; Palacas, 1988). Even though Mississippian carbonate samples average 1.39 wt% TOC, and have reached a maturity of 0.76 Ro%, they can be classified as a potential source rock with fair to very good petroleum generation quality (Peters and Cassa, 1994). Furthermore, it is likely that Mississippian source rocks are more effective in terms of hydrocarbon expulsion when compared with Woodford samples. Such interpretation is supported by data provided in table 2, which include: 1) Low free hydrocarbons S1 in Mississippian samples and higher S1 values for Woodford samples, possible evidence that Woodford samples retain more of the generated hydrocarbons, 2) Carbonate mineral content is high in Mississippian samples, indicating higher brittleness rock than the Woodford Shale, and 3) Solid bitumen structures in Mississippian samples form connected microstructural pathways; in contrast, Woodford samples contain isolated bitumen clasts. This is not to say that the Woodford Shale is not an effective source rock in north-central Oklahoma. In fact, many studies have shown how rich and productive the Woodford Shale is (Comer and Hinch, 1987; Jones and Philp, 1990). Instead, this evidence support the premise that Mississippian carbonate rocks have generated hydrocarbons in addition to the significant hydrocarbon contribution from the Woodford.

4.2 Source Rock and Oil Geochemistry

4.2.1 Source rock n-alkanes and biomarkers

Rock extracts of both Mississippian carbonate and Woodford Shale exhibit a similar n-alkane profile typical of marine-derived organic matter (Fig. 10). Both samples exhibit unimodal distribution of n-alkanes and maximizing at n-C_{13}. More specifically, Mississippian samples maximize at n-C_{13} and n-C_{14}, whereas Woodford samples maximize at n-C_{13} followed by n-C_{12}. Also Mississippian rocks tend to have slightly lower ratios of both pristane/phytane (Pr/Ph) and odd-to-even predominance (OEP) than Woodford Shale samples (Table 4).

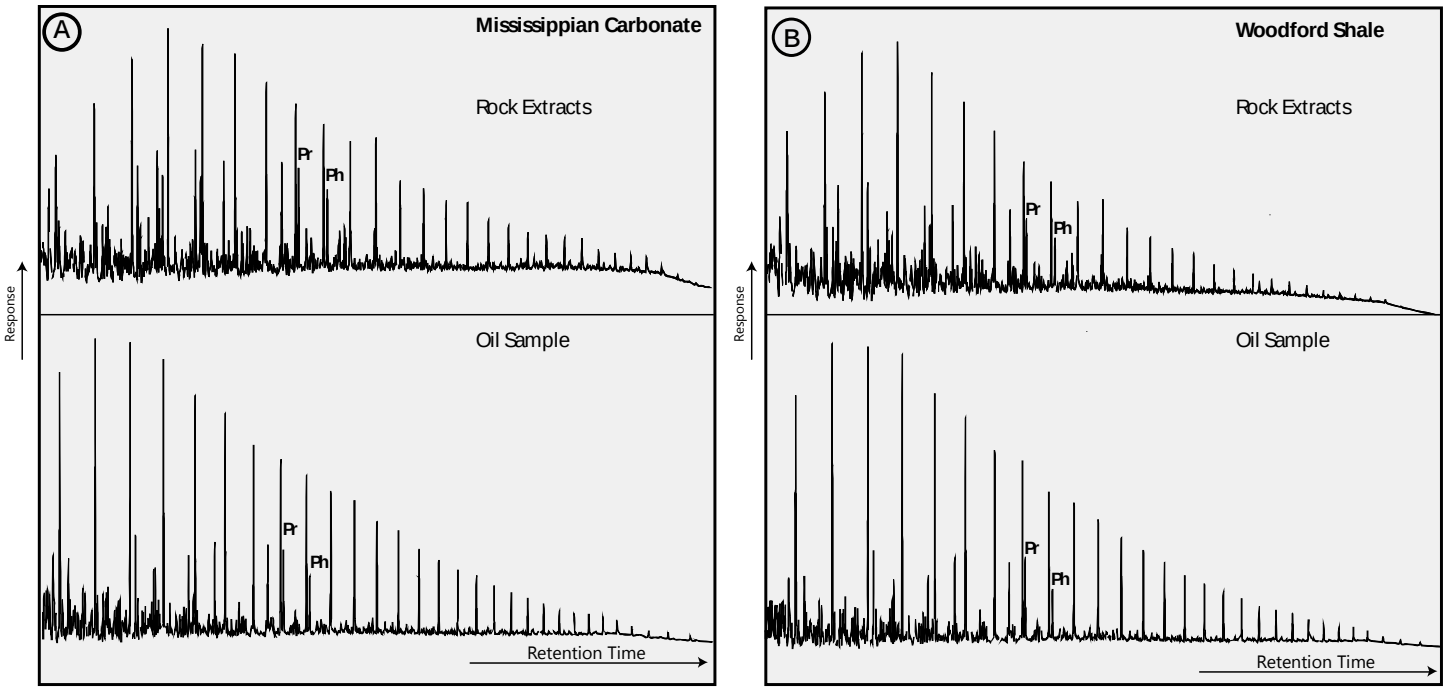

Figure 11. Gas chromatograms of both rock extract and related oil samples, from (A) Mississippian carbonate and (B) Woodford Shale intervals.

Mississippian source rocks exhibit unique biomarkers and diamondoids that are distinctive from those in the Woodford Shale. Mississippian rock extracts show the presence of extended tricyclic terpanes up to C_{35}, together with high C_{27} input relative to C_{28} and C_{29} regular and rearranged steranes (Fig 12). Such results corroborate the results of previous studies that examined Mississippian (Osage) samples over the Anadarko basin (Da Wang and Philp, 1997; Kim and Philp, 2001). Also, we observe high gammacerane in Mississippian samples possibly indicating stratified

water column, however, gammacerane could be coeluting with C_{34} extended tricyclic terpane, and high bisnorhopane relative to hopane reflecting more influence of algal as opposed to bacterial organic matter input (Table 5) (Kim and Philp, 2001; Peters et al., 2005; Schoell et al., 1992). In contrast, the Woodford Shale showed low abundance of extended tricyclic terpanes (up to C_{31}), together with high C_{29} input relative to C_{28} and C_{27} regular steranes. Despite minimum terrestrial organics input in the marine Woodford Shale, the abundance of C_{29} regular sterane in the Woodford appears to be of marine origin, and this is confirmed by the abundance of C_{30} sterane (Fig. 11) (Da Wang and Philp, 1997; Jones and Philp, 1990; Romero and Philp, 2012).

4.2.2 Crude oil n-alkanes and biomarkers

Most of the crude oil samples show similar n-alkane profiles peaking at n-C_{11-13}. Such profiles are believed to be indicative of marine derived petroleum. Similarly, Pr/Ph ratio is relatively similar for most of the oil samples ranging from 1.26 to 1.65, and with average of 1.51. The one exception is sample El-Py-3 that has a Pr/Ph of 0.77. Therefore, bulk chemical characteristics would not be sufficient to define differences between end-members of Mississippian carbonate and Woodford Shale derived oils (Engel et al., 1988). Hence, we looked for more organic matter sensitive biomarkers.

Unlike n-alkanes, biomarker ratios varied among crude oil samples and were useful in delineating end-members of Mississippian and Woodford Shale derived oils (Table 5). Some of the oil samples exhibit the presences of extended tricyclic terpanes up to C_{35}, with the extended tricyclic ratio ranging from 0.43 to 0.94 (Fig. 13)(Table 5). Moreover, samples such as Me-Py-1 and To-Py-1 plot close to C_{27} sterane and exhibit high input of C_{27} relative to C_{28} and C_{29} steranes (Fig. 12). However, Ka-Al-1 and Me-Py-1 samples showed high input of C_{29} relative to C_{28} and C_{27} in both regular and rearranged steranes. Such variations are also observed with other biomarkers such as gammacerane/hopane and pregnanes (Table 5).

Table 5. Selected molecular markers and ratios of both rock extracts and oil samples.

Sample ID	OEP	Pr/Ph	Pr/*n*-C_{17}	Ph/*n*-C_{18}	Terpane					Sterane				Triaromatic Steroids	
					TetC_{24}/Hop	Gam/Hop	Bisnorhop/Hop	HHI	Extended TT	$C_{22}/(C_{21}+C_{22})$	$C_{22}/(C_{22}+C_{27})$	Dia/Reg	C_{27}/C_{29}	MA(I)/MA(I+II)	TA(I)/TA(II)
Ad-Lo-5	0.94	1.24	1.24	1.24	0.35	0.41	0.57	0.23	0.96	0.23	0.39	0.35	1.32	0.19	0.54
Ad-Lo-6	0.98	1.46	1.46	1.46	0.34	0.31	0.47	0.25	0.91	0.26	0.38	0.30	1.19	0.23	0.72
Da-Wo-1	0.96	1.57	1.57	1.57	0.17	0.06	0.06	0.06	0.50	0.42	0.53	0.27	0.68	0.19	0.33
El-Py-3	1.04	0.77	0.77	0.77	0.15	0.10	0.09	0.08	0.70	0.41	0.34	0.26	0.87	0.16	0.27
Je-Py-1	1.02	1.65	1.65	1.65	0.16	0.11	0.11	0.10	0.73	0.40	0.44	0.28	0.87	0.20	0.34
Ka-Al-1	0.96	1.50	1.50	1.50	0.19	0.09	0.13	0.07	0.71	0.41	0.53	0.27	0.69	0.27	0.49
Me-Py-1	1.01	1.66	1.66	1.66	0.16	0.08	0.12	0.04	0.68	0.42	0.49	0.26	0.54	0.22	0.38
Ri-Wo-1	1.01	1.40	1.40	1.40	0.14	0.09	0.07	0.06	0.43	0.45	0.45	0.24	0.66	0.17	0.25
St-Al-1	0.99	1.61	1.61	1.61	0.19	0.07	0.07	0.11	0.63	0.44	0.50	0.24	0.79	0.24	0.45
To-Py-1	0.98	1.65	1.65	1.65	0.15	0.10	0.12	0.10	0.66	0.40	0.34	0.24	1.06	0.17	0.31
Wd-Py-1	1.02	1.39	1.39	1.39	0.22	0.11	0.15	0.09	0.60	0.46	0.60	0.35	0.32	0.24	0.54
Wh-Lo-1	0.95	1.53	1.53	1.53	0.13	0.10	0.10	0.07	0.72	0.43	0.44	0.24	0.75	0.20	0.39
Wh-Lo-2	1.03	1.48	1.48	1.48	0.16	0.08	0.10	0.07	0.73	0.39	0.45	0.26	0.84	0.21	0.38
Wi-Py-1	0.97	1.25	1.25	1.25	0.25	0.20	0.26	0.15	0.78	0.33	0.54	0.26	1.00	0.21	0.36
Wi-Py-6	1.00	1.63	1.63	1.63	0.21	0.23	0.09	0.13	0.85	0.33	0.42	0.31	1.24	0.27	0.59

[a] OEP, odd-to-even predominance(Scalan and Smith, 1970); Pr/Ph, pristine/phytane ratio; TetC_{24}/Hop, $C_{24}H_{42}$ tetracyclic terpane/ hopane ratio; Gam/Hop, gammacerane/hopane ratio; Bisnorhop/Hop, 17α(H), 21β(H)-28,30-bisnorhopane/hopane ratio; HHI, homohopane index = C_{35}αβ(S+R)/(ΣC_{31}-C_{35}αβS+R); Extended TT, extended tricyclic terpane= extended trycyclic Σ$C_{28\text{-}40}$(S+R)/ (Σ$C_{28\text{-}40}$(S+R)+hopane); $C_{21}/(C_{21}+C_{22})$, C_{21}αβ sterane/(C_{21}αβ sterane+ C_{22}αβ sterane); $C_{22}/ C_{22}+C_{27}$, C_{22}αβ sterane/(C_{22}αβ steranes+ C_{27}αα 20R sterane); Dia/Reg, C_{27} βα 20S+R diasterane/(C_{27} βα 20S+R diasterane+ C_{27}αα20[S+R]+ C_{27}ββ20[S+R] regular steranes); C_{27}/C_{29} , C_{27}αα 20R sterane/ C_{29}αα 20R sterane

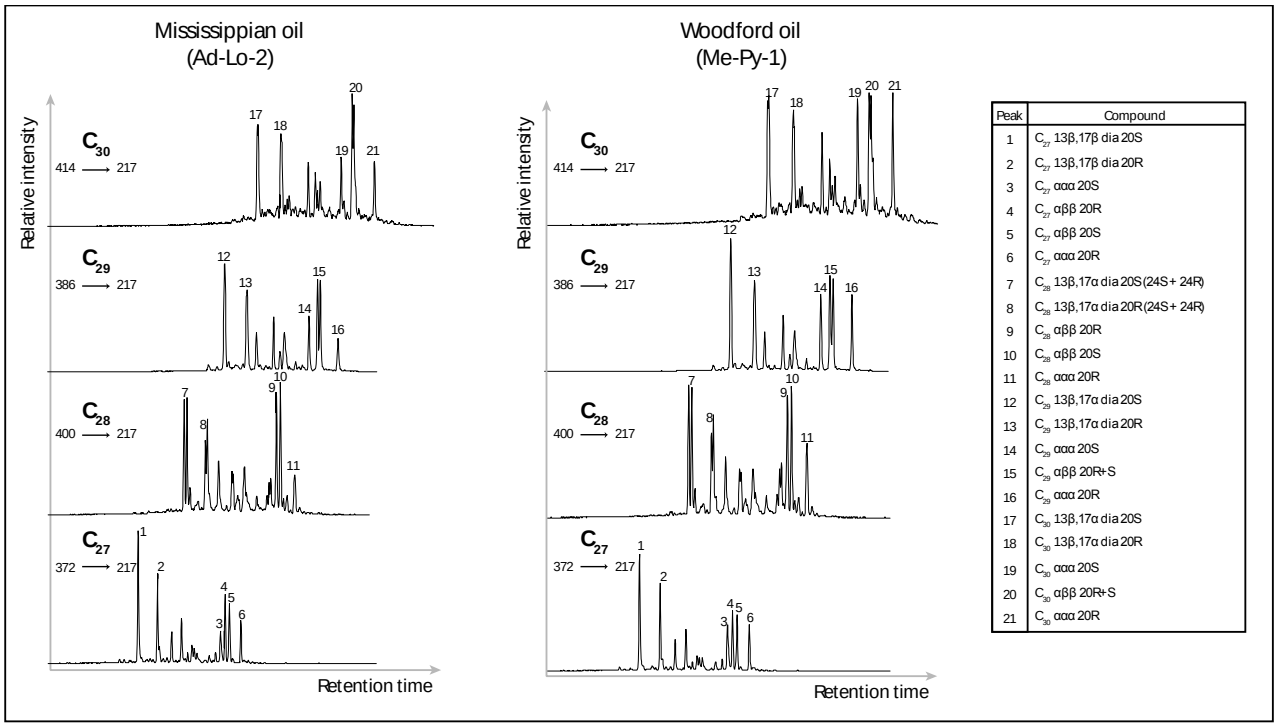

Figure 12. GC-MS-MS of C_{27}-C_{30} steranes analysis showing end-members of both Woodford and Mississippian oils.

4.2.3 Source rock-crude oil correlation

The use of biomarkers is crucial for understanding petroleum systems by relating source rocks to genetically related oils (Curiale, 2008; Magoon and Dow, 1994; Peters et al., 2005). Diagnostic biomarkers were identified that appear to represent the contribution of the Mississippian carbonate source rock. Mississippian carbonate and related oils (i.e. Ad-Lo-5, Ad-Lo-6 and Wi-Py-1) exhibit OEP<1, the presence of extended tricyclic terpane series up to C_{35}, high gammacerane/hopane, and high C_{27} sterane together with 28, 30-bisnorhopane relative to hopane (Fig 12). Such markers are likely to indicate both carbonate lithology and large input of marine algal organics. Moreover, algal input of Mississippian kerogen is proposed by previous studies to result from an algal blooming event that occurred during Mississippian deposition (De Grande et al., 1993; Kim and Philp, 2001; Peters et al., 2005). Woodford Shale and related oils (i.e. Wd-Py-1, Me-Py-1 and Ri-Wo-1) display OEP>1, high C_{29} sterane, low gammacerane and high

homoprenange relative to pregnanes (Table 5). These markers have been previously observed and are a typical signature of siliciclastic marine shale source rock (Jones and Philp, 1990; Peters et al., 2005; Romero and Philp, 2012; Wang et al., 2015). Maturity biomarker ratios indicate that the majority of the samples are within the early to mid-oil window with MA(I)/MA(I+II) and TA(I)/TA(II) ratios averaging at 0.23 and 0.45 respectively

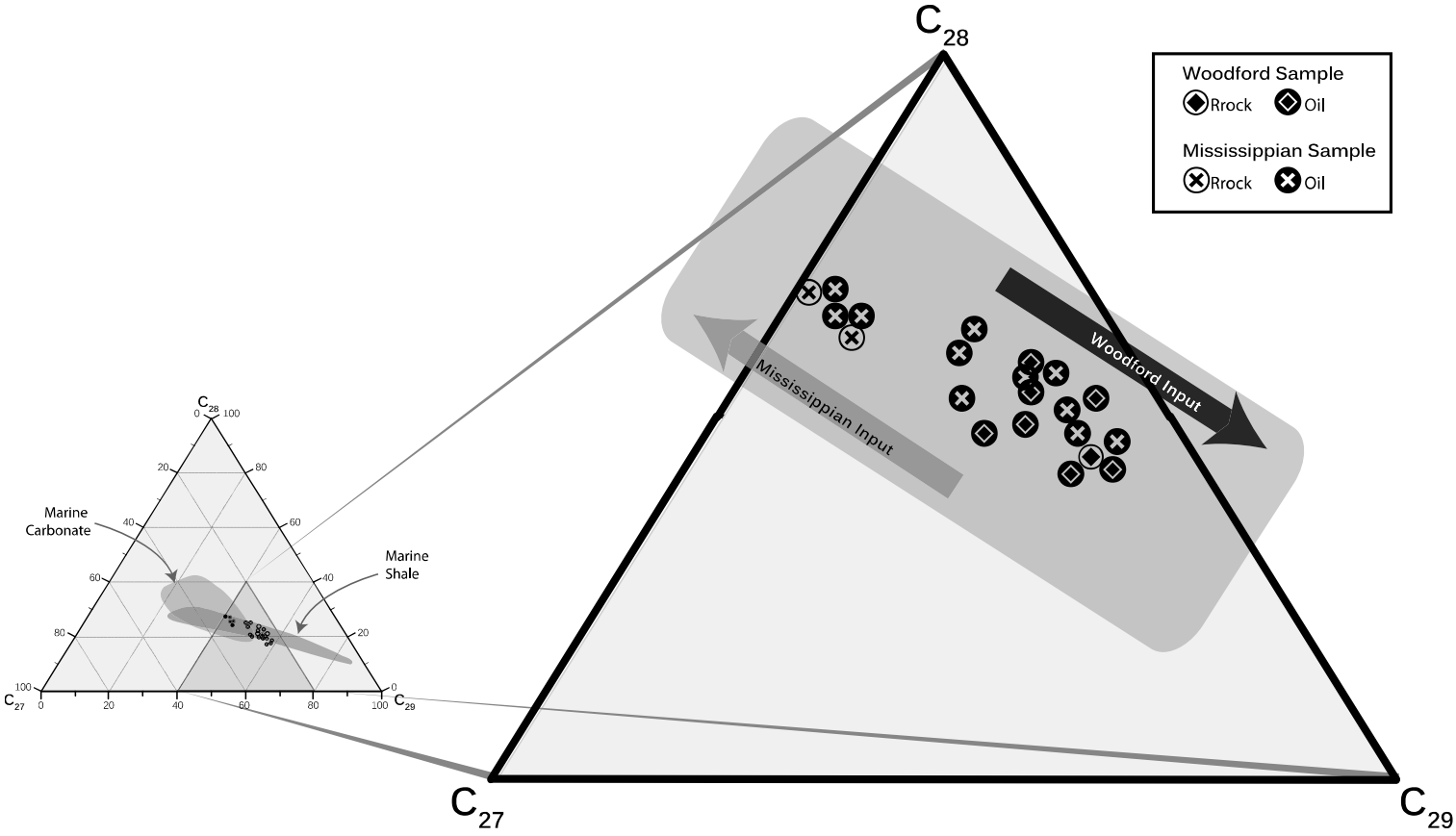

Figure 13. Ternary diagram of relative concentrations of ααα-C_{27}, C_{28} and C_{29} regular steranes of Woodford Shale and Mississippian carbonate as measured by GC-MSMS plot modified from (Moldowan et al., 1985)

4.2.4 Diamondoids and oil mixing

Biomarkers when supplemented with diamondoids are an effective tool for unraveling co-sourcing and oil mixing (Moldowan et al., 2015). Summarized in Table 6 are concentration results of major diamondoid compounds in both oil and rock extract samples. Samples across the Anadarko shelf contain relatively high concentrations of both regular C_{29} sterane and diamondoids compounds, particularly alkylated adamantane and diamantane. Samples located east of the

Nemaha uplift contained relatively low concentrations of diamondoid compounds, but high regular C_{29} sterane. Thermal fragility of C_{29} sterane, combined with thermal stability of methylated diamantane provide insights into the extent of hydrocarbon cracking and mixing (Dahl et al., 1999). Mississippian oils within the Anadarko shelf are a mixture of cracked and non-cracked oils, as indicated by high 3+4-methyldiamantane (average of 4.05 ppm) and high C_{29} sterane (average of 50.43ppm) (Fig. 14). In contrast, sampled oils from east of the Nemaha uplift contained low 3+4-methyldiamantane (average of 1.84 ppm) and high C_{29} sterane (average of 26.12 ppm) (Fig. 14)

Table 6. Selected diamondoids and biomarker concentration in ppm.

Sample ID	1+2-Methyladamantane	1+2-Ethyladamantane	3+4-Methyldiamantane	C29ααα 20R sterane
West of Nemaha (Anadarko Shelf)				
Da-Wo-1	77.8	41.9	4.2	53.7
Ka-Al-1	98.4	46.9	5.1	21.7
Ri-Wo-1	121.6	86.4	3.6	85.5
St-Al-1	63.4	38.4	3.3	40.8
East of Nemaha				
Ad-Lo-5	46	29.7	2.3	11
Ad-Lo-6	40.2	20.9	2.3	14.5
El-Py-3	31.3	20.8	1.7	49.2
Je-Py-1	43.2	24.8	1.7	29.5
Me-Py-1	47.6	23.7	2	26.8
To-Py-1	39.1	19.5	1.4	38.6
Wd-Py-1	43.4	30	1.3	10.5
Wh-Lo-1	32.9	24.4	2.2	40.5
Wh-Lo-2	34.8	29	2.1	38.6
Wi-Py-1	37	29.2	1.7	14.3
Wi-Py-6	30.9	20.7	1.5	13.8

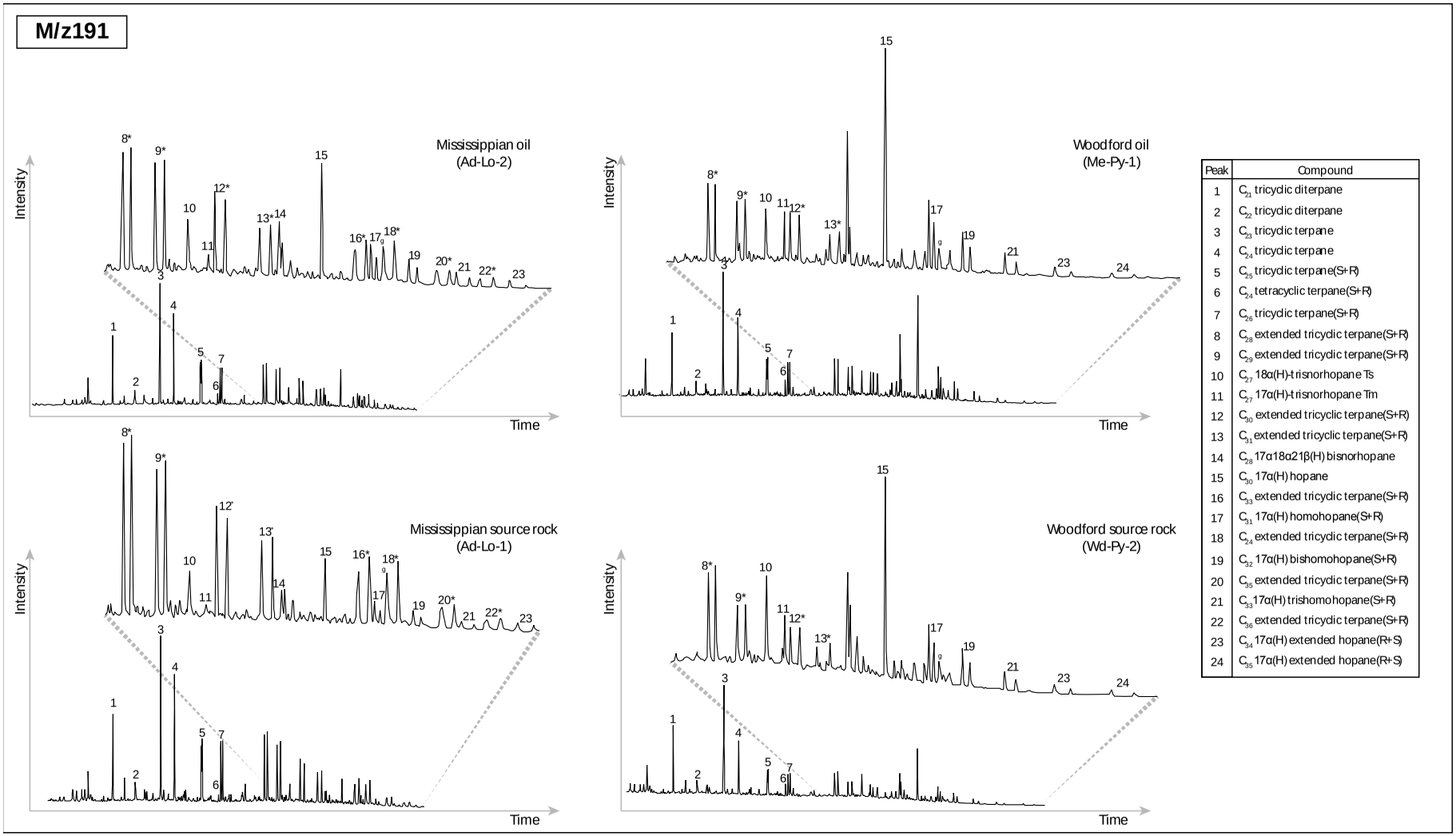

Figure 14. Mass chromatogram (m/z 191) of saturate hydrocarbons comparing end-members of Woodford oil and rock with Mississippian oil and rock (is depicting extended tricyclic terpanes).*

4.3 Implications to Hydrocarbon Charge History

A long-distance oil migration model out of the Anadarko Basin is proposed on the basis of light hydrocarbons. Moreover, the decrease in toluene of C_7 hydrocarbons away from the Anadarko Basin has been attributed to long-distance oil migration (Burruss and Hatch, 1989). Similarly, our data support the long distance migration hypothesis. However diamondoids and biomarkers in samples from Anadarko shelf suggest the presence of another early-maturity oil. The presence of low maturity parautochthonous oil mixed with more mature migrated oil could be explained by episodic hydrocarbon charge, which is composed of an early maturity hydrocarbon charge followed by a mature charge as the Anadarko basin continued to subside and expel hydrocarbons. Unlike the open migration system of the Anadarko shelf, samples from Payne and Logan counties east of the Nemaha uplift appear to be a result of a relatively closed charge system with short migration distance, and in-situ generation under much lower thermal stress as indicated by the low diamondoids concentration together with measured vitrinite and solid bitumen reflectance (Table 4).

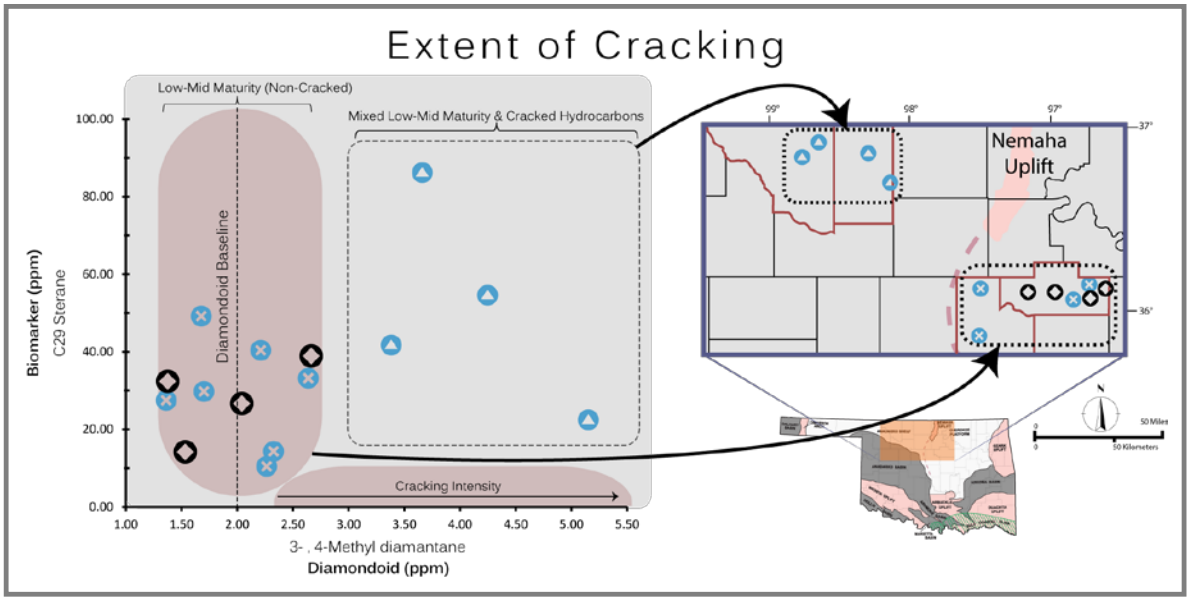

Figure 15. Extent of cracking measured by comparing concentration of ααα-C_{29} sterane and 3+4-methyldiamantane comparing samples over east and west regions with respect to the Nemaha uplift.

The Nemaha uplift is a late Mississippian or early Pennsylvanian paleostructural feature extending from southeast Nebraska to central Oklahoma. This structural-high feature separates the Cherokee Platform in northeastern Oklahoma from the Anadarko Basin and shelf (Dolton and Finn, 1989). In this tectonic context, occurrence of oil within north-central (i.e. Payne and Logan counties) is very likely to be of localized origin with very minimal if any contribution from the Anadarko or Arkoma basins. Localization is further enhanced by facies change within Mississippian section from clean carbonate to the north to argillaceous mudrocks to the south, which provided a low permeability barrier between the Cherokee Platform and Arkoma Basin (Andrews, 2007). This interpretation is supported by the low maturity of recovered fluids and rock samples. Any contribution from deeper basins (i.e. Anadarko and Arkoma) would have generated a high-maturity signature that should be observed along with high concentration of diamondoids. Additionally, because of low permeability in the Woodford Shale, it seems reasonable to expect the oil in the Woodford east of Nemaha uplift (i.e. Payne and Logan) to be generated locally and not the result of long distance migration.

.

CHAPTER V

CONCLUSION

5.1 Major Findings

The Woodford Shale and Lower Mississippian carbonates are the most important sources of hydrocarbons for the Devonian-Mississippian petroleum systems within north-central Oklahoma. Pyrolysis and reflected light microscopy suggest that in addition to the well-known potential of the Woodford Shale, organic-rich, Lower Mississippian carbonates exhibit good to fair generation potential, and have reached the early-oil window. Furthermore, hydrocarbon contribution from Lower Mississippian carbonates was revealed by the similar molecular characteristics that Mississippian-rock extracts share with some Mississippian produced oils. The diagnostic biomarker of Lower Mississippian source-rocks is the presence of extended tricyclic terpane homologs up to C_{35}. Such variations in fingerprints are believed to reflect both of organic matter type and depositional setting.

Mississippian and Woodford oils within the Anadarko shelf and east of the Nemaha uplift appear to have undergone different charging histories. Diamondoids combined with biomarkers suggests that oils within the Anadarko shelf are a result of episodic charges of non-cracked oil followed by cracked oil that probably migrated from the Anadarko Basin. In contrast, samples collected within east of the Nemaha uplift (i.e. Payne and Logan counties) are relatively depleted in diamondoids, hence indicating localized source rock that went through lower maturation levels.

It is speculated that the Nemaha uplift, which was a positive feature during the Carboniferous, contributed to the separation of the Cherokee Platform petroleum system from the Anadarko petroleum systems. Facies change within the Mississippian section in eastern Oklahoma facilitated isolation of the Cherokee platform from the Arkoma Basin petroleum kitchen.

5.2 Potential Future Work

This work could be further developed by 1) expanding the study area, 2) examining oil-bearing fluid inclusions and 3) performing selective stable isotopic analysis of both biomarkers and diamondoids. Such work will have crucial implications at both basin/petroleum system and reservoir/oil field scales.

This type of study can benefit greatly from expanding the study area to collect samples from across the Cherokee Platform. More specifically, oils and rocks samples located within areas, to the south and east of Payne and Logan counties (e.g. Pottawatomie, Lincoln and Creek counties). Examining both rock and oils from a larger area will help delineate the extent of the Mississippian petroleum system relative to the Woodford petroleum system. Such work would be valuable input and help refine existing basin models and migration pathways.

The micro-sized oil inclusions provide valuable evidence of palaeo-oil composition. When carefully and meticulously handled and examined, hydrocarbon fluid inclusions can provide a better understanding of petroleum migration and accumulation. Specifically, biomarkers provide a valuable insight into hydrocarbons inclusion composition in terms of organic matter source, sedimentary depositional settings and level of thermal stress. Such work would improve and refine this study by comparing produced oil composition and oil inclusion composition, furthermore deciphering reservoir filling history (George et al., 2007).

Since most of the analyses completed in this study are molecular-focused, adding an isotopic component to this study will further solidify its conclusions. More specifically, preforming compound specific isotopic analysis (CSIA) would enhance oil to source correlation. Moreover, analyzing the samples using gas chromatography-isotope ratio mass spectrometry (GC/IRMS) will provide isotopic data of individual biomarker or diamondoid compounds. Particularly, CSIA of diamondoids has been proven to be a useful tool when dealing with samples depleted in biomarkers due to thermal maturation (Moldowan et al., 2015).

REFERENCES

Adler, F., Henslee, H., Hicks, I., Larson, T., Rascoe Jr, B., Caplan, W., Carlson, M., Goebel, E., McCracken, M., and Wells, J., 1987, Stratigraphic distribution of oil and gas in the Mid-Continent, *in* Rascoe, B., and Hyne, N. J., eds., Petroleum geology of the Mid-continent, Tulsa Geological Society Special Publication 3, p. 25-28.

Amsden, T. M., 1975, Hunton Group (Late Ordovician, Silurian, and Early Devonian) ,*in* the Anadarko Basin of Oklahoma,, Oklahoma Geological Survey Bulletin 121, p. 214.

Andrews, R. D., 2007, Stratigraphy, production, and reservoir characteristics of the Caney Shale in southern Oklahoma: Shale Shaker, v. 58, p. 9–25.

Blakey, R., 2011, Paleogeography and geologic evolution of North America, Colorado Plateau Geosystems, Inc. http://cpgeosystems.com/nam.html

Boardman, D. R., Thompson, T. L., Godwin, C., Mazzullo, S. J., Wilhite, B. W., and Morris, B. T., 2013, High-resolution conodont zonation for Kinderhookian (Middle Tournaisian) and Osagean (Upper Tournaisian-Lower Visean) strata of the western edge of the Ozark Plateau, North America: Shale Shaker, v. 64, p. 98-151.

Boyd, D. T., 2008, Oklahoma: The ultimate oil opportunity: Shale Shaker, v. 58, no. 6, p. 205−221.

-, 2012, Oklahoma 2011 Drilling Highlights: Shale Shaker, v. 62, no. 5, p. 378-393.

Burchett, R. R., Luza, K., Van Eck, O., and Wilson, F., 1983, Seismicity and tectonic relationships of the Nemaha Uplift and Midcontinent geophysical anomaly (Final project summary): Oklahoma Geological Survey Special Publications, v. 85-2, p. 33.

Burruss, R. C., and Hatch, J. R., 1989, Geochemistry of oils and hydrocarbon source rocks, greater Anadarko basin: evidence for multiple sources of oils and long distance oil migration: Oklahoma Geological Survey Circular 90, p. 53-64.

Cardott, B. J., 2012, Thermal maturity of Woodford Shale gas and oil plays, Oklahoma, USA: International Journal of Coal Geology, v. 103, p. 109-119.

Cardott, B. J., and Lambert, M. W., 1985, Thermal maturation by vitrinite reflectance of Woodford Shale, Anadarko basin, Oklahoma: AAPG Bulletin, v. 69, no. 11, p. 1982-1998.

Carlson, M., 1971, Eastern Nebraska and north-central Kansas, *in* Cram, J. H., ed., Future Petroleum Provinces of the United States-Their Geology and Potential, AAPG, Memoir 15, p. 1,103- 101,107.

Carmalt, S., and John, B. S., 1986, Giant oil and gas fields: AAPG, Memoir 40, p. 11-53.

Comer, J. B., and Hinch, H. H., 1987, Recognizing and quantifying expulsion of oil from the Woodford Formation and age-equivalent rocks in Oklahoma and Arkansas: AAPG Bulletin, v. 71, no. 7, p. 844-858.

Cronenwett, C., 1956, A subsurface study of the Simpson Group in east-central Oklahoma: Shale Shaker Digest, no. II, p. 171-187.

Curiale, J., 2008, Oil–source rock correlations–limitations and recommendations: Organic Geochemistry, v. 39, no. 8, p. 1150-1161.

Curtis, D. M., and Champlin, S. C., 1959, Depositional environments of Mississippian limestones of Oklahoma: Tulsa Geological Society Digest, v. 27, p. 90-103.

Da Wang, H., and Philp, R. P., 1997, Geochemical study of potential source rocks and crude oils in the Anadarko Basin, Oklahoma: AAPG Bulletin, v. 81, no. 2, p. 249-275.

Dahl, J., Moldowan, J. M., Peters, K., Claypool, G., Rooney, M., Michael, G., Mello, M., and Kohnen, M., 1999, Diamondoid hydrocarbons as indicators of natural oil cracking: Nature, v. 399, no. 6731, p. 54-57.

De Grande, S. M. B., Aquino Neto, F. R., and Mello, M. R., 1993, Extended tricyclic terpanes in sediments and petroleums: Organic Geochemistry, v. 20, no. 7, p. 1039-1047.

Dolton, G. L., and Finn, T. M., 1989, Petroleum geology of the Nemaha Uplift, central Mid-Continent: U.S. Geological Survey, Open-File Report 88-450-D, p. 30.

George, S. C., Volk, H., and Ahmed, M., 2007, Geochemical analysis techniques and geological applications of oil-bearing fluid inclusions, with some Australian case studies: Journal of Petroleum Science and Engineering, v. 57, no. 1–2, p. 119-138.

Gilbert, M. C., 1992, Speculations on the origin of the Anadarko basin, Basement Tectonics 7, Springer, p. 195-208.

Gutschick, R. C., and Sandberg, C. A., 1983, Mississippian continental margins of the conterminous United States: Special Publications of SEPM, no. 33, p. 79-96.

Higley, D. K., 2013, 4D Petroleum system model of the Mississippian System in the Anadarko basin province, Oklahoma, Kansas, Texas, and Colorado, USA: The Mountain Geologist, v. 50, no. 3, p. 81-98.

Hunt, J. M., 1996, Petroleum Geochemistry and Geology, New York, W H Freeman Limited, 743 p. http://www.searchanddiscovery.com/documents/2003/mcbee/

Hunt, J. M., and McNichol, A. P., 1984, The Cretaceous Austin Chalk of south Texas--a petroleum source rock, *in* G., P. J., ed., Petroleum Geochemistry and Source Rock Potential of Carbonate Rocks: AAPG Studies in Geology, p. 117-126.

Jiang, C., Li, M., Osadetz, K. G., Snowdon, L. R., Obermajer, M., and Fowler, M. G., 2001, Bakken/Madison petroleum systems in the Canadian Williston basin. Part 2: molecular markers diagnostic of Bakken and Lodgepole source rocks: Organic Geochemistry, v. 32, no. 9, p. 1037-1054.

Johnson, K. S., 1989, Geologic evolution of the Anadarko basin, *in* Johnson, K. S., ed., Anadarko basin symposium: , Oklahoma Geological Survey Circular 90, p. 3-12.

Jones, P. J., and Philp, R. P., 1990, Oils and source rocks from Pauls Valley, Anadarko Basin, Oklahoma, U.S.A: Applied Geochemistry, v. 5, no. 4, p. 429-448.

Jordan, L., and Rowland, T. L., 1959, Mississippian rocks in northern Oklahoma: Tulsa Geological Society Digest, v. 27, p. 124-136.

Kim, D., and Philp, R. P., 2001, Extended tricyclic terpanes in Mississippian rocks from the Anadarko basin, Oklahoma, *in* J., K. S., ed., Silurian, Devonian, and Mississippian Geology and Petroleum in the Southern Midcontinent, 1999 Symposium, Oklahoma Geological Survey Circular 105, p. 109-127.

Kirkland, D. W., and Evans, R., 1981, Source-rock potential of evaporitic environment: AAPG Bulletin, v. 65, no. 2, p. 181-190.

Lane, H. R., and De Keyser, T., 1980, Paleogeography of the late Early Mississippian (Tournaisian 3) in the central and southwestern United States, *in* Fouch, T. D., and Magathan, E. R, ed., Paleozoic Paleogeography of West-Central United States, West-Central U.S., Rocky Mountain Section (SEPM), p. 149-162.

Magoon, L. B., and Dow, W. G., 1994, The petroleum system—From source to trap: AAPG Memoir 60, p. 3-24.

Malek-Aslani, M., 1980, Environmental and diagenetic controls of carbonate and evaporite source rocks: Gulf Coast Association of Geological Societies Transactions, v. 30, p. 445-458.

Mazzullo, S., Boardman, D. R., Wilhite, B. W., Godwin, C., and Morris, B. T., 2013, Revisions of outcrop lithostratigraphic nomenclature in the Lower to Middle Mississippian Subsystem (Kinderhookian to Basal Meramecian Series) along the shelf-edge in southwest Missouri, northwest Arkansas, and northeast Oklahoma: Shale Shaker, v. 63, p. 414-454.

Mazzullo, S., Wilhite, B. W., and Boardman II, D. R., 2011, Lithostratigraphic architecture of the Mississippian Reeds Spring Formation (Middle Osagean) in southwest Missouri, northwest Arkansas, and northeast Oklahoma: Outcrop analog of subsurface petroleum reservoirs: Shale Shaker, v. 61, p. 254-269.

McBee, W., 2003, Nemaha strike-slip fault zone: American Association of Petroleum Geologists, Search and Discovery, 6 p. ht

Moldowan, J. M., Dahl, J., Zinniker, D., and Barbanti, S. M., 2015, Underutilized advanced geochemical technologies for oil and gas exploration and production-1. The diamondoids: Journal of Petroleum Science and Engineering, v. 126, p. 87-96.

Moldowan, J. M., Seifert, W. K., and Gallegos, E. J., 1985, Relationship between petroleum composition and depositional environment of petroleum source rocks: AAPG Bulletin, v. 69, no. 8, p. 1255-1268.

Noble, P. J., 1993, Paleoceanographic and tectonic implications of a regionally extensive Early Mississippian hiatus in the Ouachita system, southern mid-continental United States: Geology, v. 21, no. 4, p. 315-318.

Oehler, J. H., 1984, Carbonate source rocks in the Jurassic Smackover trend of Mississippi, Alabama, and Florida, *in* G., P. J., ed., Petroleum Geochemistry and Source Rock Potential of Carbonate Rocks: AAPG Studies in Geology 18, p. 63-69.

Palacas, J. G., 1984, Petroleum geochemistry and source rock potential of carbonate rocks, AAPG Studies in Geology 18, 208 p.

-, 1988, Characteristics of carbonate source rocks of petroleum: Petroleum Systems of the United States: U.S. Geological Survey Bulletin, v. 1870, p. 20-25.

Perry, W., 1995, Arkoma Basin Province (062), *in* DL Gautier, G. D., KI Takahashi and KL Varnes, ed., 1995 National assessment of United States oil and gas resources — Results, methodology, and supporting data: U.S. Geological Survey Digital Data Series 30, CD-ROM.

Peters, K. E., and Cassa, M. R., 1994, Applied source rock geochemistry, *in* Magoon, L. B., and Dow, W. G., eds., The petroleum system--from source to trap, Volume Memoir 60: AAPG, p. 93-120.

Peters, K. E., and Fowler, M. G., 2002, Applications of petroleum geochemistry to exploration and reservoir management: Organic Geochemistry, v. 33, no. 1, p. 5-36.

Peters, K. E., Walters, C., and Moldowan, J., 2005, The biomarker guide: Biomarkers and isostopes in the environment and human history, Cambridge University Press, 704 p.

Rice, D. D., 1984, Occurrence of indigenous biogenic gas in organic-rich, immature chalks of Late Cretaceous age, eastern Denver basin, *in* G., P. J., ed., Petroleum Geochemistry and Source Rock Potential of Carbonate Rocks: AAPG Studies in Geology 18, p. 135-150.

Rogers, S. M., 2001, Deposition and diagenesis of Mississippian chat reservoirs, north-central Oklahoma: AAPG Bulletin, v. 85, no. 1, p. 115-129.

Romero, A. M., and Philp, R. P., 2012, Organic geochemistry of the Woodford Shale, southeastern Oklahoma: How variable can shales be?: AAPG Bulletin, v. 96, no. 3, p. 493-517.

Scalan, E. S., and Smith, J. E., 1970, An improved measure of the odd-even predominance in the normal alkanes of sediment extracts and petroleum: Geochimica et Cosmochimica Acta, v. 34, no. 5, p. 611-620.

Schoell, M., McCaffrey, M. A., Fago, F. J., and Moldowan, J. M., 1992, Carbon isotopic compositions of 28,30-bisnorhopanes and other biological markers in a Monterey crude oil: Geochimica et Cosmochimica Acta, v. 56, no. 3, p. 1391-1399.

Suneson, N. H., 2012, Arkoma basin petroleum-past, present, and future: Shale Shaker, v. 36, no. 1, p. 38-70.

Sutherland, P. K., 1988, Late Mississippian and Pennsylvanian depositional history in the Arkoma basin area, Oklahoma and Arkansas: Geological Society of America Bulletin, v. 100, no. 11, p. 1787-1802.

Tissot, B., Deroo, G., and Hood, A., 1978, Geochemical study of the Uinta Basin: formation of petroleum from the Green River Formation: Geochimica et Cosmochimica Acta, v. 42, no. 10, p. 1469-1485.

Walper, J. L., 1977, Paleozoic tectonics of the southern margin of North America: Gulf Coast Association of Geological Societies Transactions, v. 27, p. 230-239.

Wang, G., Chang, X., Wang, T. G., and Simoneit, B. R. T., 2015, Pregnanes as molecular indicators for depositional environments of sediments and petroleum source rocks: Organic Geochemistry, v. 78, p. 110-120.

Zumberge, J. E., 1984, Source rocks of the La Luna Formation (Upper Cretaceous) in the Middle Magdalena Valley, Colombia, *in* G., P. J., ed., Petroleum Geochemistry and Source Rock Potential of Carbonate Rocks: AAPG Studies in Geology 18, p. 127-133.

APPENDIX I

Organic and Inorganic Carbon Data

Table 1. Carbon analysis data including total, inorganic and organic carbon.

Well	Depth(ft)	Formation	Total Carbon	Inorganic Carbon	Organic Carbon
Wd-Py	3360	Woodford	2.94	0.05	2.89
	3367	Woodford	7.38	0.07	7.31
	3371	Woodford	8.66	0.32	8.34
	3377	Woodford	8.76	0.60	8.16
Wi-Py	5144	Mississippian	12.16	0.43	11.73
	5146	Mississippian	3.82	2.16	1.66
	5154	Mississippian	5.42	5.00	0.42
	5156	Mississippian	3.89	2.64	1.25
	5157	Mississippian	5.89	4.10	1.79
	5159	Mississippian	5.97	3.49	2.48
	5162	Mississippian	2.66	1.21	1.45
	5164	Mississippian	6.91	1.04	5.87
	5185	Mississippian	5.66	6.14	-0.48
	5197	Mississippian	3.27	1.86	1.41
	5246	Mississippian	4.22	3.00	1.22
	5250	Mississippian	5.12	4.22	0.90
	5254	Mississippian	5.59	4.69	0.90
	5271	Mississippian	4.30	3.76	0.54
	5273	Mississippian	5.70	2.92	2.78
	5276	Mississippian	4.88	3.54	1.34
	5278	Mississippian	5.52	4.30	1.22
	5280	Mississippian	6.42	5.32	1.10
	5281	Mississippian	5.55	4.52	1.03
	5298	Mississippian	5.84	1.61	4.23
	5302	Mississippian	6.75	6.05	0.70
	5748	Mississippian	6.76	6.31	0.45
El-Py	4363	Mississippian	5.68	3.26	2.42
	4365	Mississippian	7.32	4.78	2.54
	4367	Mississippian	5.89	3.36	2.53
	4371	Mississippian	6.69	4.82	1.87
	4462	Mississippian	7.72	6.20	1.52
	4481	Mississippian	4.99	4.14	0.85
Ad-Lo	5518	Mississippian	4.89	0.38	5.27
	5524	Mississippian	4.40	0.61	5.01
	5525	Mississippian	4.16	0.56	4.72
	5568	Mississippian	4.92	1.49	6.41
	5568	Mississippian	4.97	1.46	6.43
	5570	Mississippian	1.63	3.53	5.16
	5574	Mississippian	3.64	1.48	5.12
	5576	Mississippian	4.59	1.01	5.60

	5578	Mississippian	3.04	1.08	4.12
	5582	Mississippian	0.98	0.88	1.86
	5583	Mississippian	4.17	0.83	5.00
	5588	Mississippian	5.22	0.94	6.16
	5589	Mississippian	5.32	1.14	6.46
	5591	Mississippian	6.39	1.00	7.39
	5631	Mississippian	4.93	0.75	5.68
	5633	Mississippian	4.40	1.27	5.67
	5698	Mississippian	2.84	1.18	4.02
	5701	Mississippian	3.05	2.15	5.20
	5716	Mississippian	3.18	0.68	3.86
	5716	Mississippian	2.29	0.94	3.23
	5720	Mississippian	5.03	0.92	5.95
	5736	Mississippian	5.32	1.50	6.82
	5746	Mississippian	4.75	1.13	5.88
	5757	Mississippian	0.88	1.15	2.03
	5765	Mississippian	7.94	0.65	8.59
	5801	Mississippian	3.70	0.88	4.58
	5820	Mississippian	0.07	1.96	2.03

APPENDIX II

Rock-Eval Pyrolysis Data and Pyrograms

APPENDIX II

Table 2. Rock-Eval parameters data

Well Name	Formation	Depth(ft)	Carbonate(wt %)	TOC (wt%)	S1 (mgHC/g)	S2 (mgHC/g)	S3 (mgCO2/g)	T_{max}
Ad-Lo	Mississippian	5570	34.06	1.33	1.15	3.06	0.51	443
Ad-Lo	Mississippian	5589	42.42	0.99	0.58	2.46	0.41	445
Ad-Lo	Mississippian	5633	36.59	1.17	1.09	2.97	0.47	444
Ad-Lo	Mississippian	5701	39.50	1.29	0.82	3.27	0.43	440
El-Py	Mississippian	4365	44.50	2.07	0.83	10.23	0.45	431
El-Py	Mississippian	4462	55.07	0.87	0.67	3.01	0.46	440
Wd-Py	Woodford	3367	3.85	7.41	3.97	44.45	0.43	442
Wd-Py	Woodford	3381	6.30	8.34	3.23	42.46	0.45	436
Wi-Py	Mississippian	5144	22.14	1.93	0.71	7.30	0.35	437
Wi-Py	Mississippian	5157	38.04	2.58	1.27	11.73	0.58	441
Wi-Py	Mississippian	5162	46.06	1.25	0.59	4.19	0.38	442
Wi-Py	Mississippian	5185	21.36	1.03	0.29	2.16	0.50	435
Wi-Py	Mississippian	5271	35.89	0.83	0.43	2.39	0.48	443
Wi-Py	Mississippian	5281	40.21	1.30	0.77	3.85	0.47	444

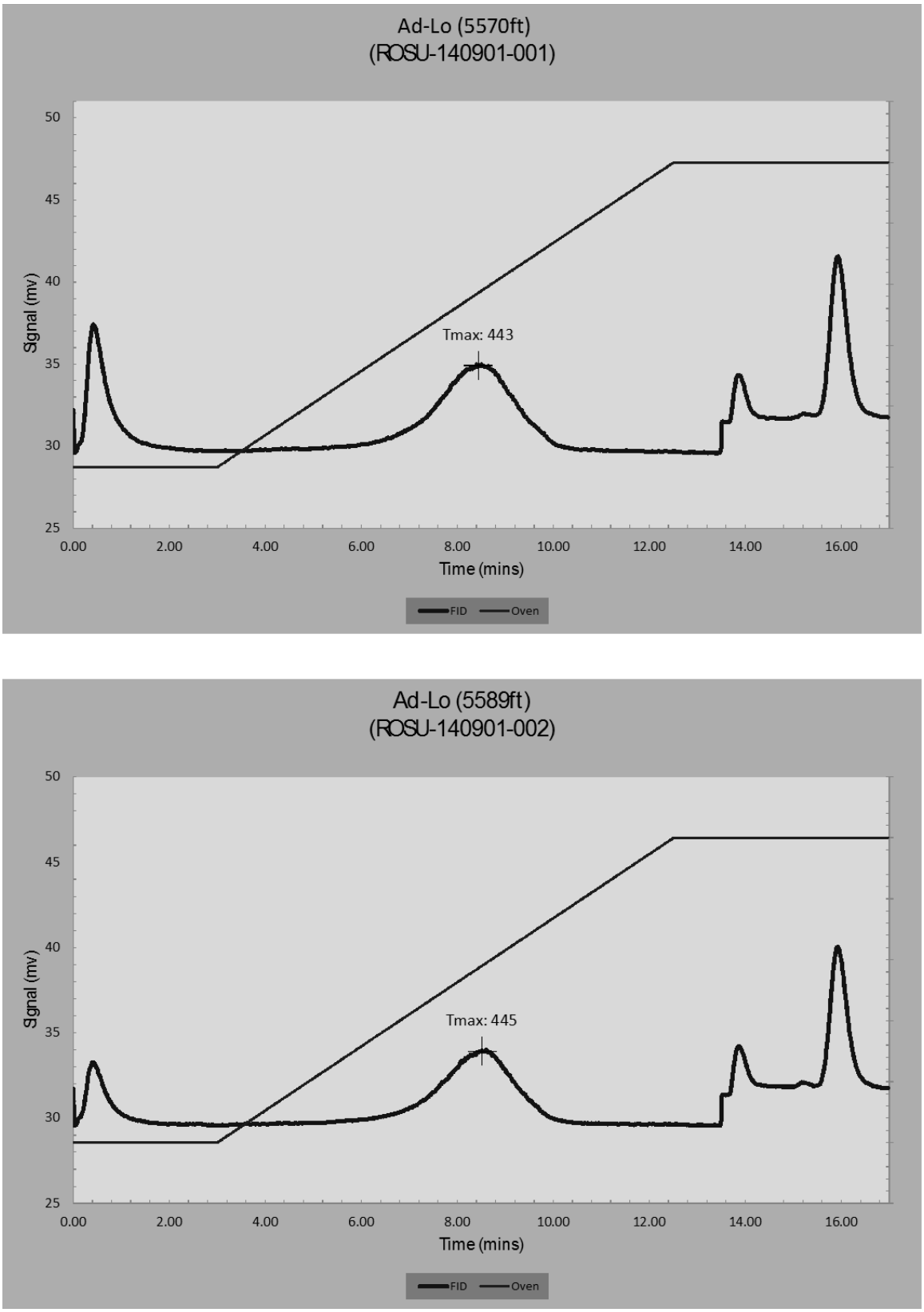

Figure 1 Pyrograms of both Mississippian and Woodford samples

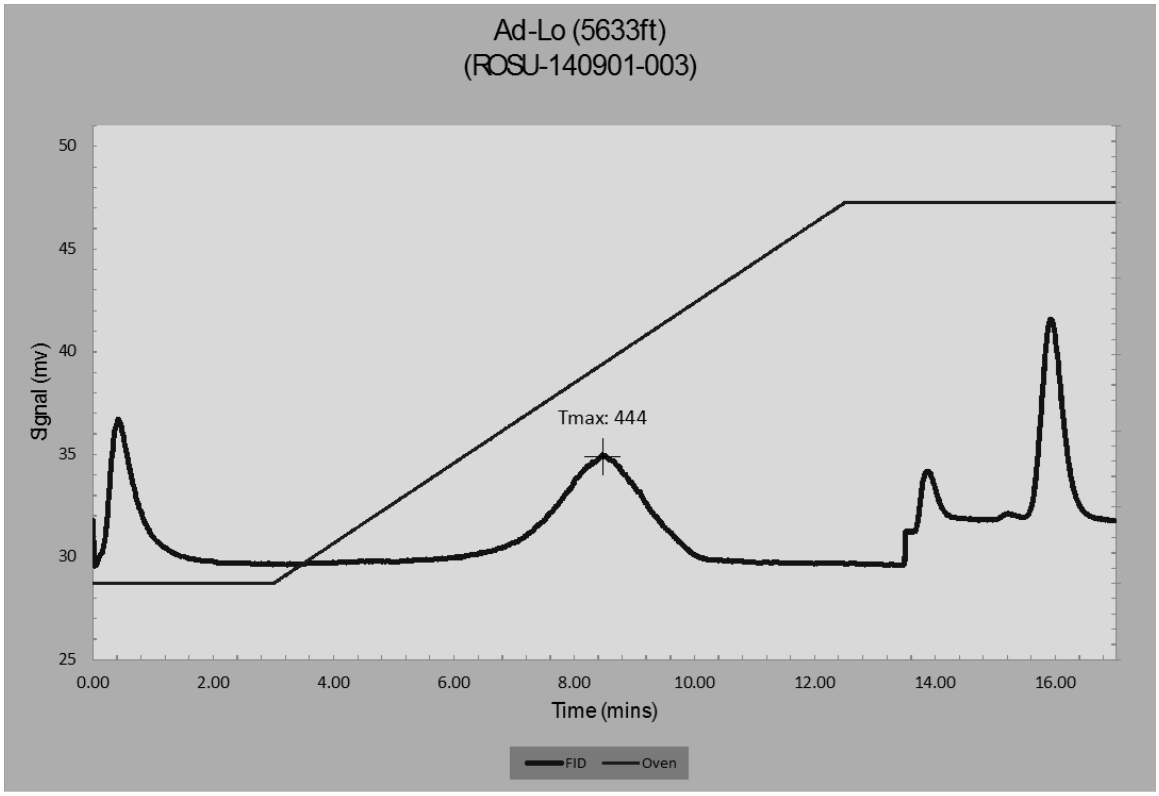

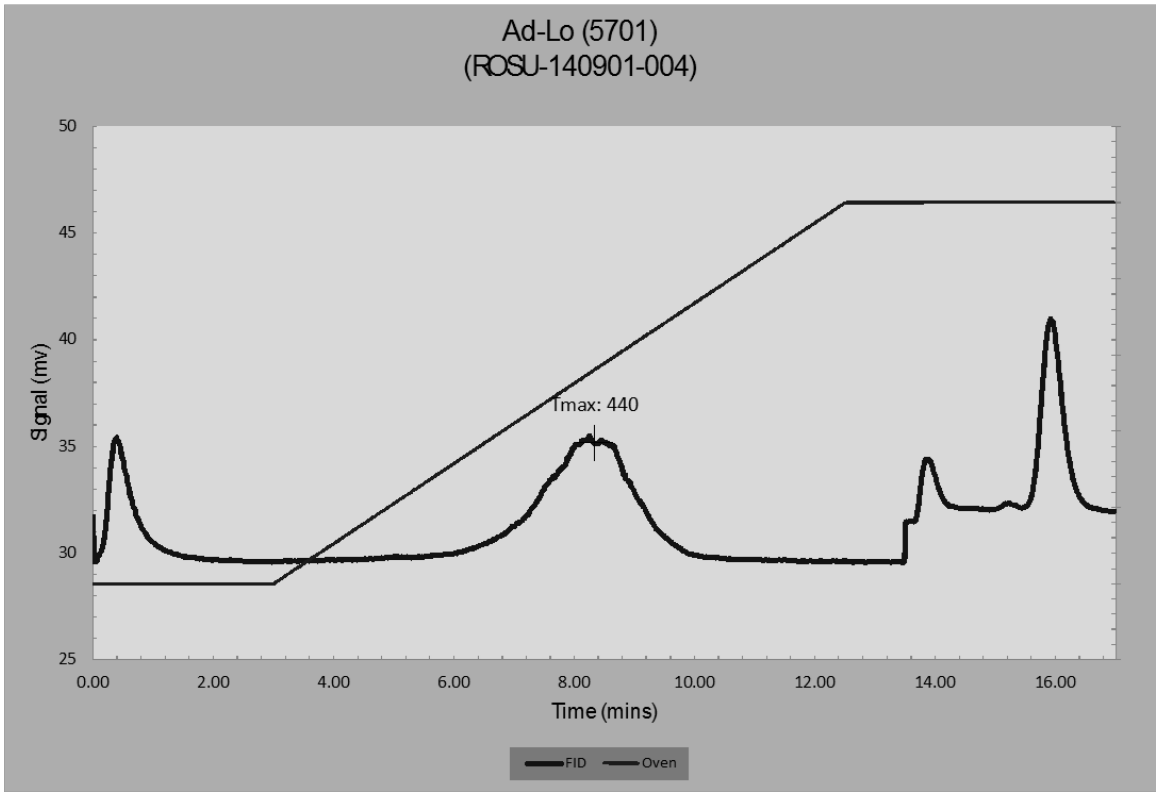

Figure 1 continued

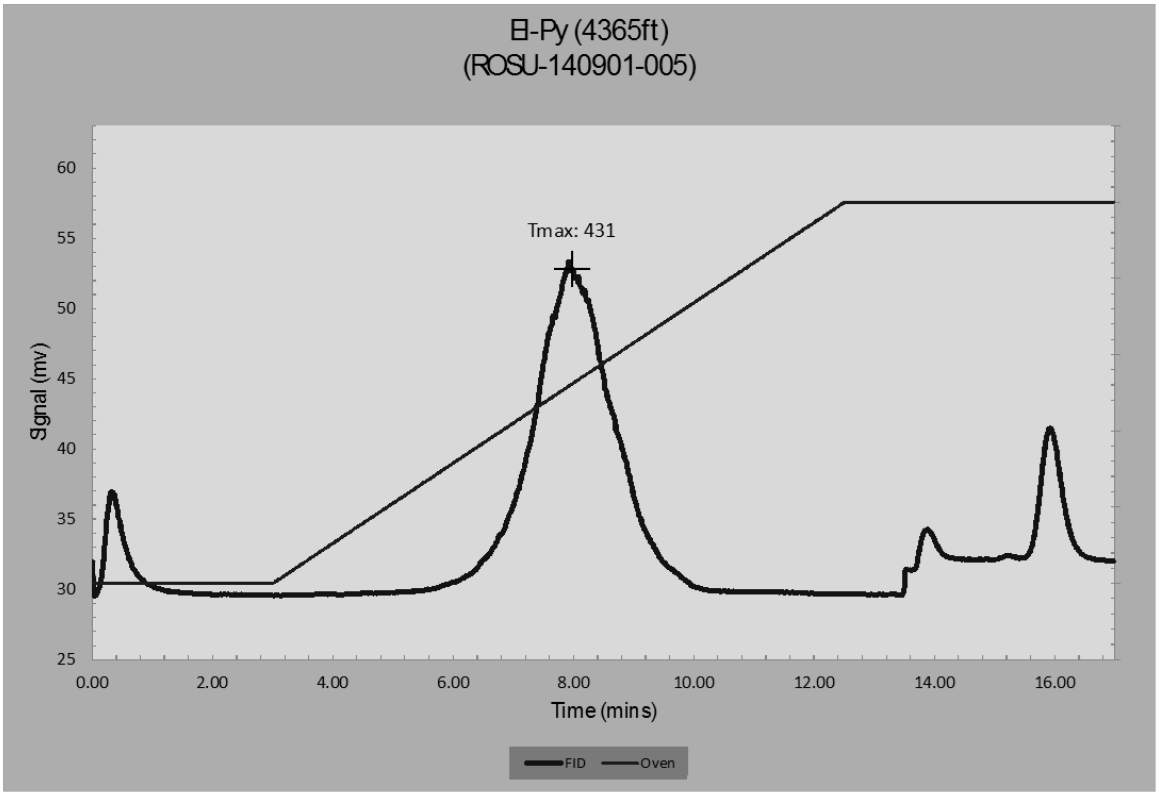

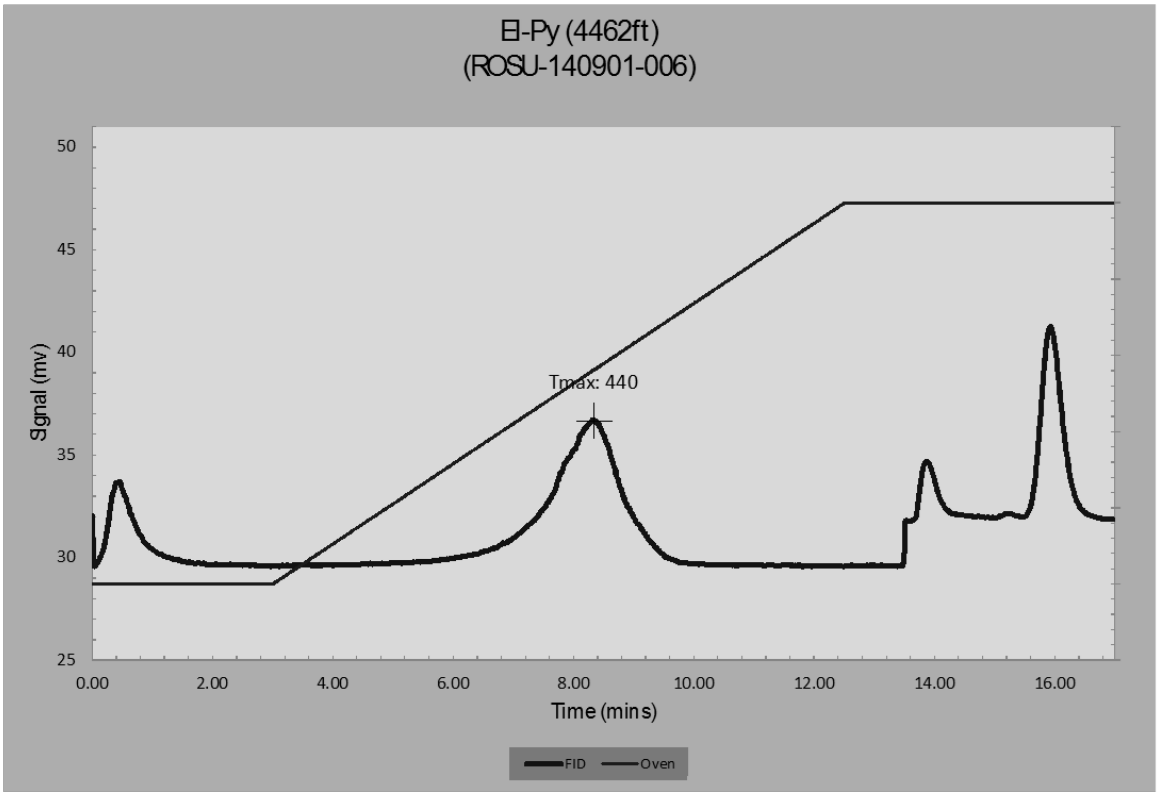

Figure 1 continued

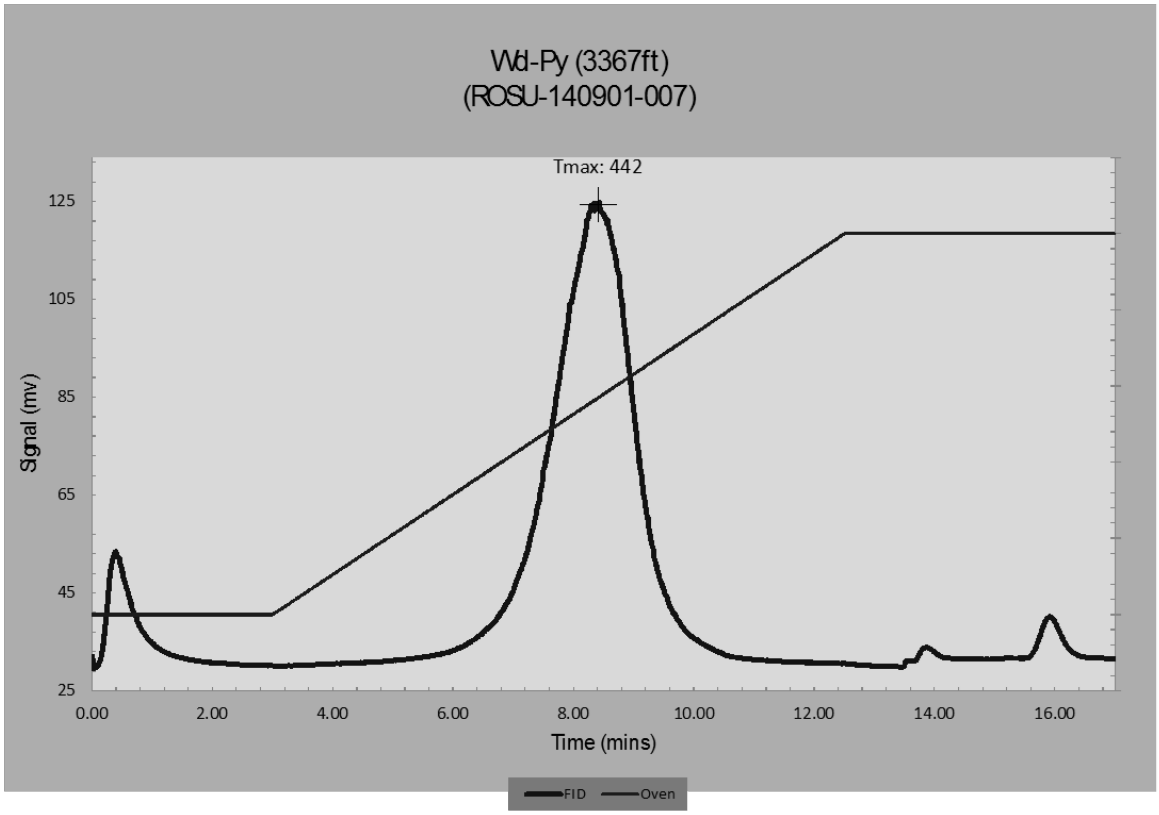

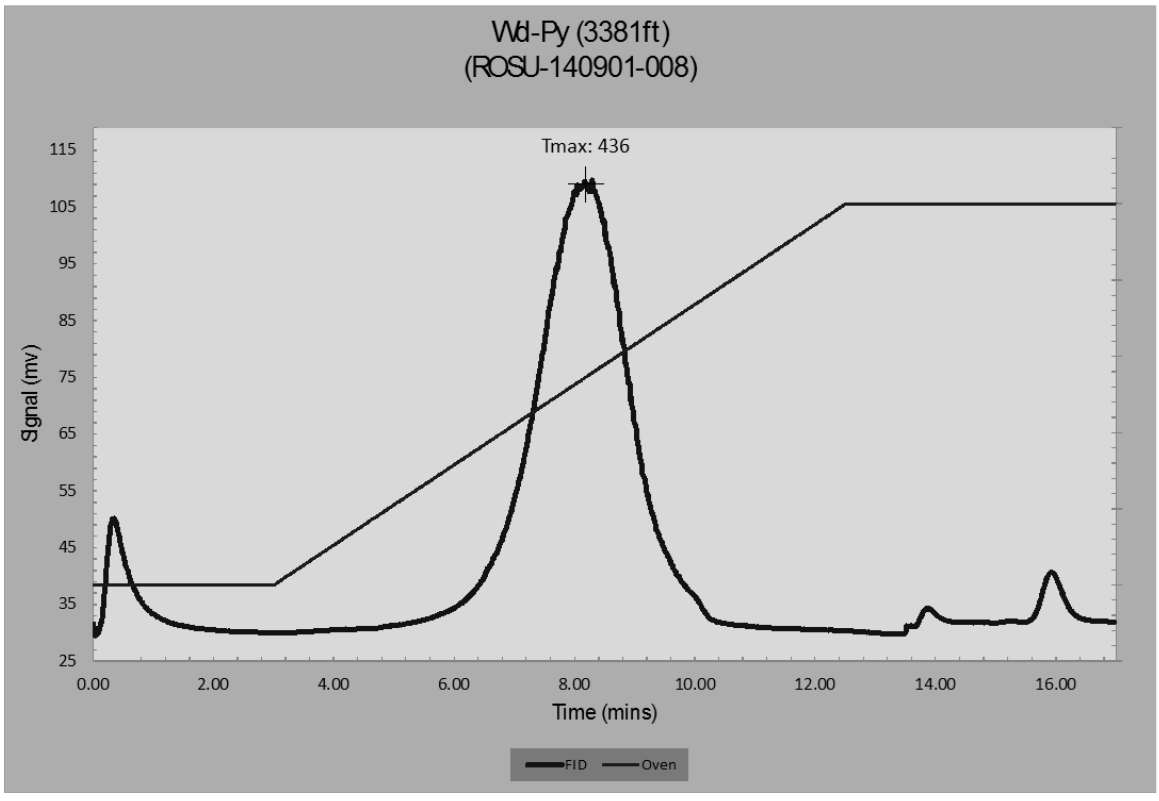

Figure 1 continued

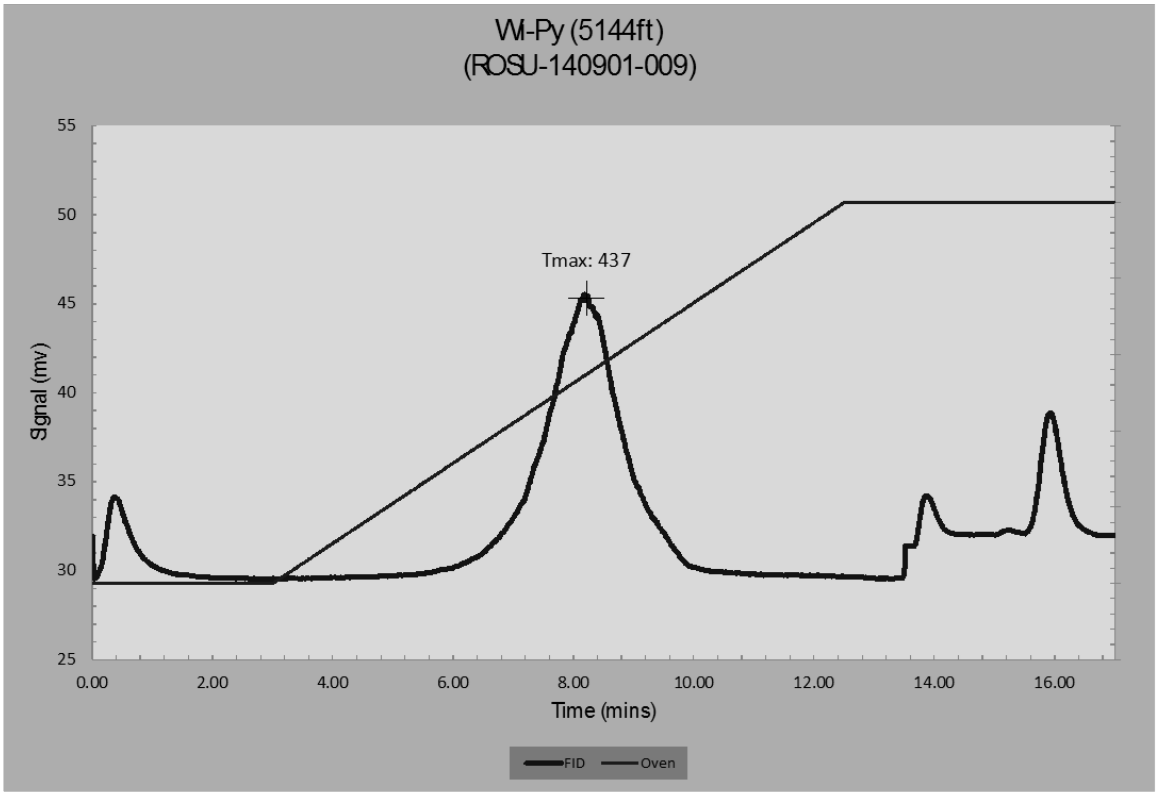

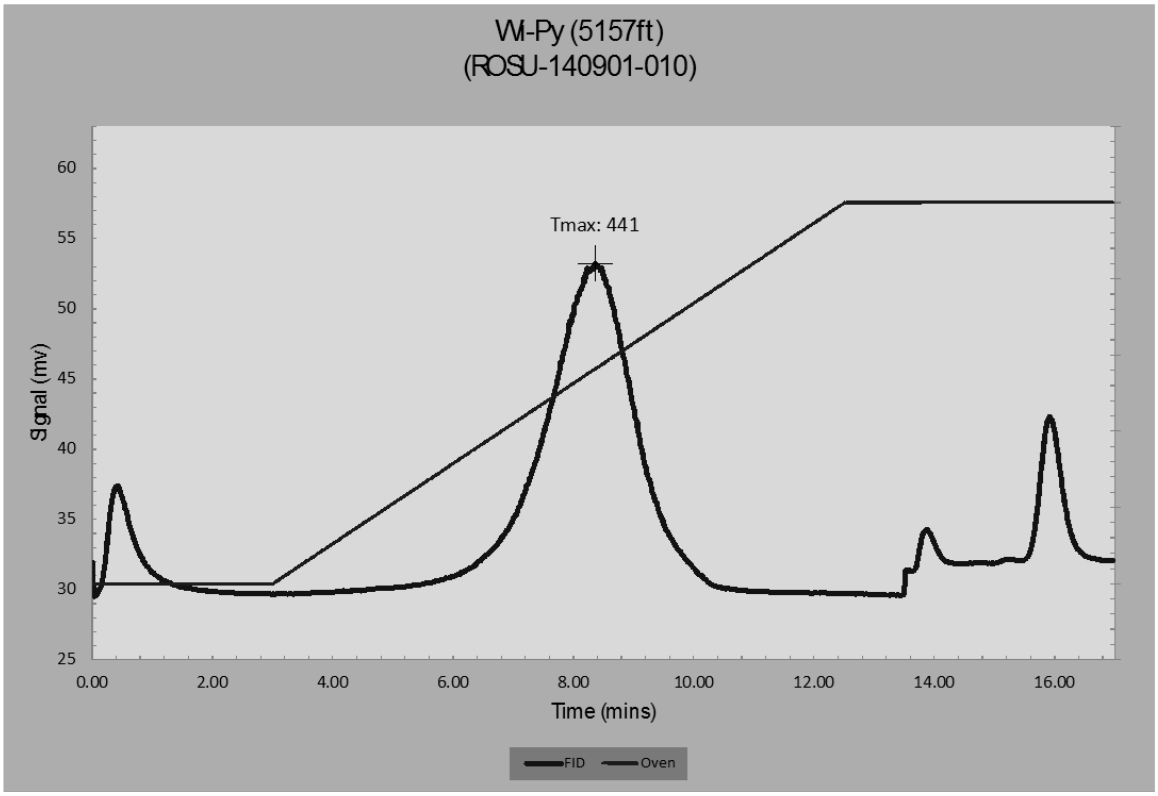

Figure 1 continued

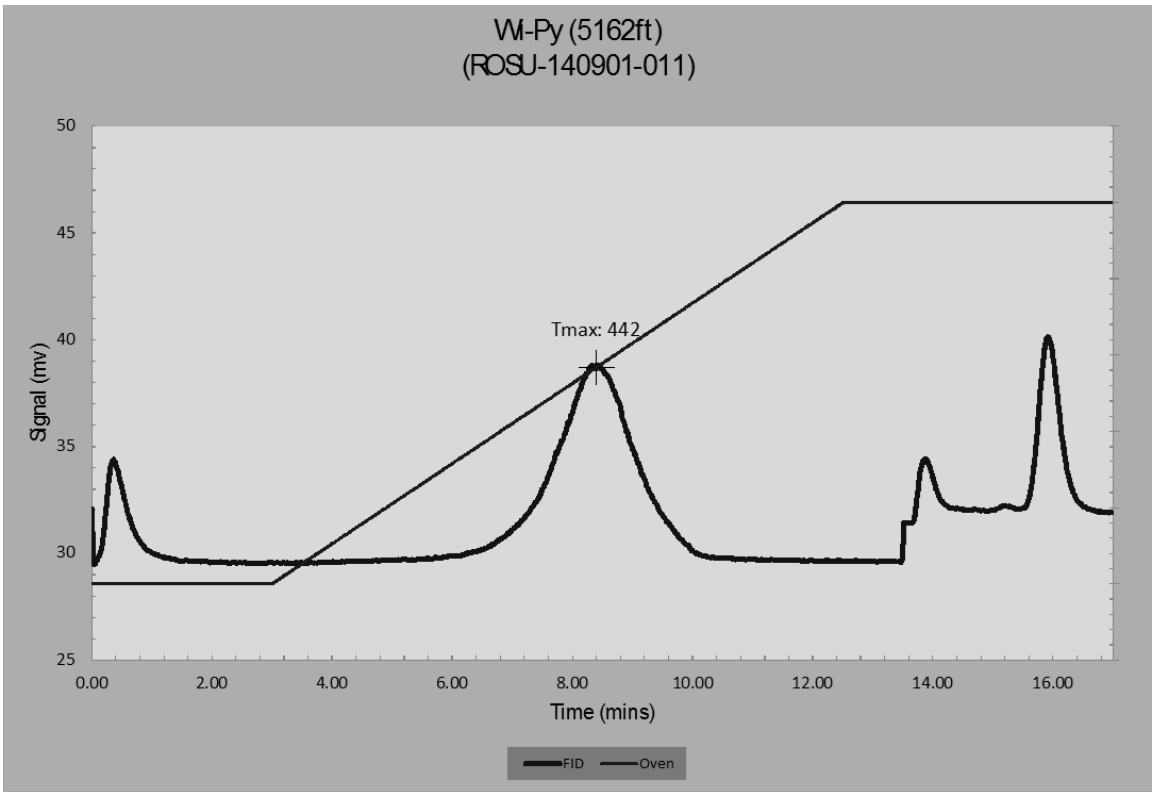

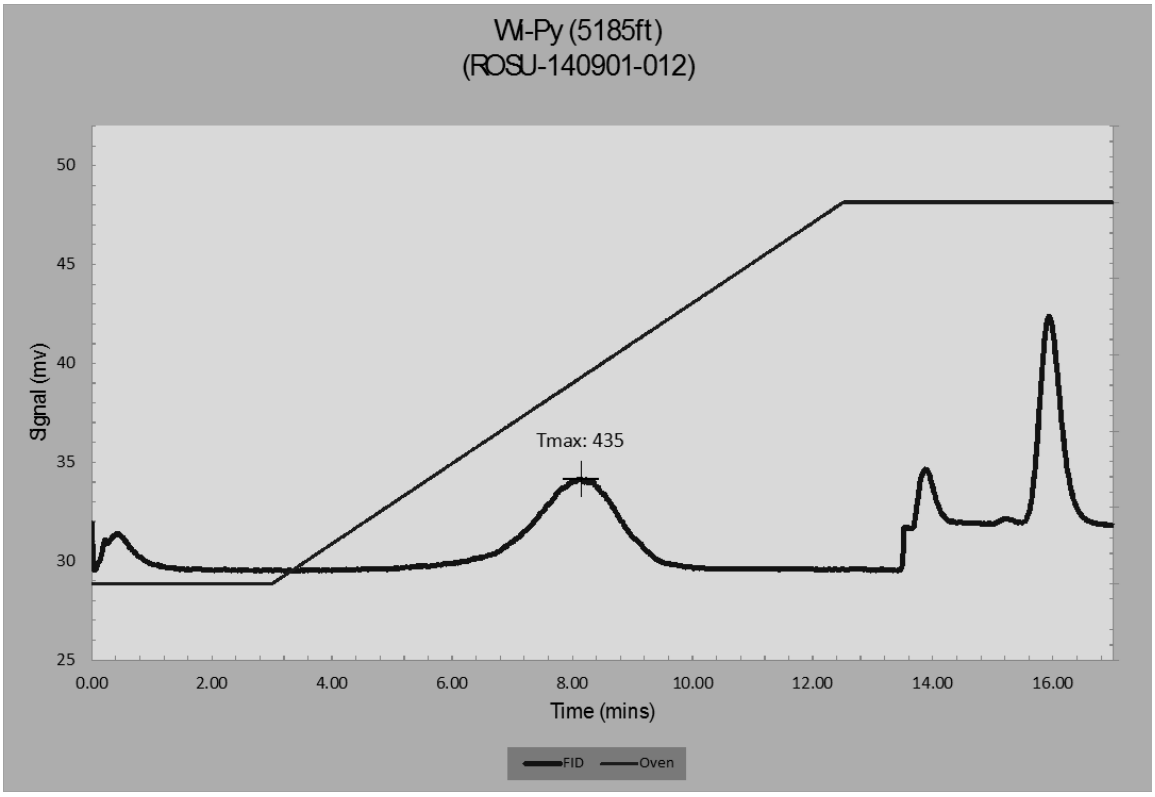

Figure 1 continued

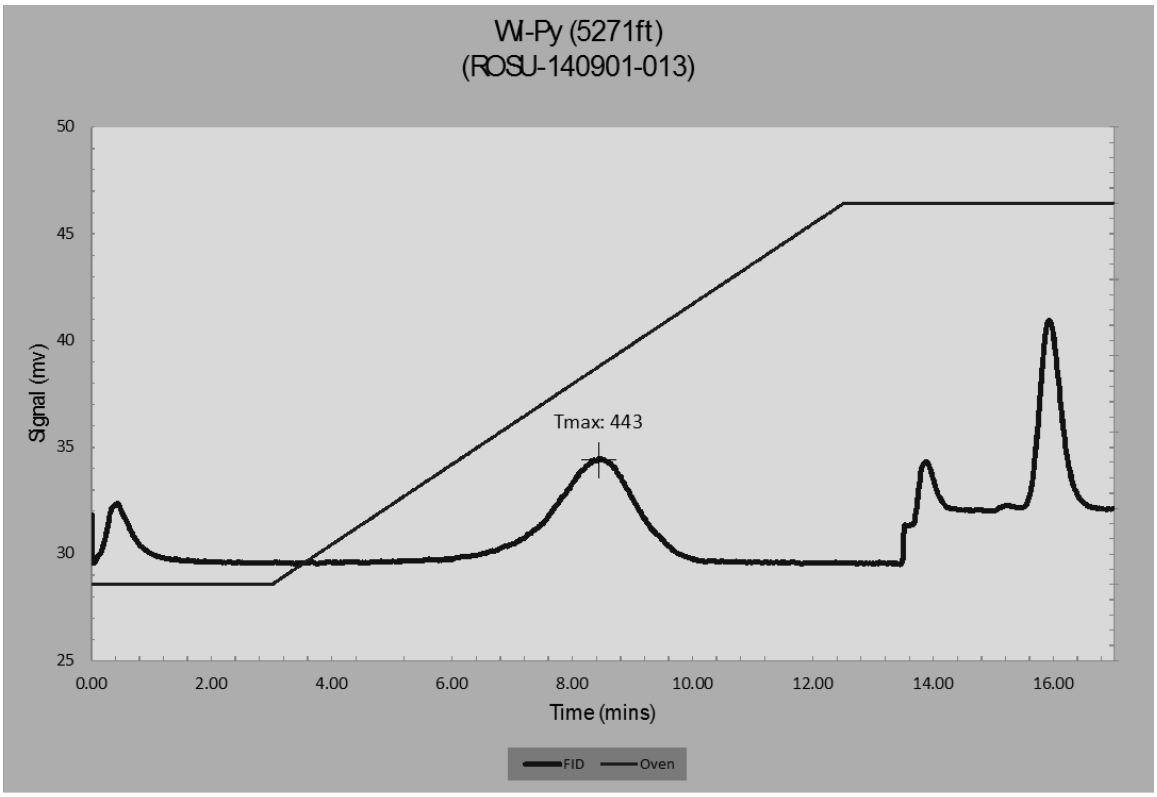

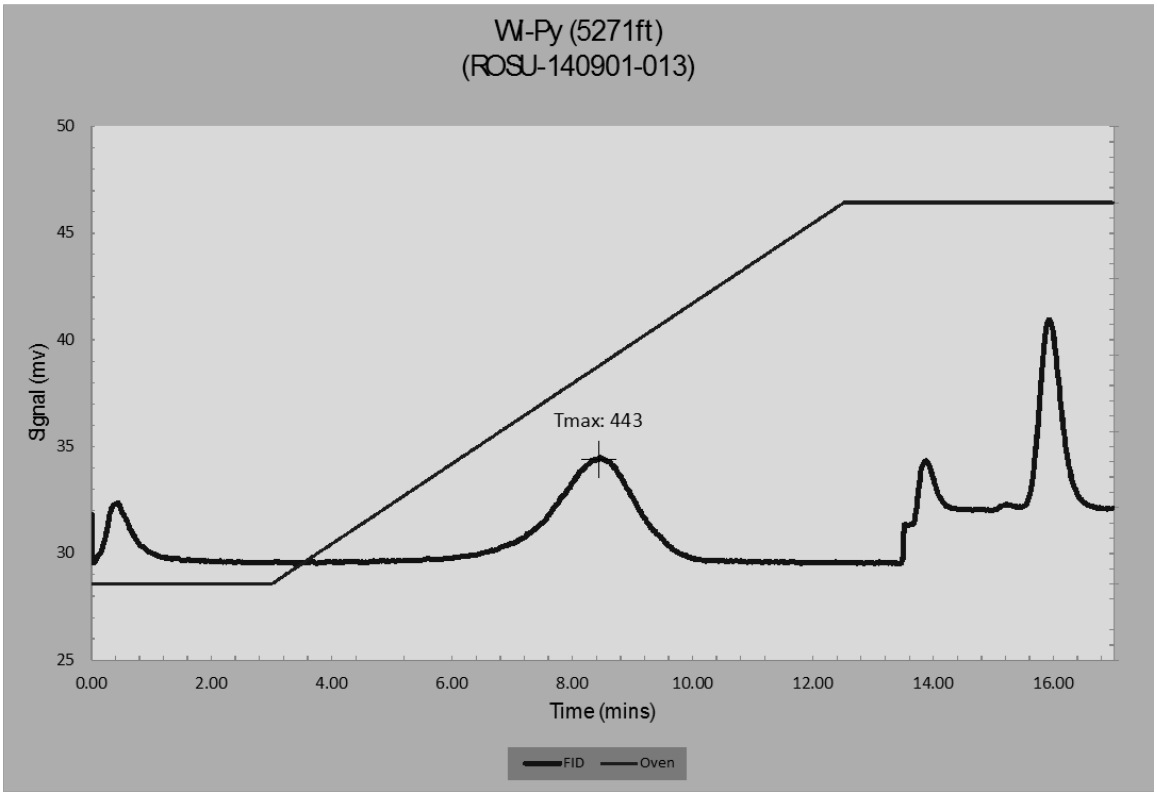

Figure 1 continued

APPENDIX III

Photomicrographs and Vitrinite Reflectance Reports

APPENDIX III

Organic Petrography

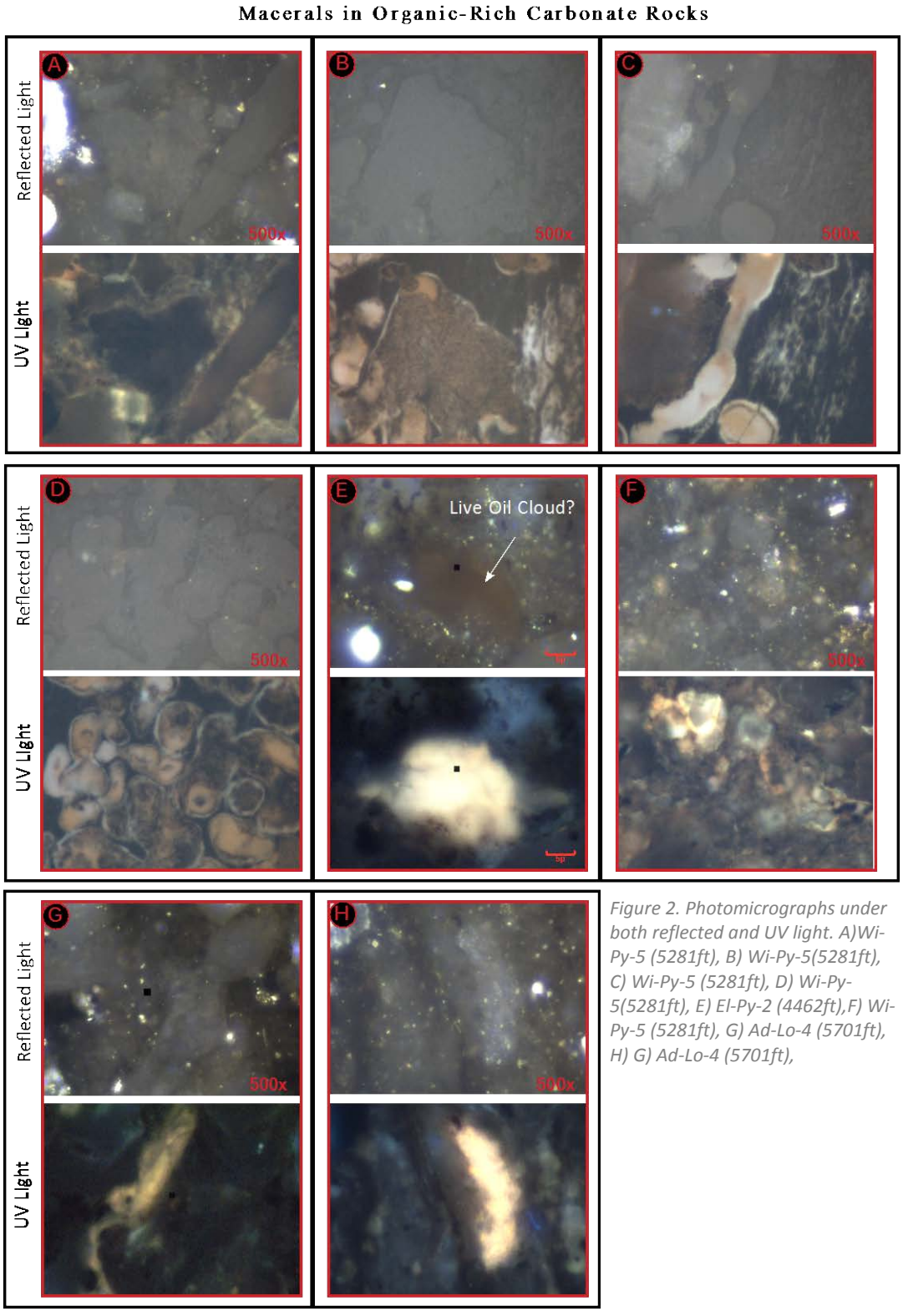

Figure 2. Photomicrographs under both reflected and UV light. A)Wi-Py-5 (5281ft), B) Wi-Py-5(5281ft), C) Wi-Py-5 (5281ft), D) Wi-Py-5(5281ft), E) El-Py-2 (4462ft),F) Wi-Py-5 (5281ft), G) Ad-Lo-4 (5701ft), H) G) Ad-Lo-4 (5701ft),

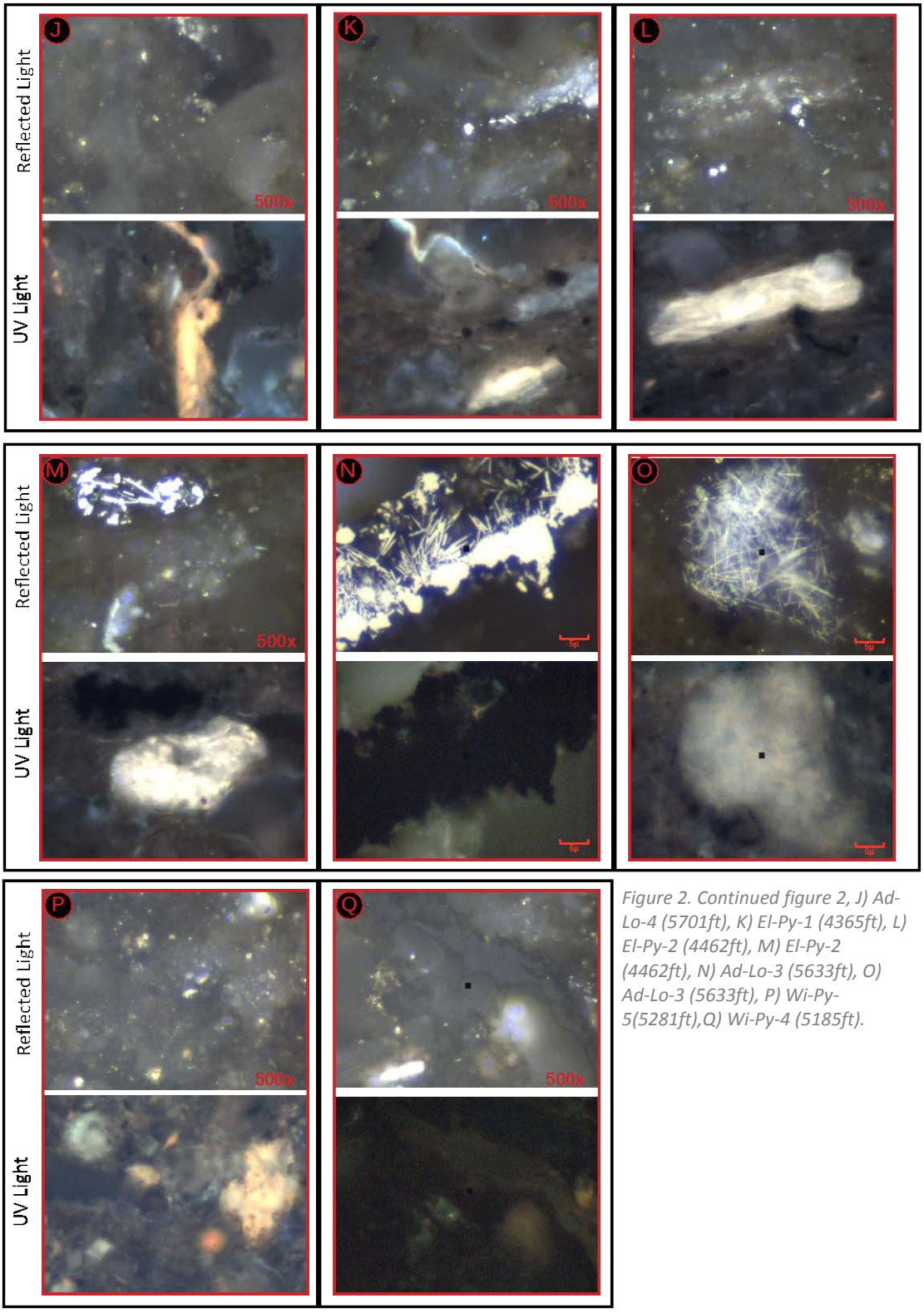

Figure 2. Continued figure 2, J) Ad-Lo-4 (5701ft), K) El-Py-1 (4365ft), L) El-Py-2 (4462ft), M) El-Py-2 (4462ft), N) Ad-Lo-3 (5633ft), O) Ad-Lo-3 (5633ft), P) Wi-Py-5(5281ft),Q) Wi-Py-4 (5185ft).

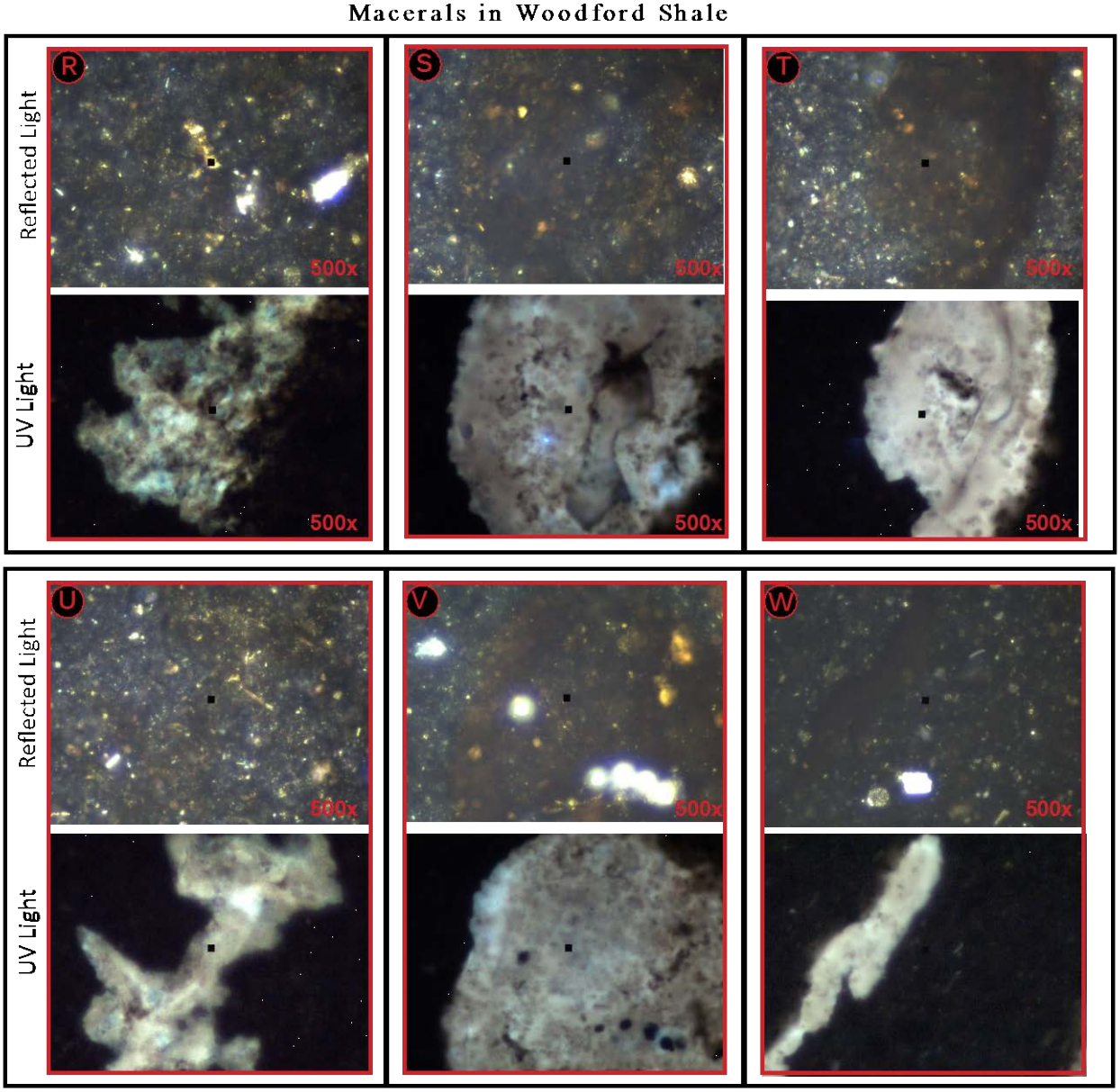

Figure 2. Continued figure 2, R-T) Wd-Py-1 (3368ft), U-W) Wd-Py-2 (3381ft).

DISPERSED VITRINITE REFLECTANCE REPORT

SAMPLE INFORMATION

Submitted by:	Ibrahim
Date Submitted:	07-14-14
Project:	M.Sc. Thesis
Sample ID:	**Sample Ad-Lo-1**
Lab ID:	OKState
Sample Type:	Core
Date Analyzed:	07-13-14
Operator:	Ibrahim
Protocol:	ASTM D7708

RESULTS

No. Measurements:	23
maceral type:	Vitrnite & Solid Bitumen
mean R_o (%):	0.77
s.d.:	0.11

Example Photograph:

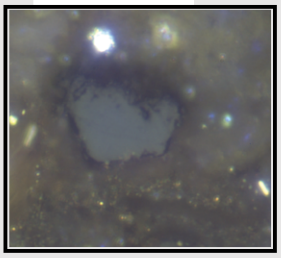

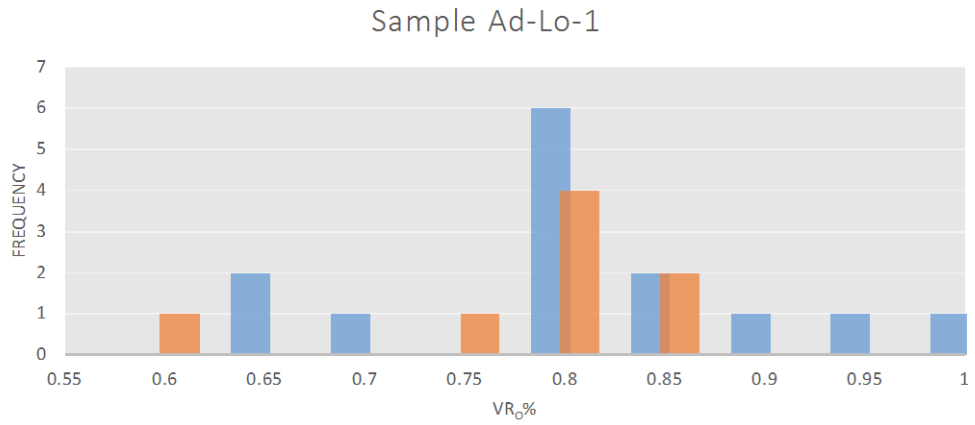

DATA

0.92	0.78	0.66	0.77	0.60	0.76
0.88	0.78	0.85	1.00	0.80	0.78
0.81	0.95	0.62	0.75	0.82	0.79
0.75	0.75	0.60	0.58	0.80	

min: 0.58 max: 1.00

COMMENT

The sample is rich in organics with 8 bitumen fragments and 19 vitrinite clasts to measure. Reflectance measurements of the solid bitumen were corrected to vitrinite reflectance equivalence using (Landis & Castano 1994) equation. Under UV light the sample showed bright yellow and light orange fluorescence of liptinite mainly alginite. Inertinite maceral also appear in very low abundance in form of fusinite and semifusinite fragments. Polishing quality 2B.

DISPERSED VITRINITE REFLECTANCE REPORT

SAMPLE INFORMATION

Submitted by:	Ibrahim
Date Submitted:	07-14-14
Project:	M.Sc. Thesis
Sample ID:	**Sample Ad-Lo-2**
Lab ID:	OKState
Sample Type:	Core
Date Analyzed:	07-13-14
Operator:	Ibrahim
Protocol:	ASTM D7708

RESULTS

No. Measurements:	24
maceral type:	Vitrnite & Solid Bitumen
mean R_o (%):	0.84
s.d.:	0.11

Example Photograph:

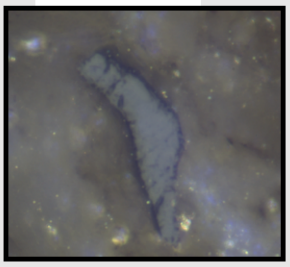

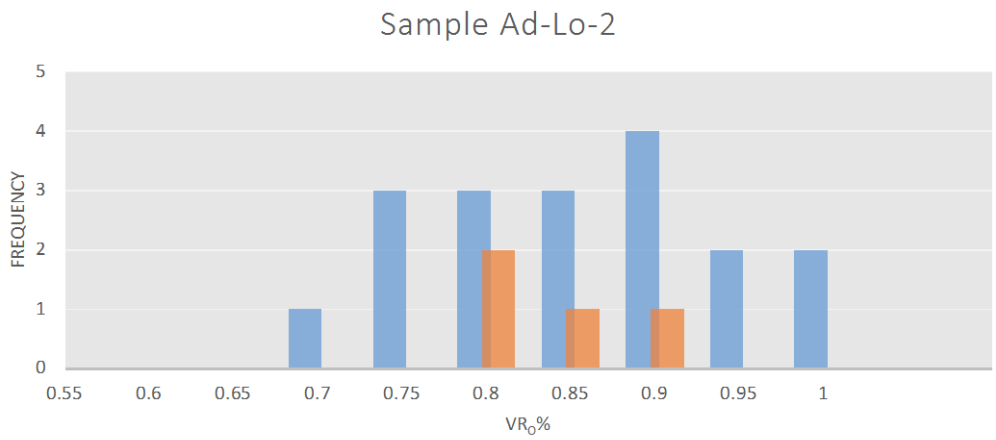

DATA

1.03	0.86	0.77	0.83	0.80
0.80	0.65	0.89	0.93	0.74
0.92	0.84	1.00	0.99	0.73
0.89	0.88	1.07	0.76	0.74

min: 0.65 max: 1.07

COMMENT

The sample is rich in organics with 4 bitumen fragments and 20 vitrinite clasts to measure. Reflectance measurements of the solid bitumen were corrected to vitrinite reflectance equivalence using (Landis & Castano 1994) equation. Under UV light the sample showed bright yellow and light orange fluorescence of liptinite mainly alginite. Inertinite maceral also appear in very low abundance in form of fusinite and semifusinite fragments. Polishing quality 2B.

DISPERSED VITRINITE REFLECTANCE REPORT

SAMPLE INFORMATION

Submitted by:	Ibrahim
Date Submitted:	07-14-14
Project:	M.Sc. Thesis
Sample ID:	**Sample Ad-Lo-3**
Lab ID:	OKState
Sample Type:	Core
Date Analyzed:	07-13-14
Operator:	Ibrahim
Protocol:	ASTM D7708

RESULTS

No. Measurements:	27
maceral type:	Vitrnite & Solid Bitumen
mean R_o (%):	0.81
s.d.:	0.11

Example Photograph:

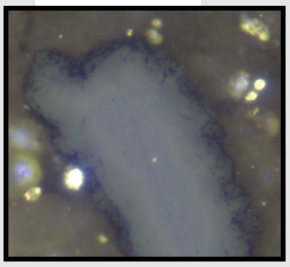

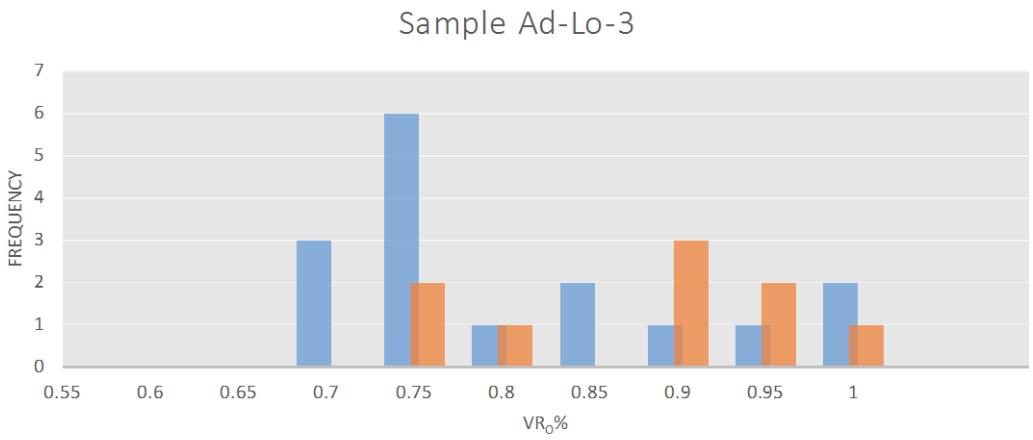

DATA

0.66	0.66	0.72	0.75	0.96	0.68	0.87
0.77	0.83	0.72	0.97	1.04	0.82	0.82
0.73	1.02	0.68	0.84	0.90	0.89	0.66
0.74	0.93	0.72	0.85	0.81	0.73	

min: 0.66 max: 1.04

COMMENT

The sample is rich in organics with 9 bitumen fragments and 18 vitrinite clasts to measure. Reflectance measurements of the solid bitumen were corrected to vitrinite reflectance equivalence using (Landis & Castano 1994) equation. Under UV light the sample showed bright yellow and light orange fluorescence of liptinite mainly alginite. Inertinite maceral also appear in very low abundance in form of fusinite and semifusinite fragments. Polishing quality 2B.

DISPERSED VITRINITE REFLECTANCE REPORT

SAMPLE INFORMATION

Submitted by:	Ibrahim
Date Submitted:	07-14-14
Project:	M.Sc. Thesis
Sample ID:	**Sample Ad-Lo-4**
Lab ID:	OKState
Sample Type:	Core
Date Analyzed:	07-13-14
Operator:	Ibrahim
Protocol:	ASTM D7708

RESULTS

No. Measurements:	29
maceral type:	Vitrnite & Solid Bitumen
mean R_o (%):	0.82
s.d.:	0.13

Example Photograph:

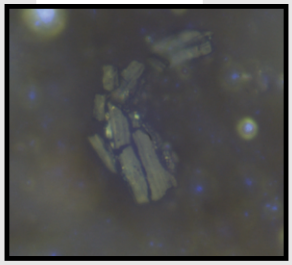

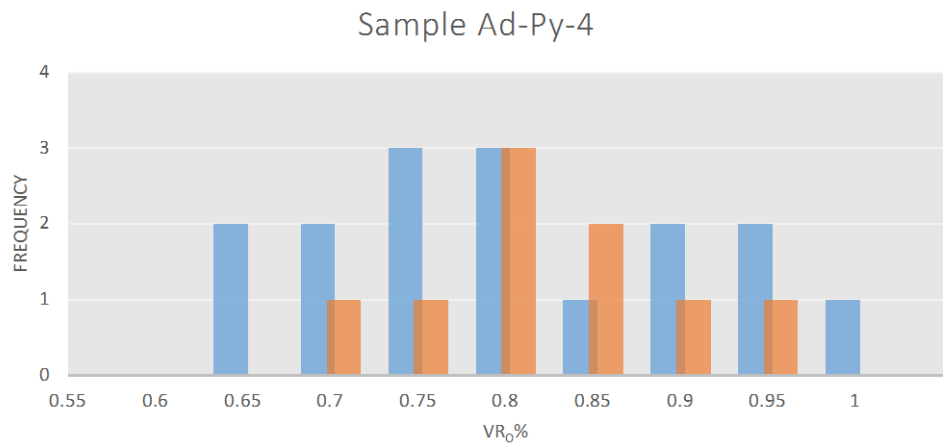

DATA

0.68	0.80	0.76	0.68	0.87	0.79	0.75	0.84
0.72	0.96	0.94	0.73	0.95	0.89	0.85	
1.03	0.95	0.97	0.62	0.93	0.76	0.73	
1.04	0.63	0.79	0.71	0.69	0.80	0.85	

min: 0.62 max: 1.04

COMMENT

The sample is rich in organics with 9 bitumen fragments and 20 vitrinite clasts to measure. Reflectance measurements of the solid bitumen were corrected to vitrinite reflectance equivalence using (Landis & Castano 1994) equation. Under UV light the sample showed bright yellow and light orange fluorescence of liptinite mainly alginite. Inertinite maceral also appear in very low abundance in form of fusinite and semifusinite fragments. Polishing quality 2B.

DISPERSED VITRINITE REFLECTANCE REPORT

SAMPLE INFORMATION

Submitted by:	Ibrahim
Date Submitted:	07-14-14
Project:	M.Sc. Thesis
Sample ID:	**Sample Ad-Lo-5**
Lab ID:	OKState
Sample Type:	Core
Date Analyzed:	07-13-14
Operator:	Ibrahim
Protocol:	ASTM D7708

RESULTS

No. Measurements:	24
maceral type:	Vitrnite & Solid Bitumen
mean R_o (%):	0.86
s.d.:	0.12

Example Photograph:

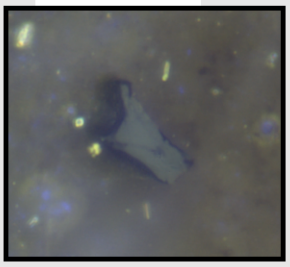

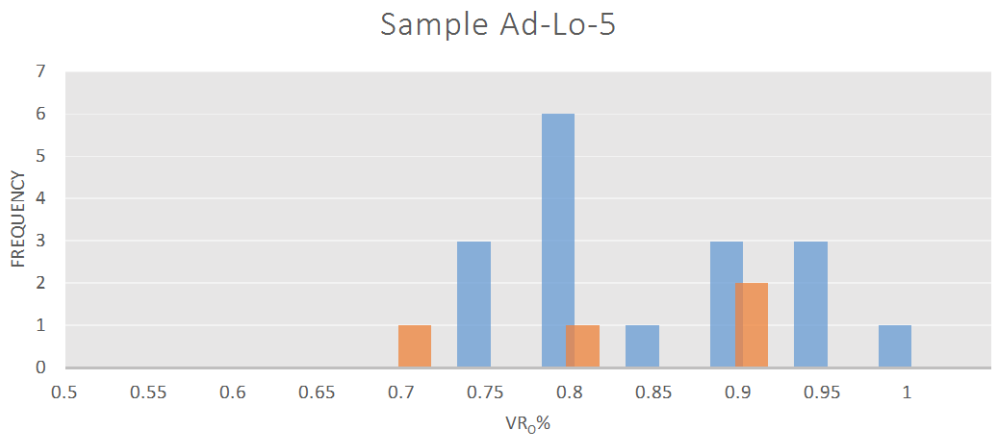

DATA

Vitrinite Solid Bitumen Corrected

0.73	0.91	0.88	0.74	0.87	0.87
0.90	0.76	0.85	0.80	1.16	0.67
1.08	0.80	0.95	0.85	0.75	0.85
0.95	0.80	0.79	0.79	1.13	0.77

min: 0.67 max: 1.16

COMMENT

The sample is rich in organics with 4 bitumen fragments and 20 vitrinite clasts to measure. Reflectance measurements of the solid bitumen were corrected to vitrinite reflectance equivalence using (Landis & Castano 1994) equation. Under UV light the sample showed bright yellow and light orange fluorescence of liptinite mainly alginite. Inertinite maceral also appear in very low abundance in form of fusinite and semifusinite fragments. Polishing quality 2B.

DISPERSED VITRINITE REFLECTANCE REPORT

SAMPLE INFORMATION

Submitted by:	Ibrahim
Date Submitted:	07-14-14
Project:	M.Sc. Thesis
Sample ID:	**Sample El-Py-1**
Lab ID:	OKState
Sample Type:	Core
Date Analyzed:	07-13-14
Operator:	Ibrahim
Protocol:	ASTM D7708

RESULTS

No. Measurements:	23
maceral type:	Vitrnite & Solid Bitumen
mean R_o (%):	0.75
s.d.:	0.10

Example Photograph:

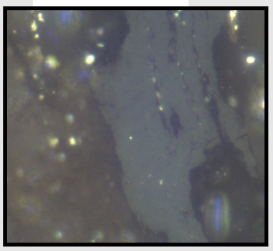

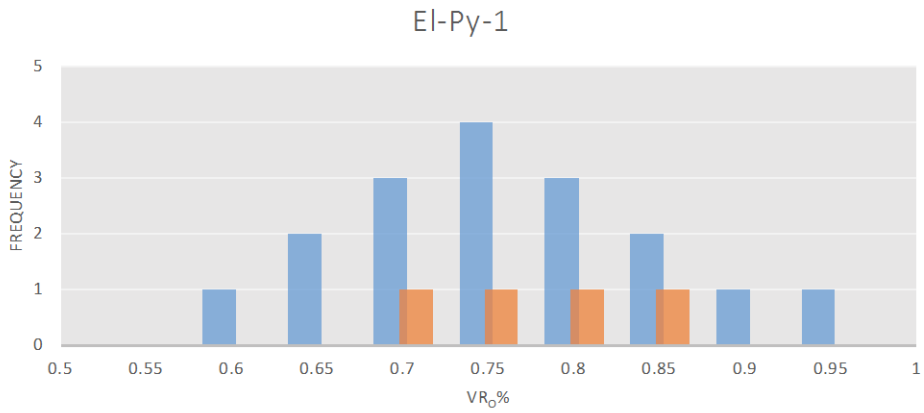

DATA

0.88	0.74	0.75	0.66	0.73	0.80
0.75	0.70	0.97	0.87	0.78	0.67
0.66	0.79	0.83	0.75	0.56	0.79
0.63	0.85	0.76	0.91	0.62	

min: 0.56 max: 0.97

COMMENT

The sample is rich in organics with 4 bitumen fragments and 19 vitrinite clasts to measure. Reflectance measurements of the solid bitumen were corrected to vitrinite reflectance equivalence using (Landis & Castano 1994) equation. Under UV light the sample showed bright yellow and light orange fluorescence of liptinite mainly alginite. Inertinite maceral also appear in very low abundance in form of fusinite and semifusinite fragments. Polishing quality 2B.

DISPERSED VITRINITE REFLECTANCE REPORT

SAMPLE INFORMATION

Submitted by:	Ibrahim
Date Submitted:	07-14-14
Project:	M.Sc. Thesis
Sample ID:	**Sample El-Py-2**
Lab ID:	OKState
Sample Type:	Core
Date Analyzed:	07-13-14
Operator:	Ibrahim
Protocol:	ASTM D7708

RESULTS

No. Measurements:	22
maceral type:	Vitrnite & Solid Bitumen
mean R_o (%):	0.85
s.d.:	0.11

Example Photograph:

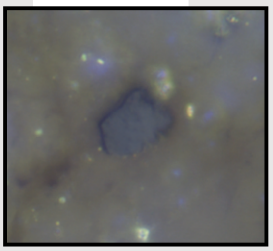

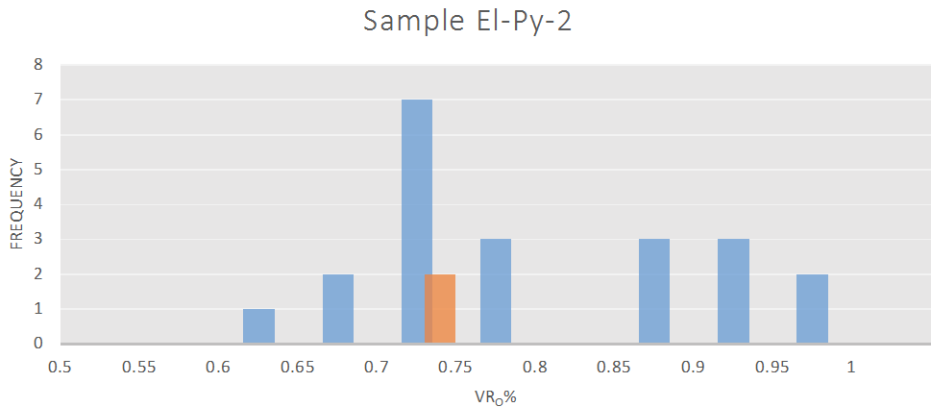

DATA

0.88	0.74	0.75	0.66	0.73	0.80
0.75	0.70	0.97	0.87	0.78	0.67
0.66	0.79	0.83	0.75	0.56	0.79
0.63	0.85	0.76	0.91	0.62	

min: 0.56 max: 0.97

COMMENT

The sample is rich in organics with 2 bitumen fragments and 20 vitrinite clasts to measure. Reflectance measurements of the solid bitumen were corrected to vitrinite reflectance equivalence using (Landis & Castano 1994) equation. Under UV light the sample showed bright yellow and light orange fluorescence of liptinite mainly alginite. Inertinite maceral also appear in very low abundance in form of fusinite and semifusinite fragments. Polishing quality 2B.

DISPERSED VITRINITE REFLECTANCE REPORT

SAMPLE INFORMATION

Submitted by:	Ibrahim
Date Submitted:	07-14-14
Project:	M.Sc. Thesis
Sample ID:	**Sample Wi-Py-1**
Lab ID:	OKState
Sample Type:	Core
Date Analyzed:	07-13-14
Operator:	Ibrahim
Protocol:	ASTM D7708

RESULTS

No. Measurements:	31
maceral type:	Vitrnite & Solid Bitumen
mean R_o (%):	0.74
s.d.:	0.06

Example Photograph:

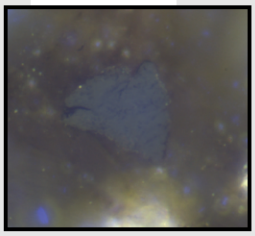

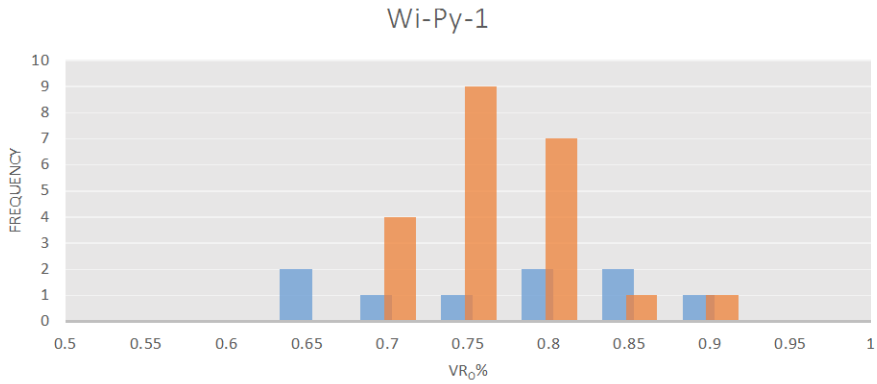

DATA

0.67	0.71	0.73	0.75	0.77	0.82	0.65	0.85
0.69	0.71	0.74	0.75	0.79	0.86	0.74	0.85
0.69	0.72	0.75	0.75	0.79	0.61	0.76	0.86
0.70	0.72	0.75	0.77	0.79	0.64	0.77	

min: 0.61 max: 0.86

COMMENT

The sample is rich in soild bitume with 22 bitumen fragments and 9 vitrinite clasts to measure. Reflectance measurements of the solid bitumen were corrected to vitrinite reflectance equivalence using (Landis & Castano 1994) equation. Under UV light the sample showed bright yellow and light orange fluorescence of liptinite mainly alginite. Inertinite maceral also appear in very few abundance in form of fusinite and semifusinite. Polishing quality 2B.

DISPERSED VITRINITE REFLECTANCE REPORT

SAMPLE INFORMATION

Submitted by:	Ibrahim
Date Submitted:	07-14-14
Project:	M.sc. Thesis
Sample ID:	**Sample Wi-Py-2**
Lab ID:	OKState
Sample Type:	Core
Date Analyzed:	07-13-14
Operator:	Ibrahim
Protocol:	ASTM D7708

RESULTS

No. Measurements:	44
maceral type:	Vitrnite & Solid Bitumen
mean R_o (%):	0.78
s.d.:	0.08

Example Photograph:

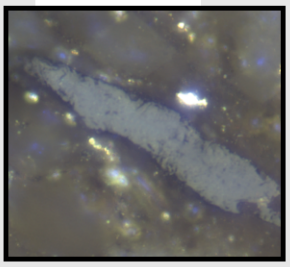

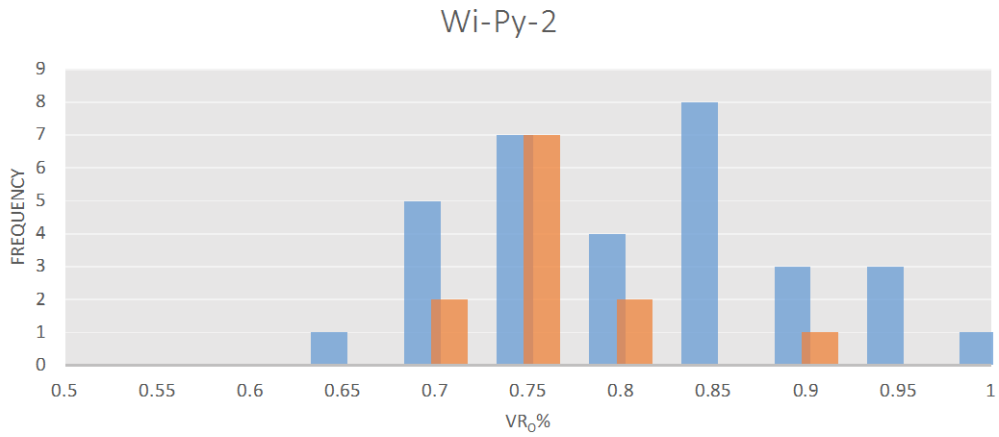

DATA

0.85	0.84	0.84	0.77	0.91	0.72	0.70	0.69	0.71	0.71	0.88
0.70	0.74	0.69	0.79	0.86	0.80	0.74	0.84	0.73	0.71	0.77
0.95	1.00	0.81	0.87	0.75	0.75	0.77	0.73	0.69	0.65	0.71
0.80	0.85	0.88	0.66	0.77	0.72	0.63	0.93	0.73	0.79	0.74

min: 0.63 max: 1.00

COMMENT

The sample is rich in organics with 12 bitumen fragments and 32 vitrinite clasts to measure. Reflectance measurements of the solid bitumen were corrected to vitrinite reflectance equivalence using (Landis & Castano 1994) equation. Under UV light the sample showed bright yellow and light orange fluorescence of liptinite mainly alginite. Inertinite maceral also appear in very few abundance in form of fusinite and semifusinite fragments. Polishing quality 2B.

DISPERSED VITRINITE REFLECTANCE REPORT

SAMPLE INFORMATION

Submitted by:	Ibrahim
Date Submitted:	07-14-14
Project:	M.Sc. Thesis
Sample ID:	**Sample Wi-Py-3**
Lab ID:	OKState
Sample Type:	Core
Date Analyzed:	07-13-14
Operator:	Ibrahim
Protocol:	ASTM D7708

RESULTS

No. Measurements:	29
maceral type:	Vitrnite & Solid Bitumen
mean R_o (%):	0.73
s.d.:	0.06

Example Photograph:

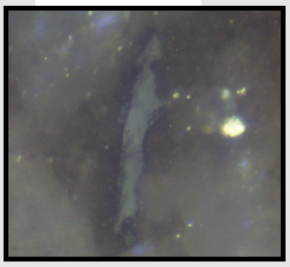

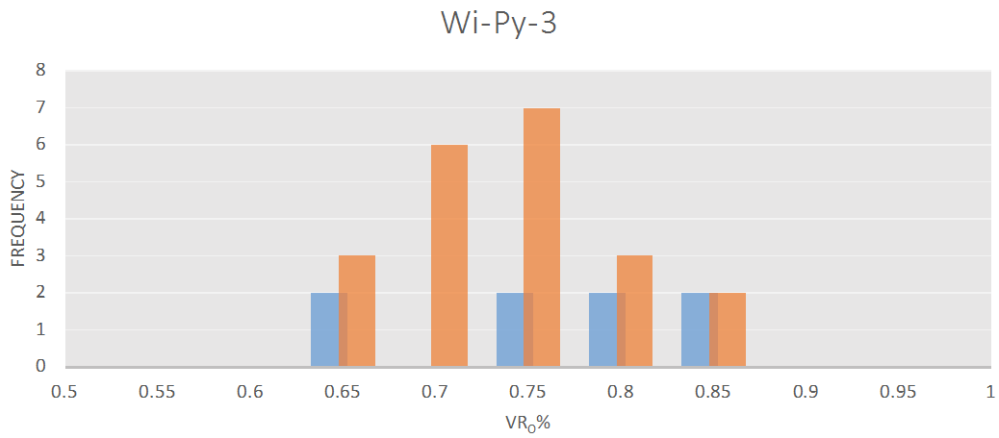

DATA

0.64	0.74	0.65	0.71	0.62	0.74	0.74	0.81
0.78	0.74	0.69	0.71	0.67	0.82	0.64	
0.64	0.80	0.78	0.69	0.68	0.75	0.75	
0.84	0.84	0.74	0.65	0.80	0.79	0.65	

min: 0.62 max: 0.84

COMMENT

The sample is rich in organics with 21 bitumen fragments and 8 vitrinite clasts to measure. Reflectance measurements of the solid bitumen were corrected to vitrinite reflectance equivalence using (Landis & Castano 1994) equation. Under UV light the sample showed bright yellow and light orange fluorescence of liptinite mainly alginite. Inertinite maceral also appear in very low abundance in form of fusinite and semifusinite fragments. Polishing quality 2B.

DISPERSED VITRINITE REFLECTANCE REPORT

SAMPLE INFORMATION

Submitted by:	Ibrahim
Date Submitted:	07-14-14
Project:	M.Sc. Thesis
Sample ID:	**Sample Wi-Py-4**
Lab ID:	OKState
Sample Type:	Core
Date Analyzed:	07-13-14
Operator:	Ibrahim
Protocol:	ASTM D7708

RESULTS

No. Measurements:	19
maceral type:	Vitrnite & Solid Bitumen
mean R_o (%):	0.79
s.d.:	0.12

Example Photograph:

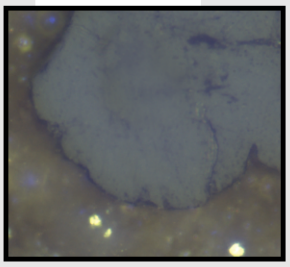

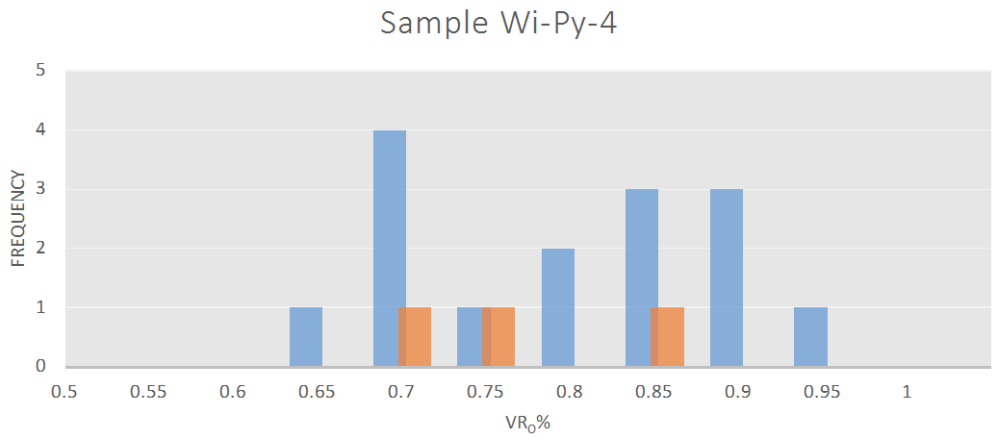

DATA

0.81	0.80	0.94	0.70	0.84
0.82	0.69	0.66	0.63	0.68
0.85	0.65	0.80	0.87	0.71
1.12	0.79	0.87	0.75	

min: 0.63 max: 1.12

COMMENT

The sample is rich in organics with 3 bitumen fragments and 16 vitrinite clasts to measure. Reflectance measurements of the solid bitumen were corrected to vitrinite reflectance equivalence using (Landis & Castano 1994) equation. Under UV light the sample showed bright yellow and light orange fluorescence of liptinite mainly alginite. Inertinite maceral also appear in very low abundance in form of fusinite and semifusinite fragments. Polishing quality 2B.

DISPERSED VITRINITE REFLECTANCE REPORT

SAMPLE INFORMATION

Submitted by:	Ibrahim
Date Submitted:	07-14-14
Project:	M.Sc. Thesis
Sample ID:	**Sample Wi-Py-5**
Lab ID:	OKState
Sample Type:	Core
Date Analyzed:	07-13-14
Operator:	Ibrahim
Protocol:	ASTM D7708

RESULTS

No. Measurements:	19
maceral type:	Vitrnite & Solid Bitumen
mean R_o (%):	0.82
s.d.:	0.10

Example Photograph:

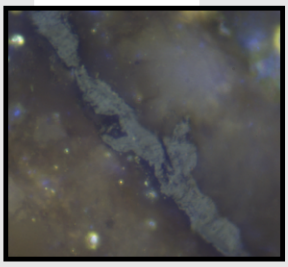

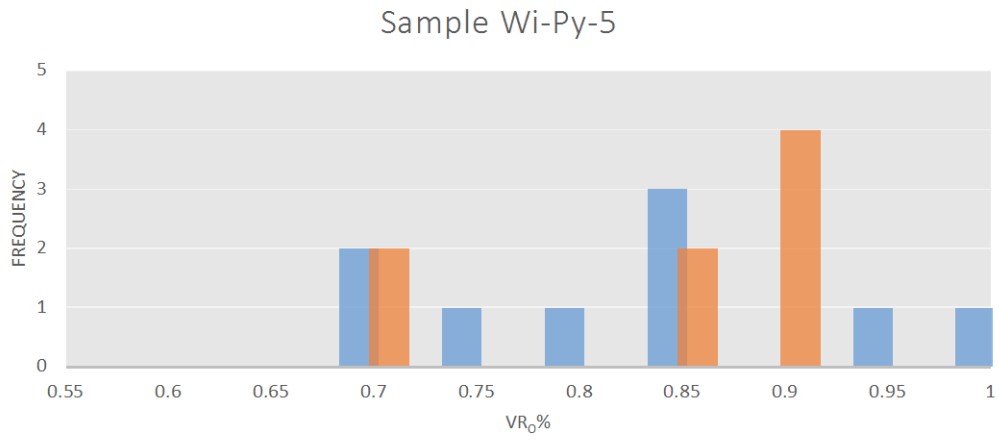

DATA

0.74	0.72	0.83	0.87	0.83
0.69	0.77	0.85	0.87	0.88
1.06	0.95	0.87	0.88	0.81
0.83	0.69	0.68	0.70	

min: 0.68 max: 1.06

COMMENT

The sample is rich in organics with 9 bitumen fragments and 10 vitrinite clasts to measure. Reflectance measurements of the solid bitumen were corrected to vitrinite reflectance equivalence using (Landis & Castano 1994) equation. Under UV light the sample showed bright yellow and light orange fluorescence of liptinite mainly alginite. Inertinite maceral also appear in very low abundance in form of fusinite and semifusinite fragments. Polishing quality 2B.

DISPERSED VITRINITE REFLECTANCE REPORT

SAMPLE INFORMATION

Submitted by:	Ibrahim
Date Submitted:	07-14-14
Project:	M.Sc. Thesis
Sample ID:	**Sample Wd-Py-1**
Lab ID:	OKState
Sample Type:	Core
Date Analyzed:	07-13-14
Operator:	Ibrahim
Protocol:	ASTM D7708

RESULTS

No. Measurements:	18
maceral type:	Vitrnite & Solid Bitumen
mean R_o (%):	0.81
s.d.:	0.08

Example Photograph:

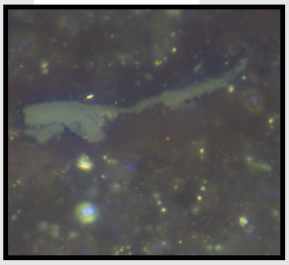

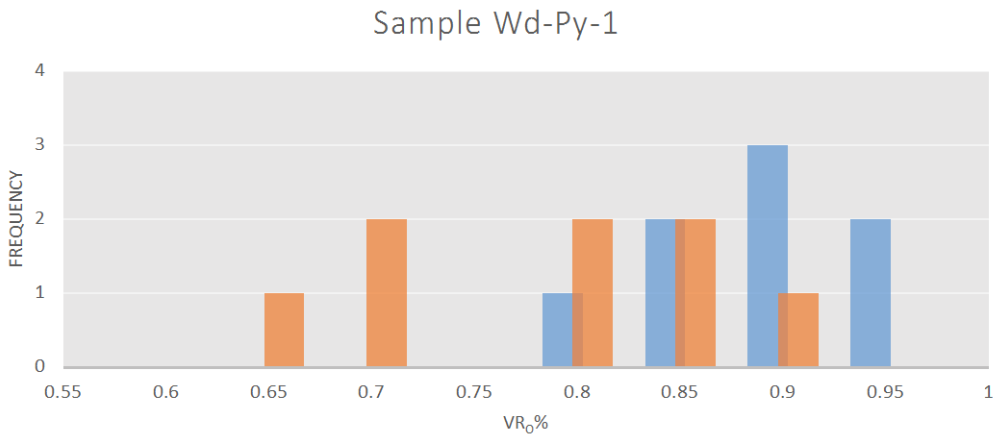

DATA

0.74	0.82	0.88	0.82	0.78
0.76	0.90	0.81	0.7	0.87
0.90	0.93	0.65	0.8	
0.81	0.93	0.67	0.82	

min: 0.65 max: 0.93

COMMENT

The sample is rich in organics with 9 bitumen fragments and 9 vitrinite clasts to measure. Reflectance measurements of the solid bitumen were corrected to vitrinite reflectance equivalence using (Landis & Castano 1994) equation. Under UV light the sample showed bright yellow and light orange fluorescence of liptinite mainly alginite. Inertinite maceral also appear in very low abundance in form of fusinite and semifusinite fragments. Polishing quality 2B.

DISPERSED VITRINITE REFLECTANCE REPORT

SAMPLE INFORMATION

Submitted by:	Ibrahim
Date Submitted:	07-14-14
Project:	M.Sc. Thesis
Sample ID:	**Sample Wd-Py-2**
Lab ID:	OKState
Sample Type:	Core
Date Analyzed:	07-13-14
Operator:	Ibrahim
Protocol:	ASTM D7708

RESULTS

No. Measurements:	23
maceral type:	Vitrnite & Solid Bitumen
mean R_o (%):	0.81
s.d.:	0.14

Example Photograph:

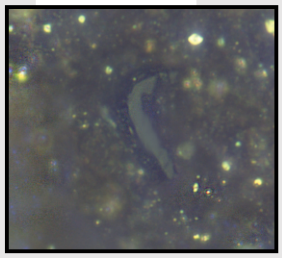

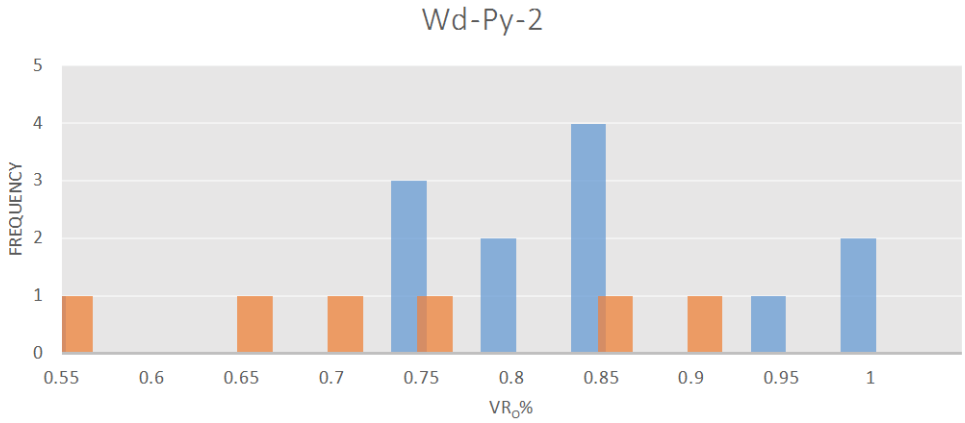

DATA

0.93	0.80	0.95	0.77	0.77	0.72
0.85	0.54	0.74	0.72	0.66	0.89
0.71	1.08	0.83	0.97	0.65	0.85
0.77	1.00	0.83	0.96	0.55	

min: 0.55 max: 1.08

COMMENT

The sample is rich in organics with 7 bitumen fragments and 16 vitrinite clasts to measure. Reflectance measurements of the solid bitumen were corrected to vitrinite reflectance equivalence using (Landis & Castano 1994) equation. Under UV light the sample showed bright yellow and light orange fluorescence of liptinite mainly alginite. Inertinite maceral also appear in very low abundance in form of fusinite and semifusinite fragments. Polishing quality 2B.

APPENDIX IV

GC-FID, GC-MS and GC-MSMS Chromatograms

GC-FID Chromatograms

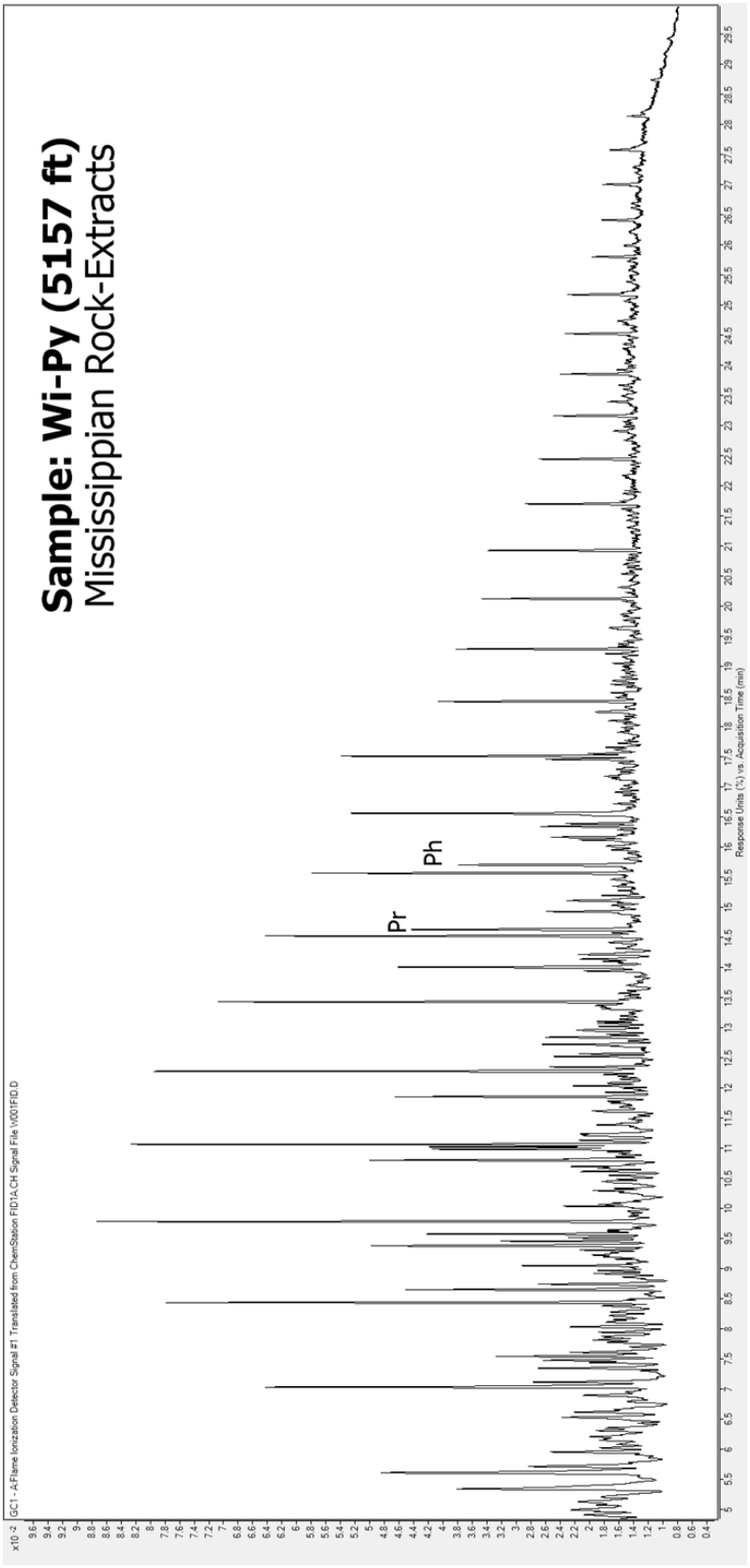

Figure 3 Gas chromatograms showing normal alkanes profile, Pr: pristane, Ph: phytane

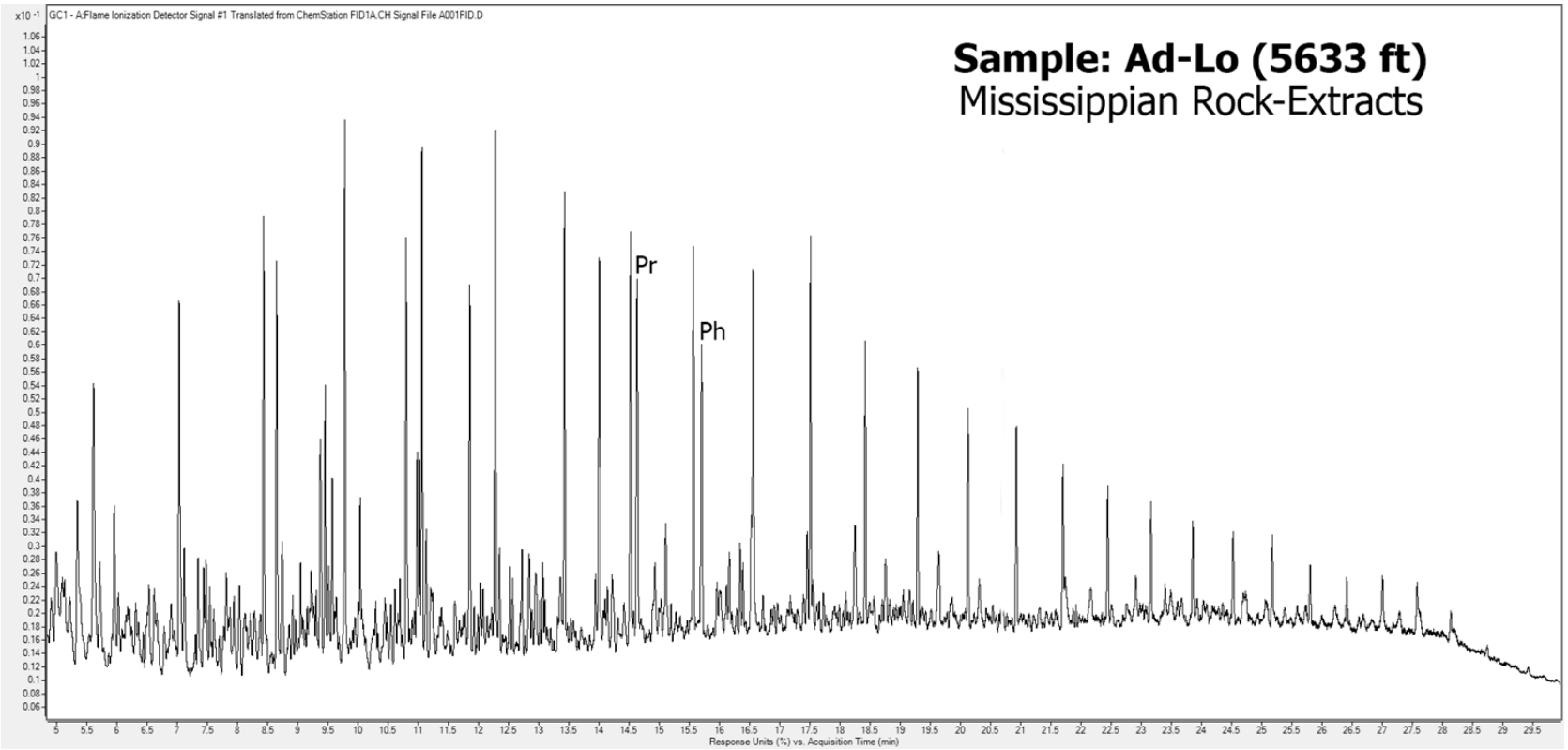

Figure 3. Continued.

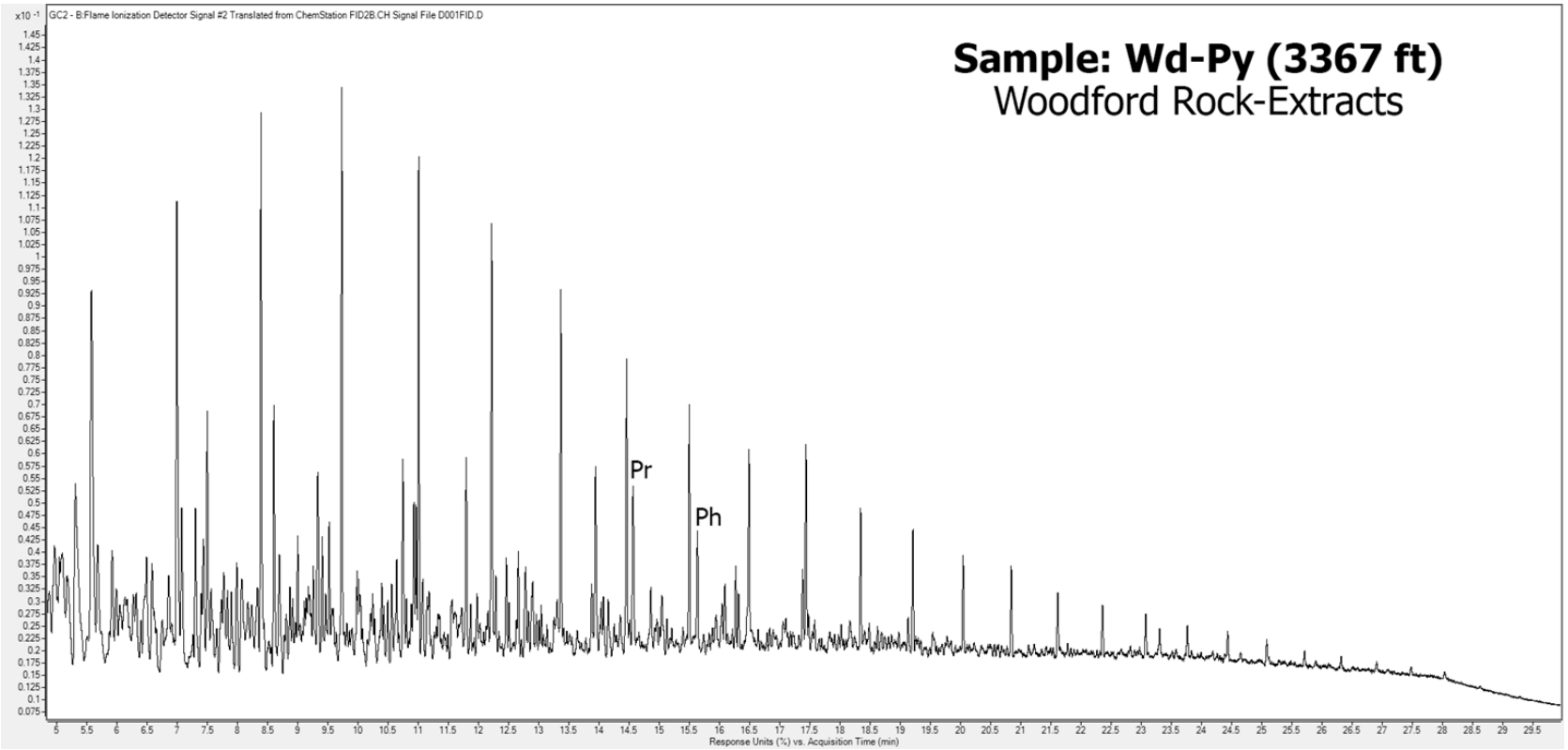

Figure 3. Continued.

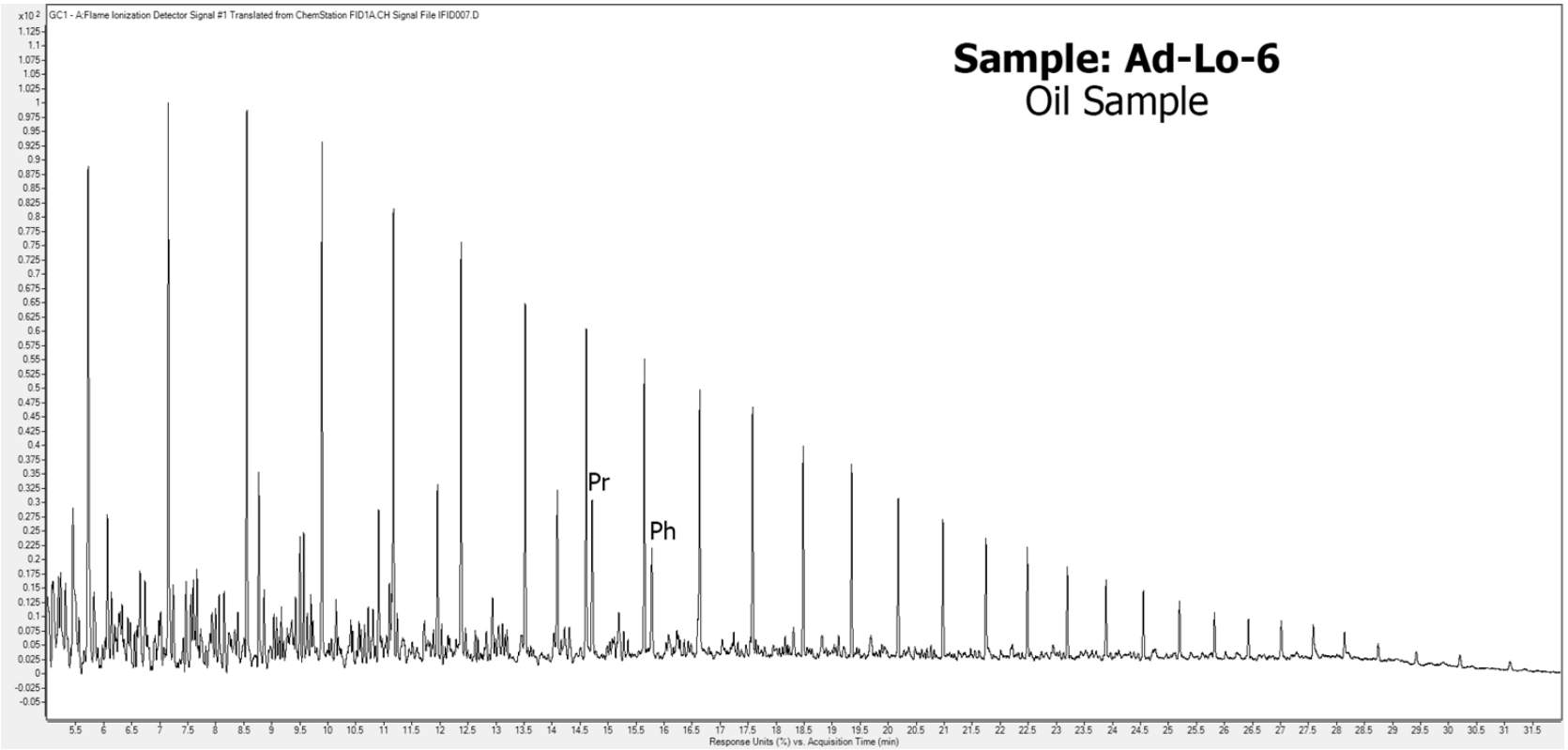

Figure 3. Continued..

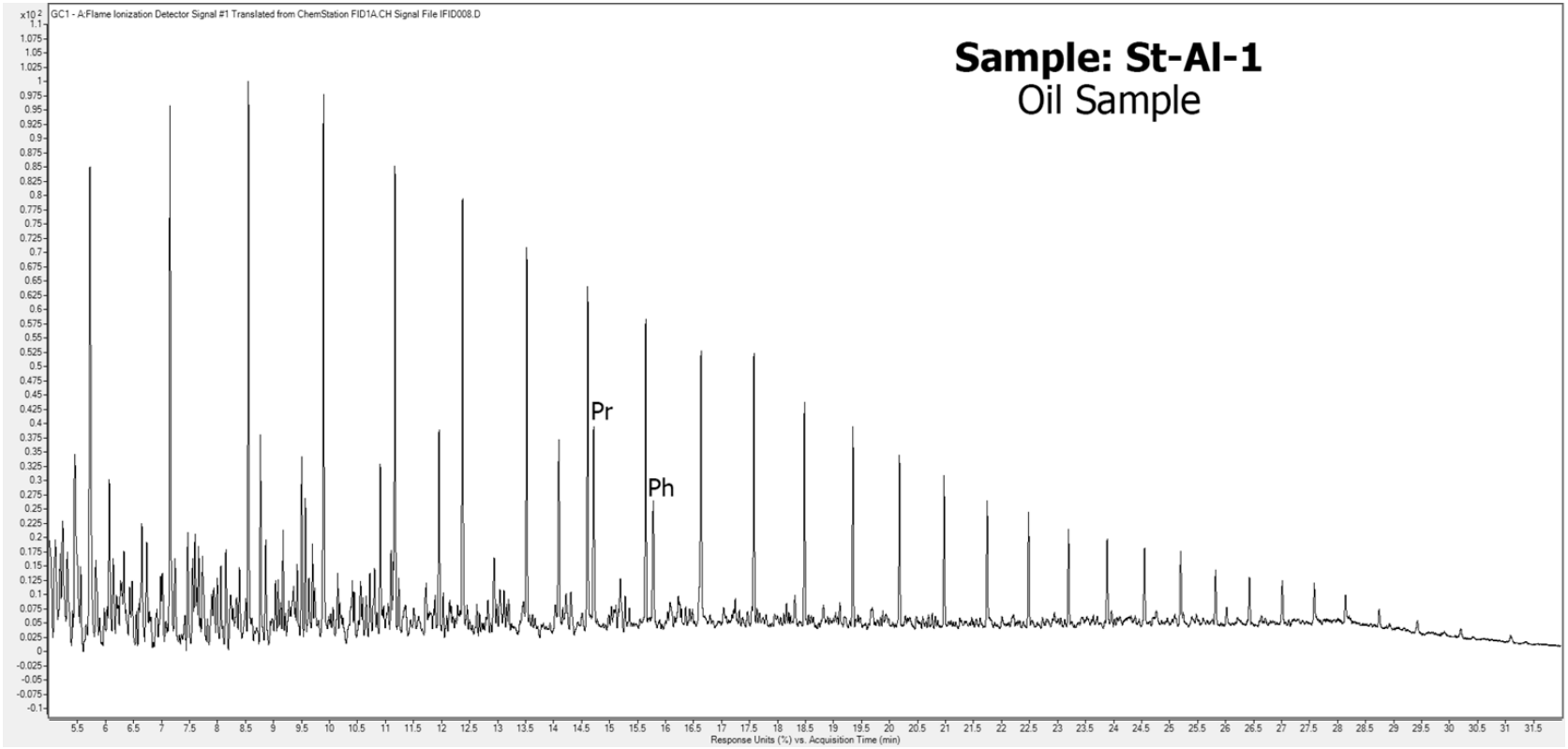

Figure 3. Continued.

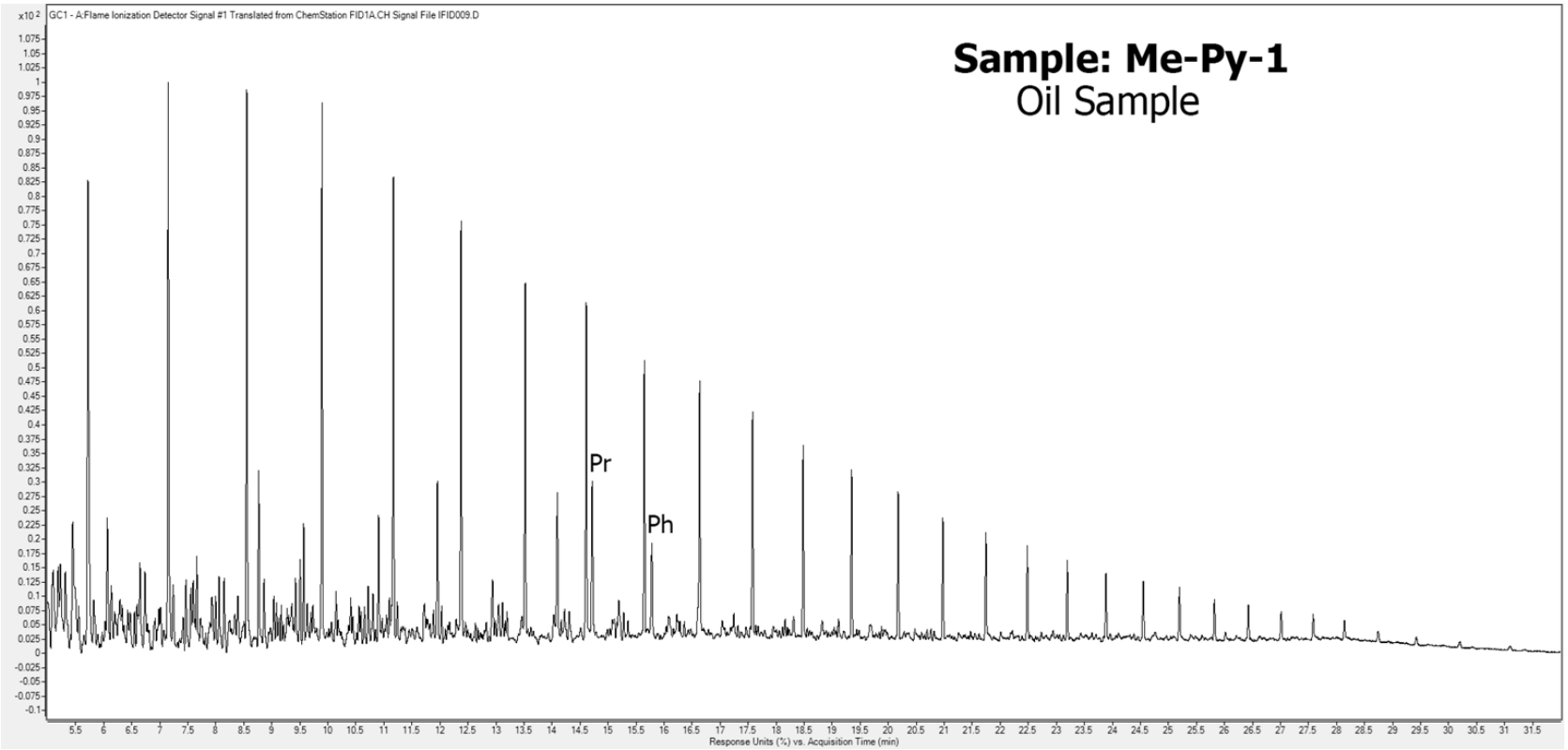

Figure 3. Continued.

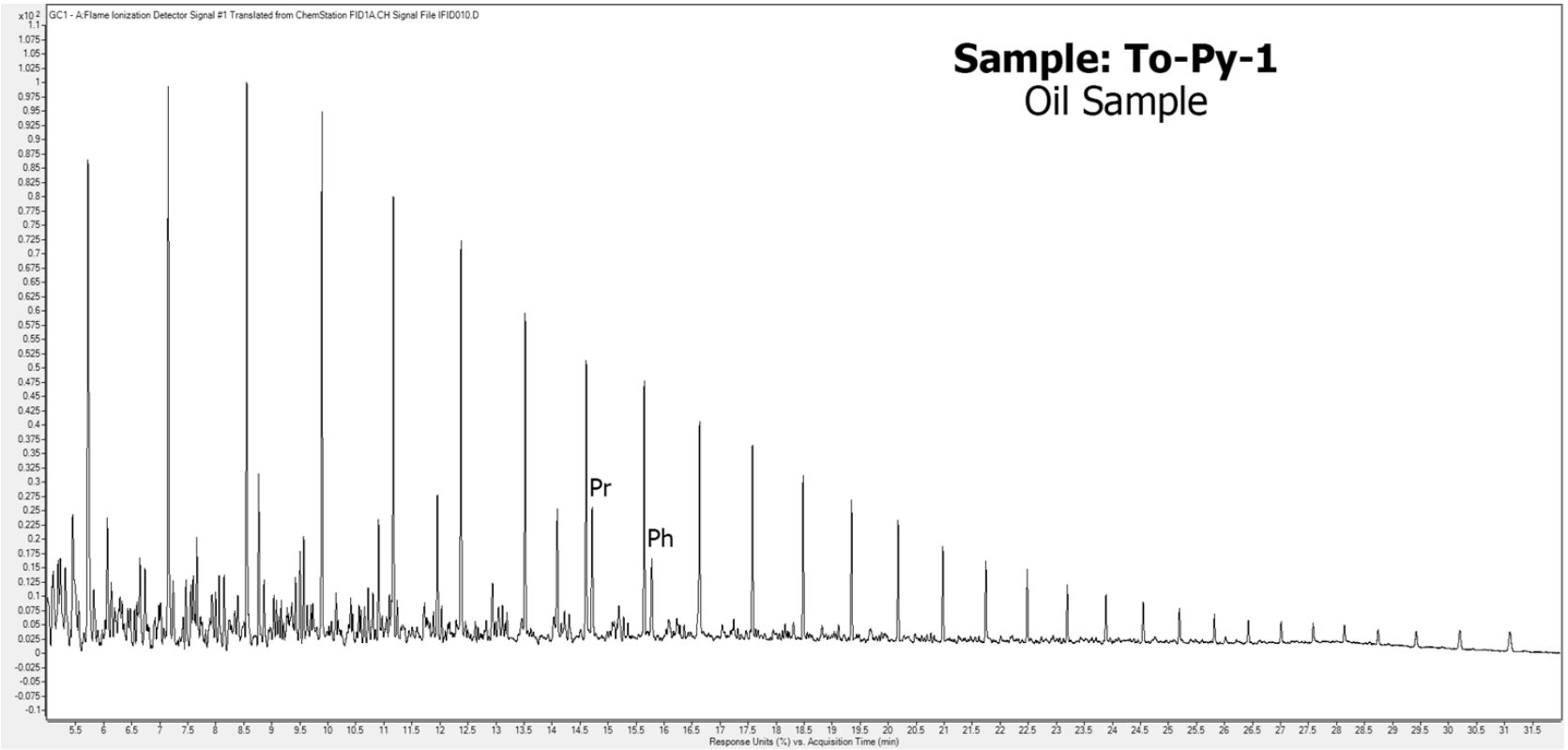

Figure 3. Continued.

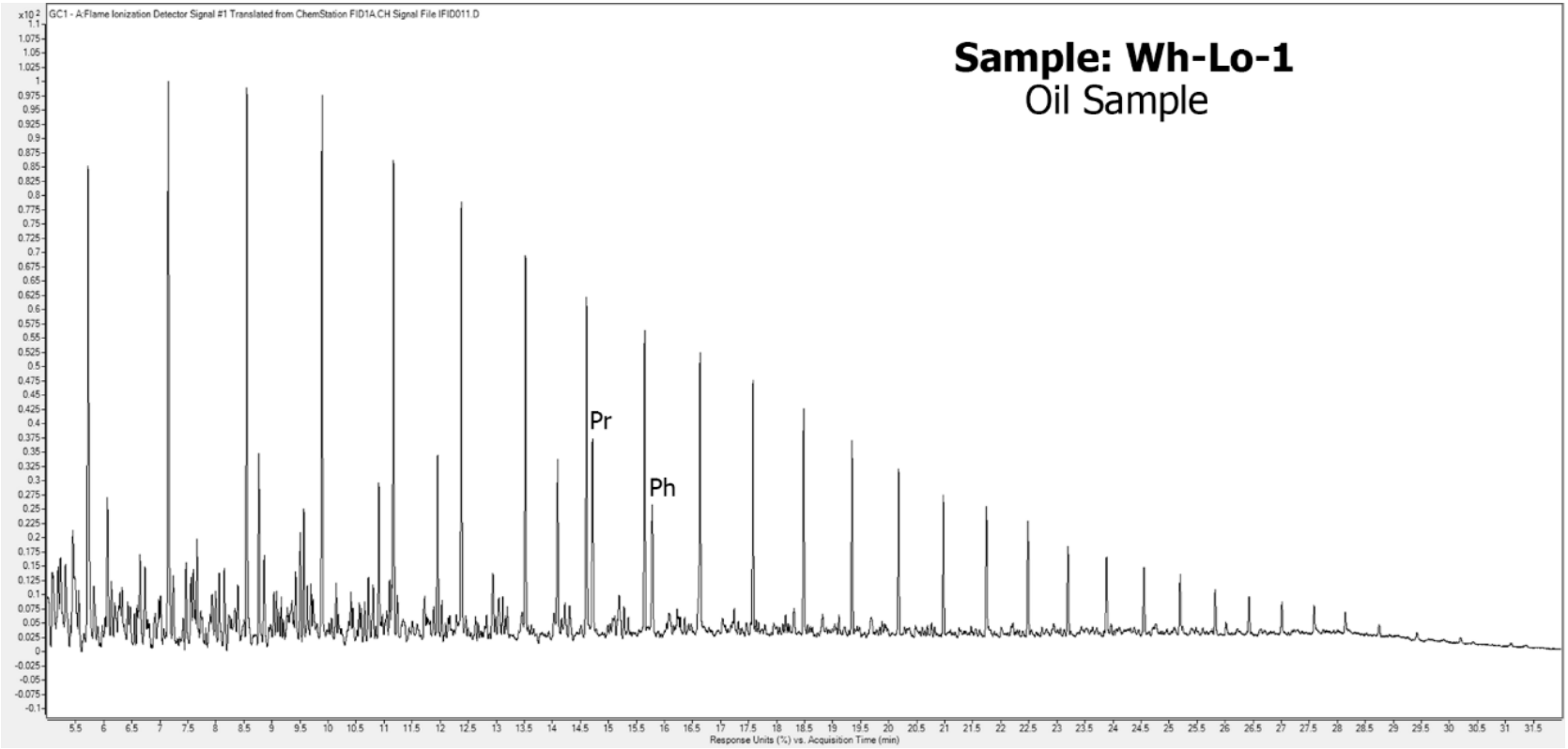

Figure 3. Continued.

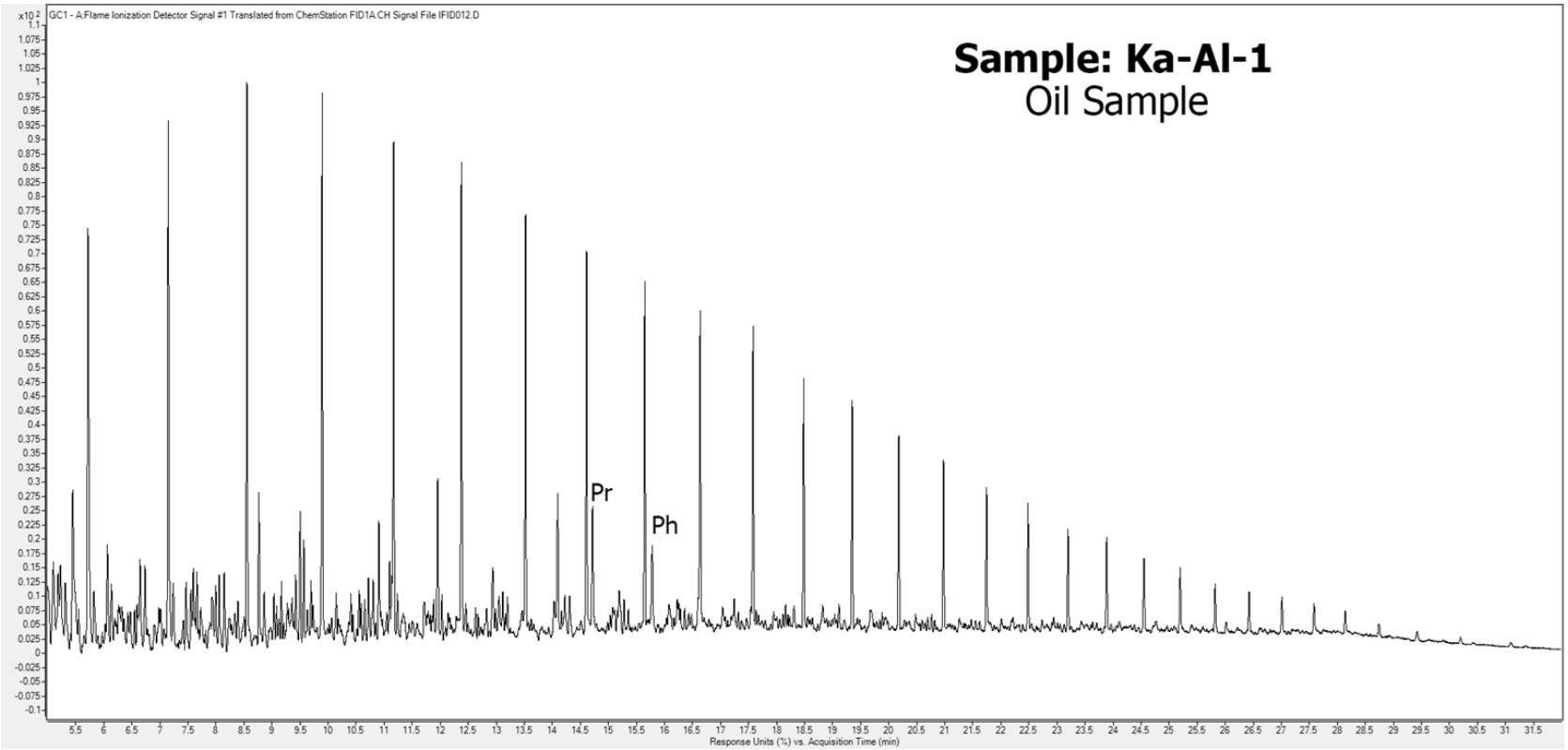

Figure 3. Continued.

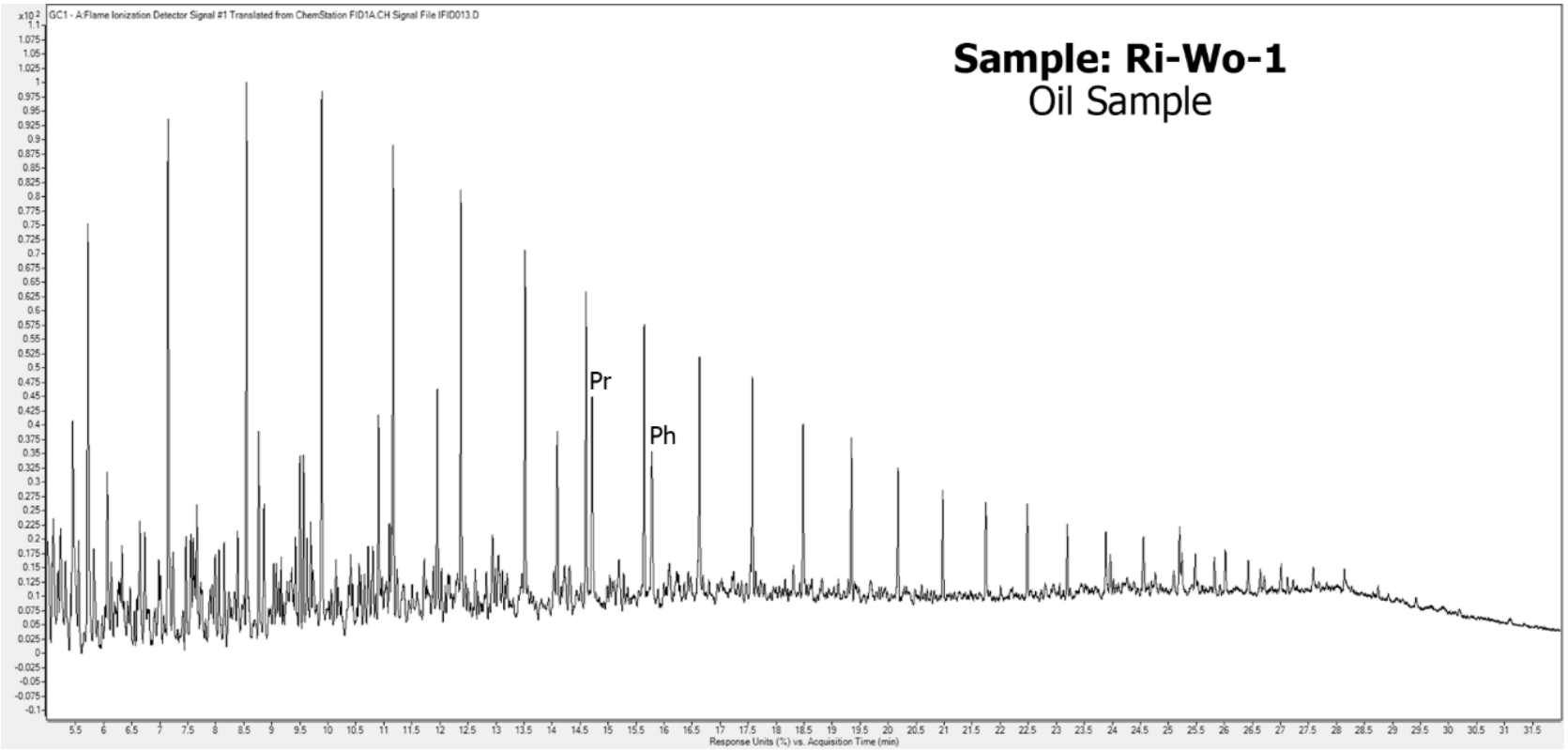

Figure 3. Continued.

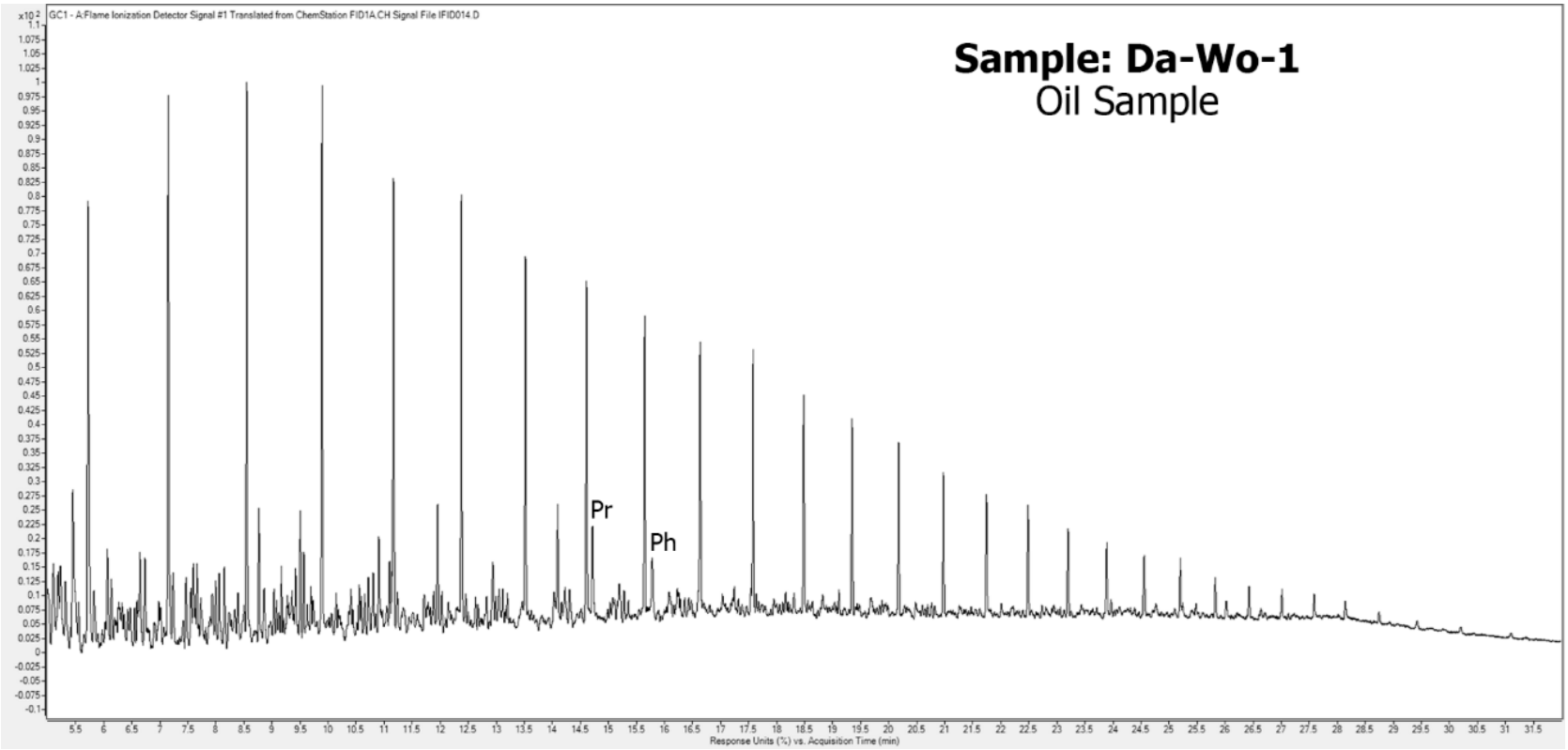

Figure 3. Continued.

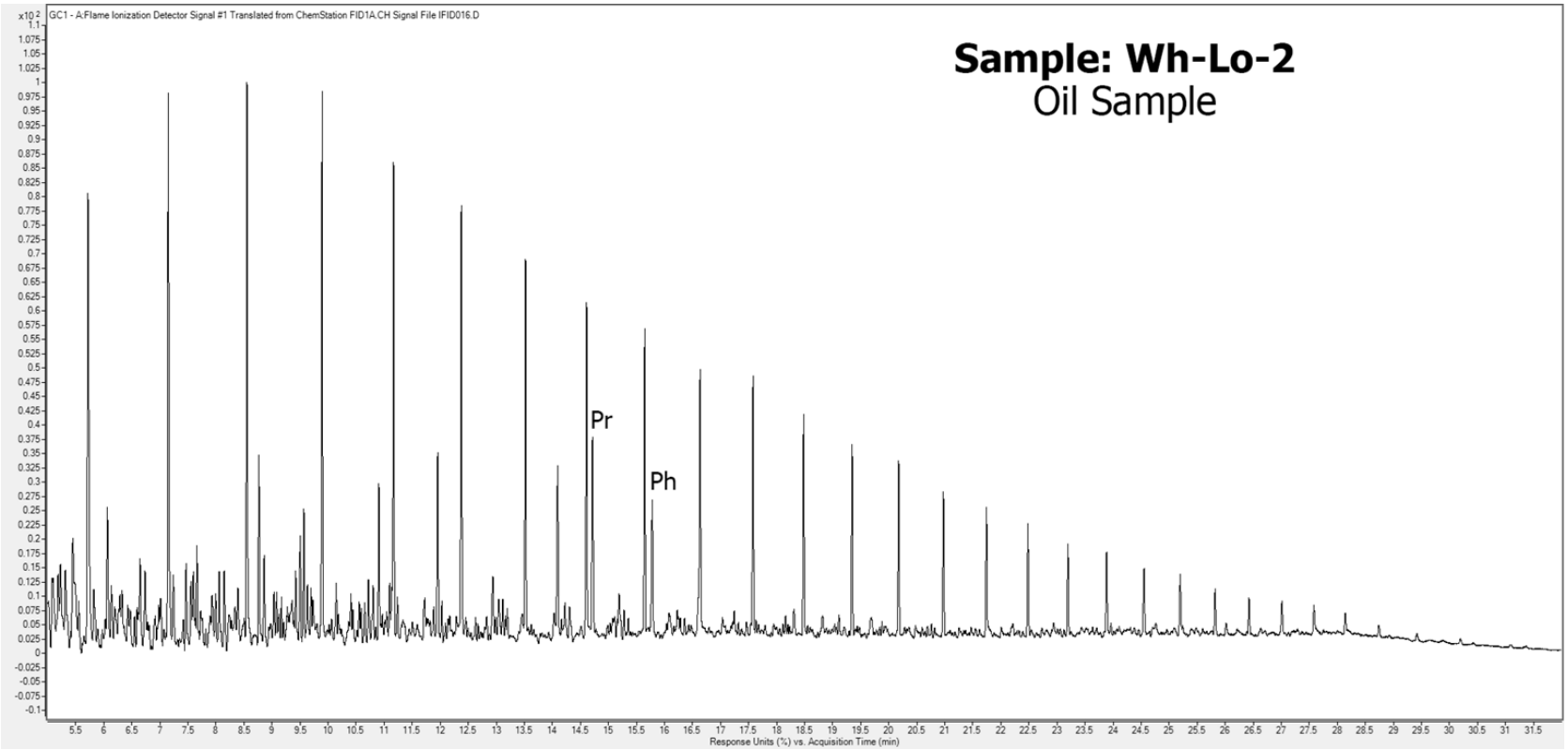

Figure 3. Continued.

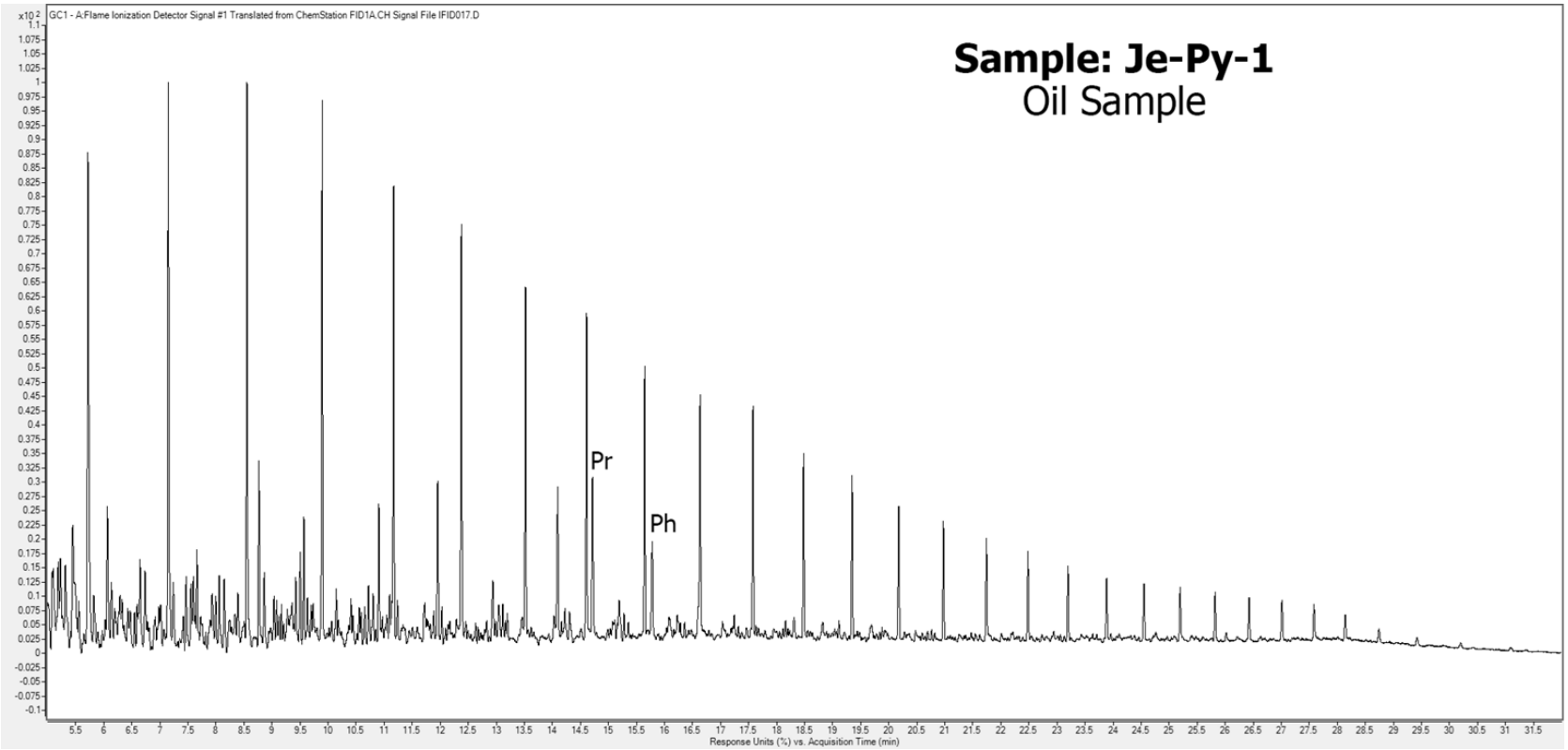

Figure 3. Continued.

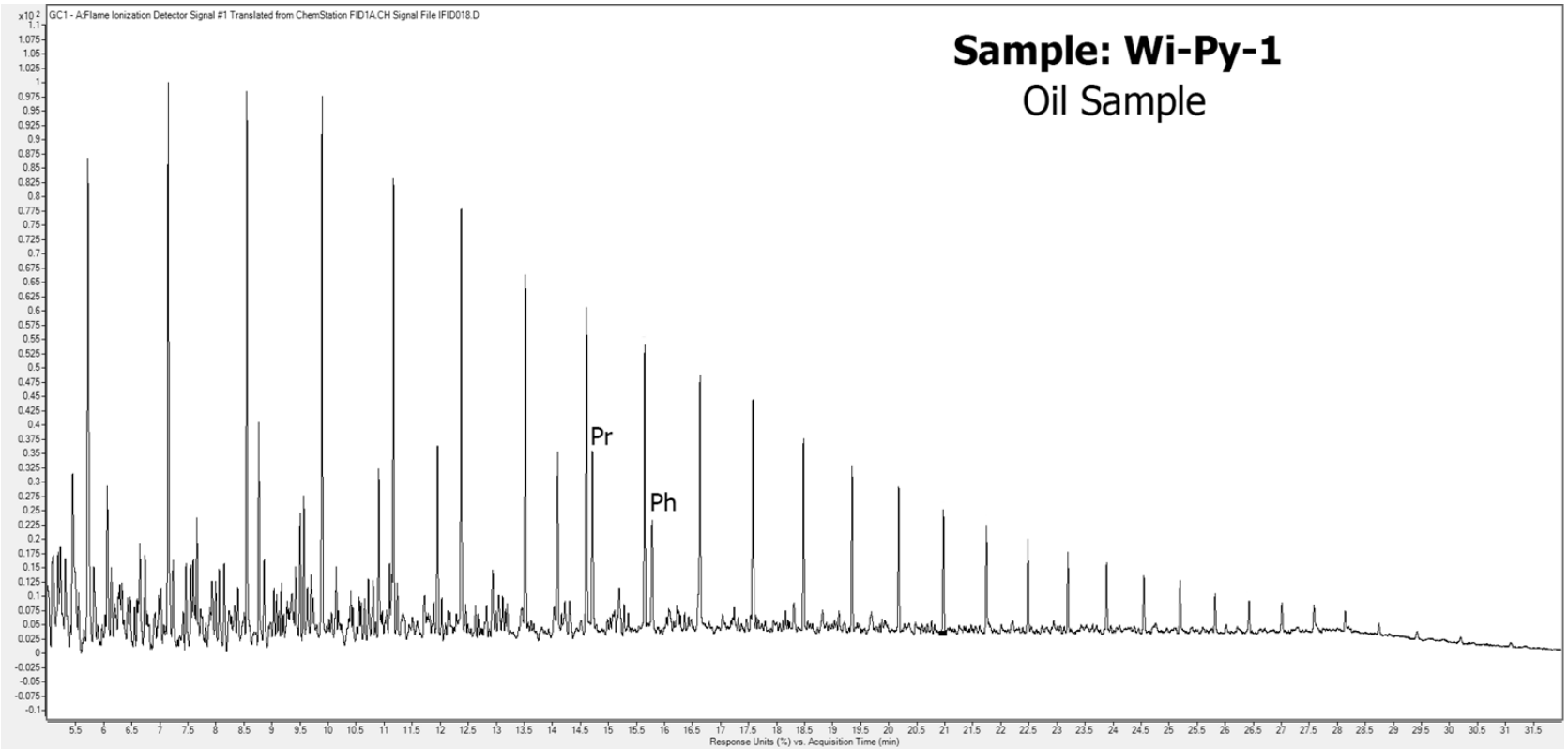

Figure 3. Continued.

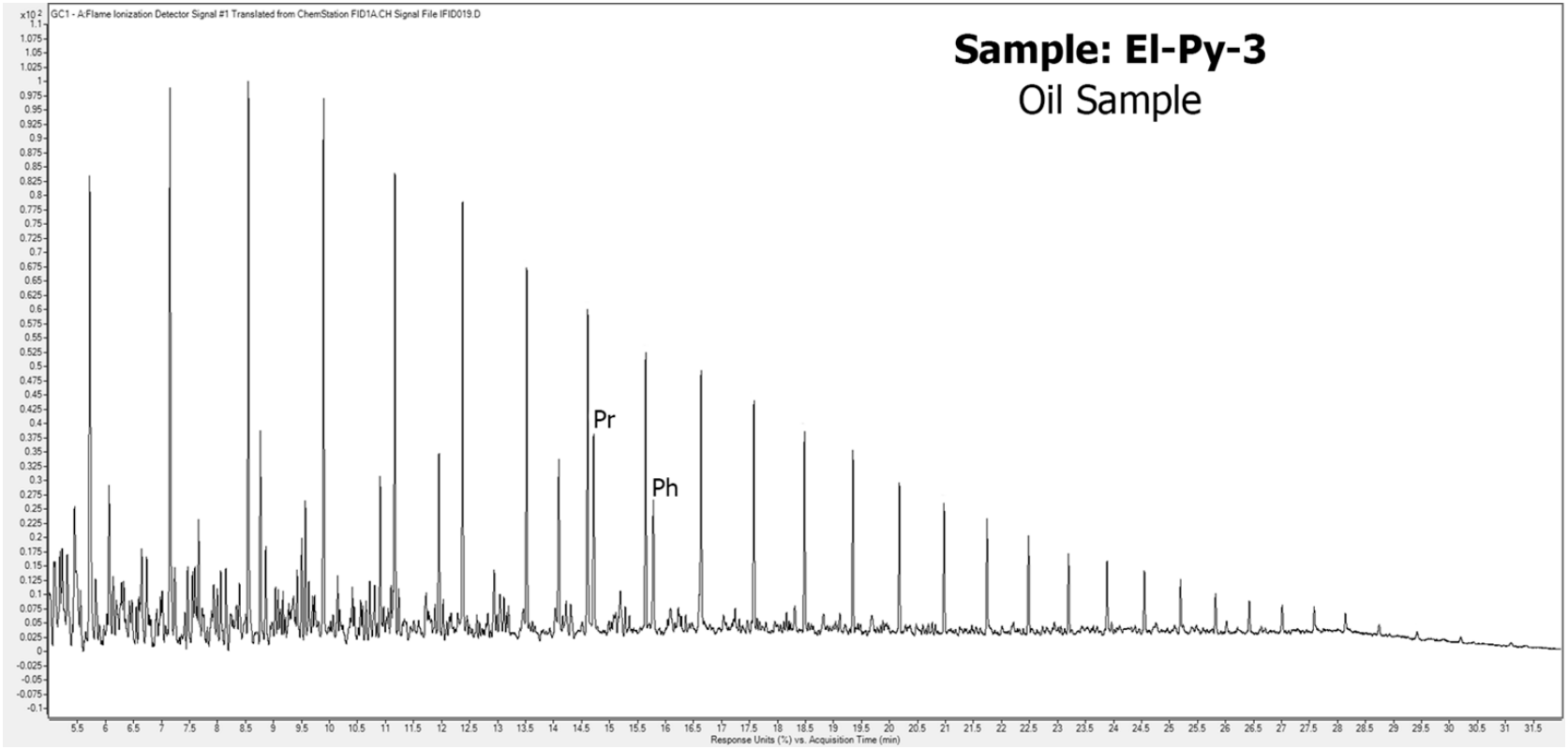

Figure 3. Continued.

GC-MS Mass Chromatograms

Sample: Ad-Lo (5633 ft)

Mississippian Rock-Extract

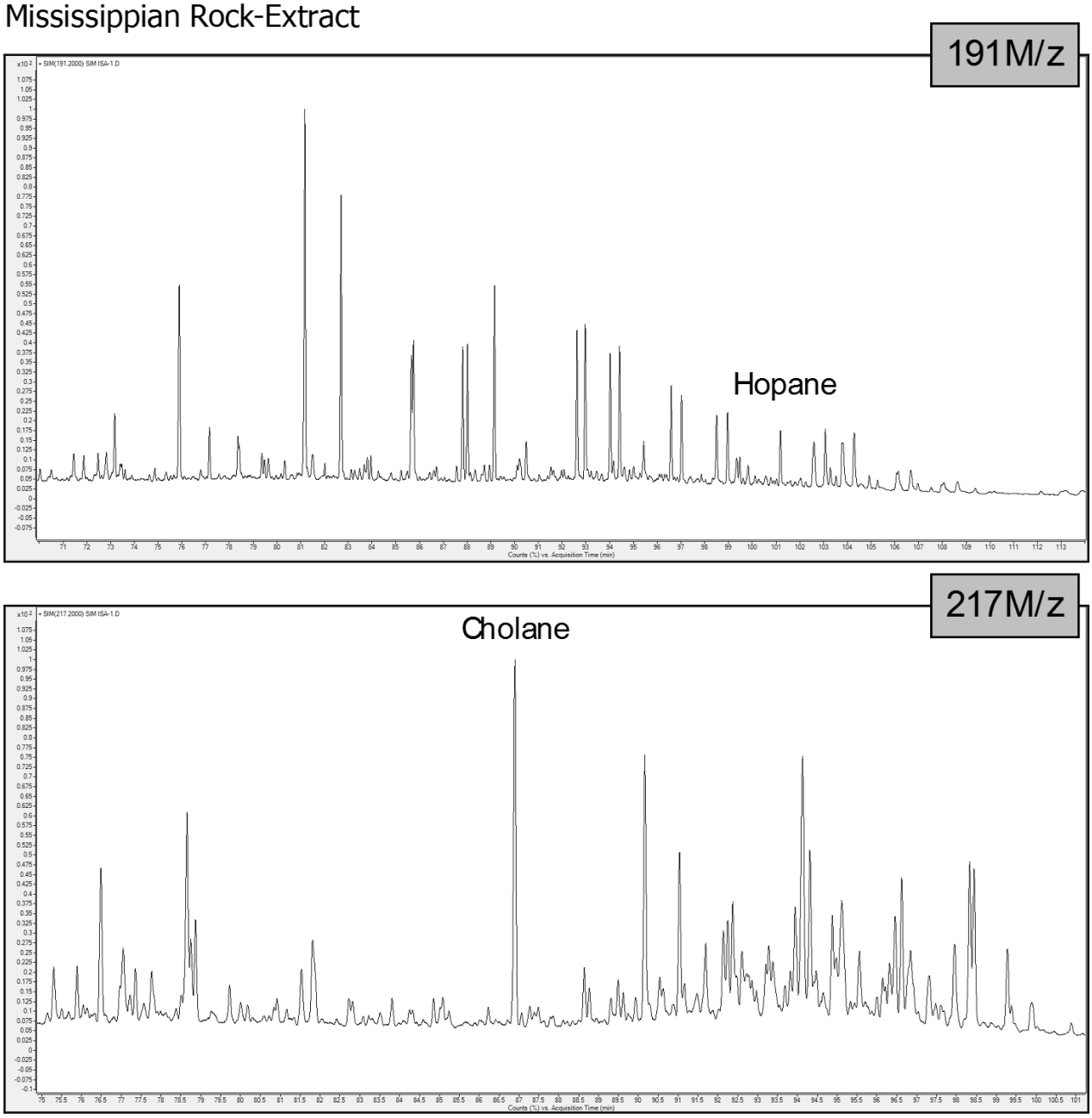

Figure 4. Mass chromatograms of terpane biomarkers (m/z191) and sterane biomarkers (m/z217).

Sample: Wi-Py (5157 ft)
Mississippian Rock-Extract

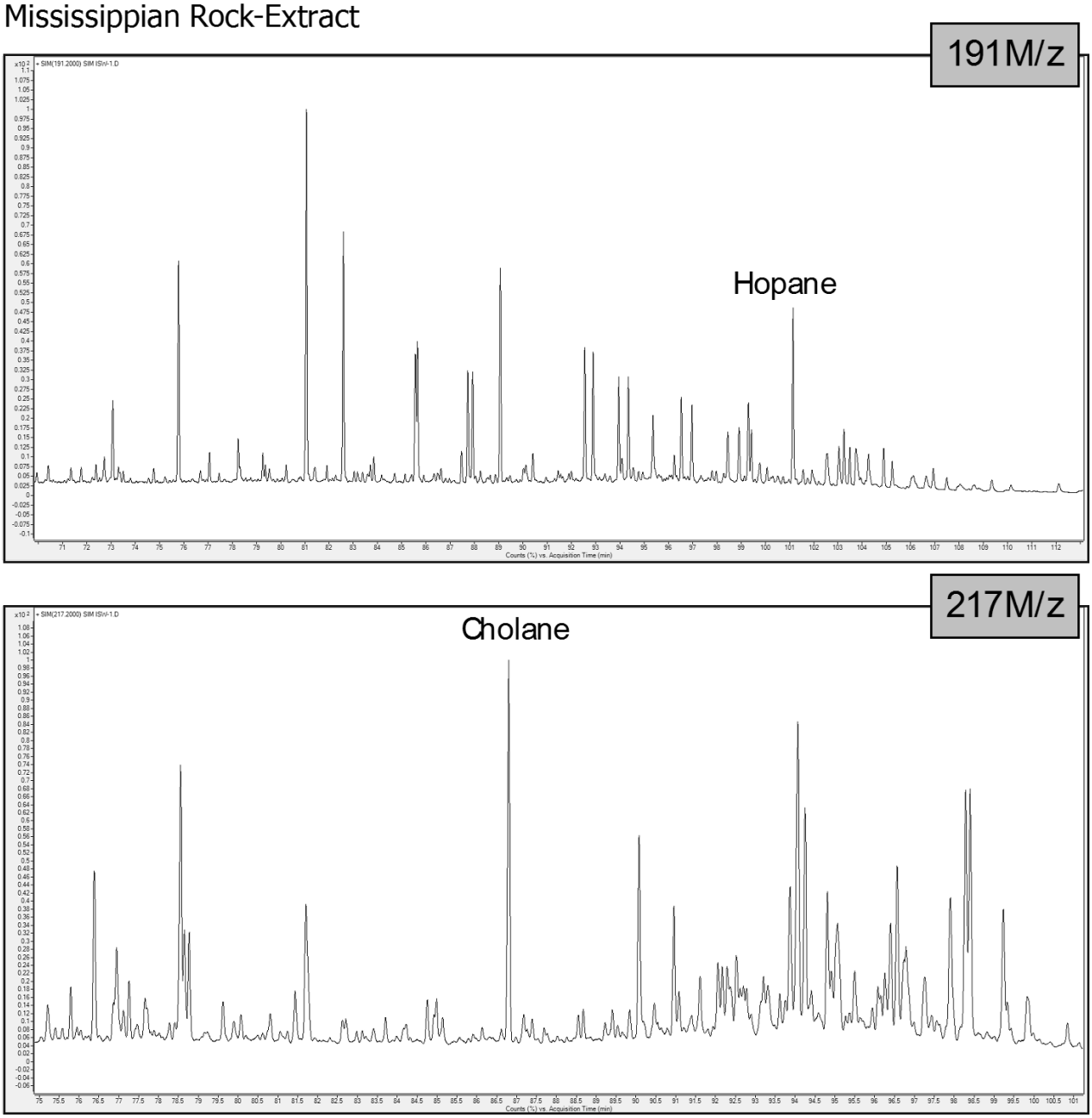

Figure 4. Continued.

Sample: Wd-Py (3367 ft)
Woodford Rock-Extract

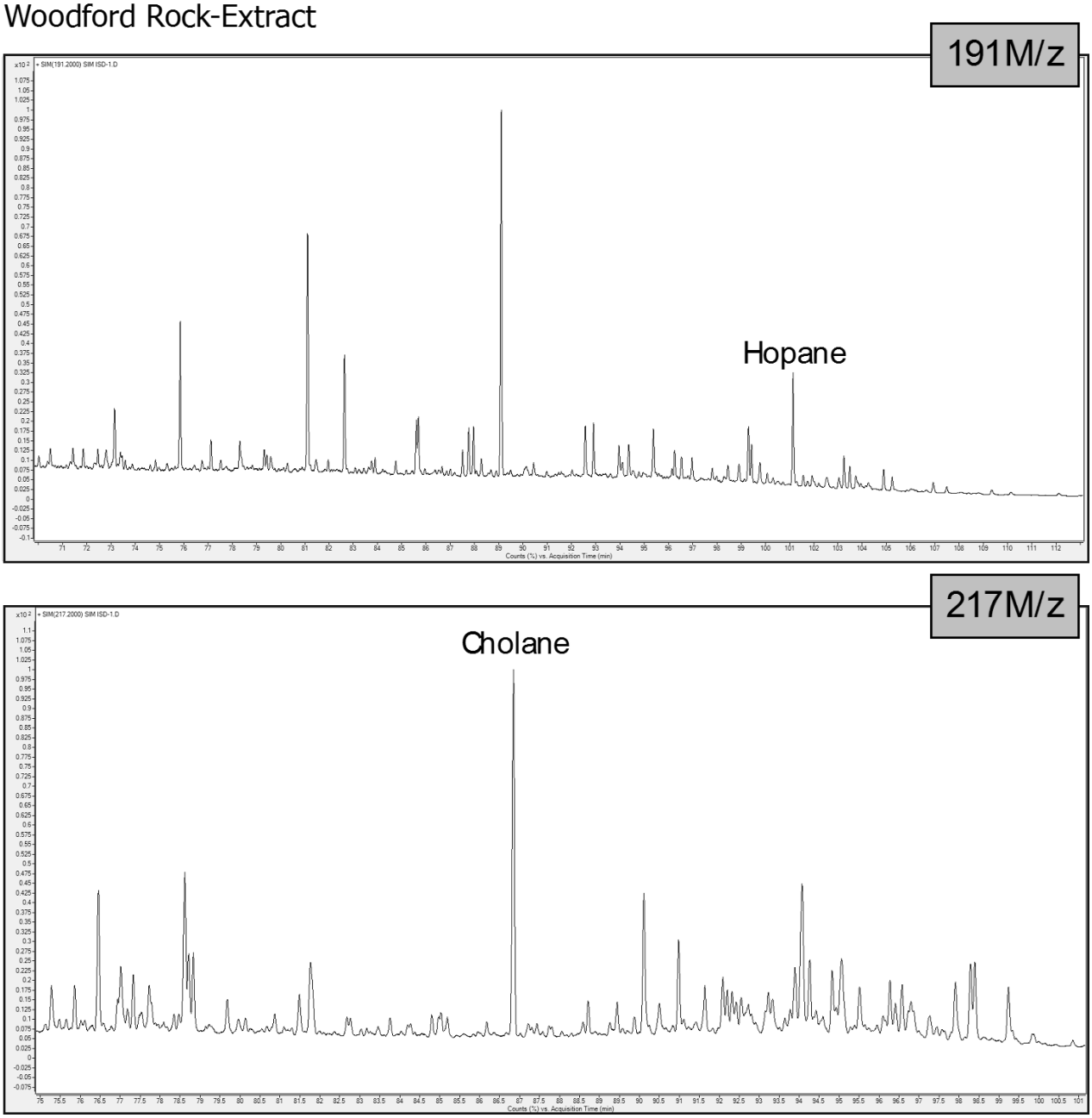

Figure 4. Continued.

Sample: Ad-Lo-6
Oil Sample

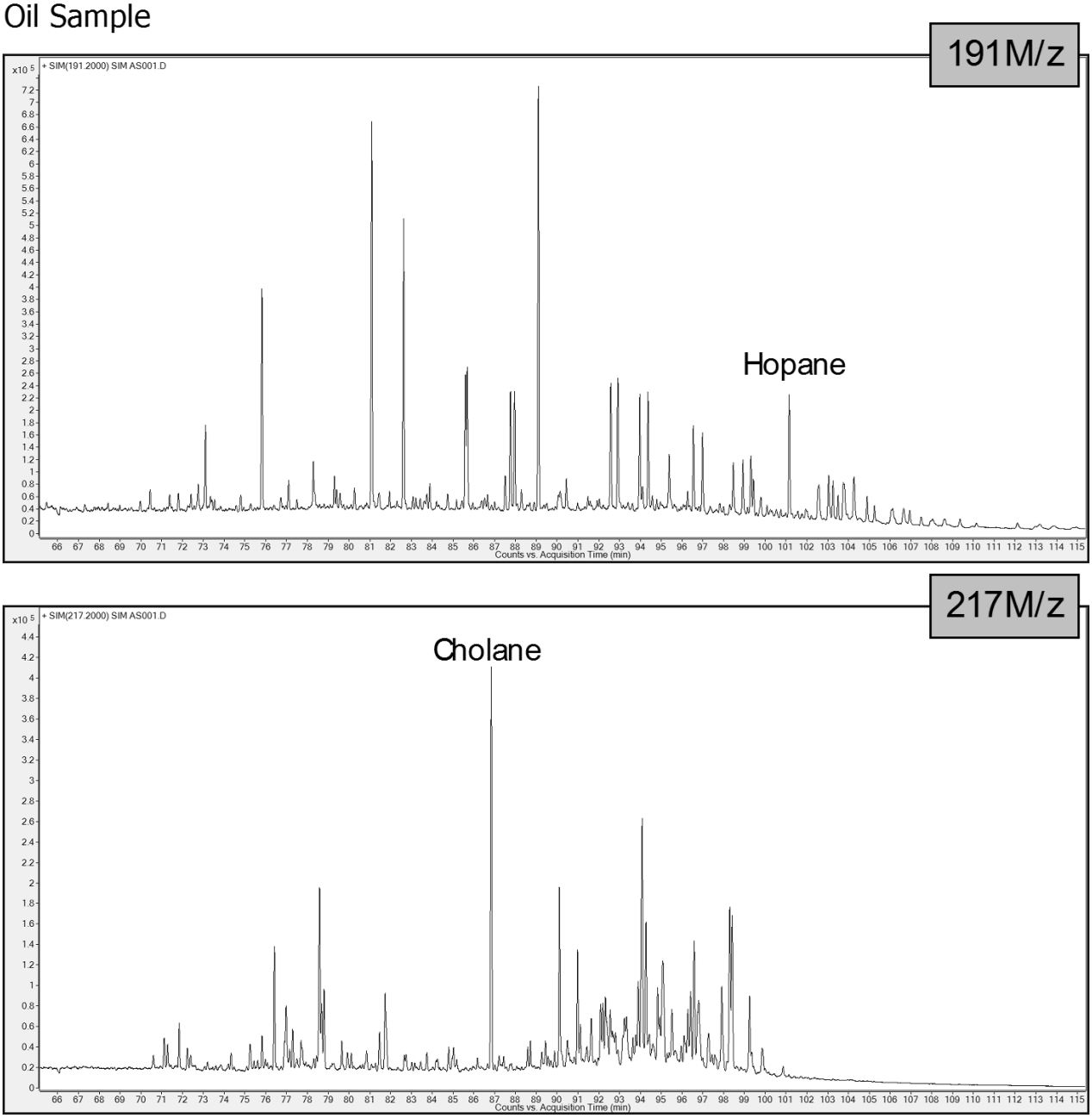

Figure 4. Continued.

Sample: St-Al-1
Oil Sample

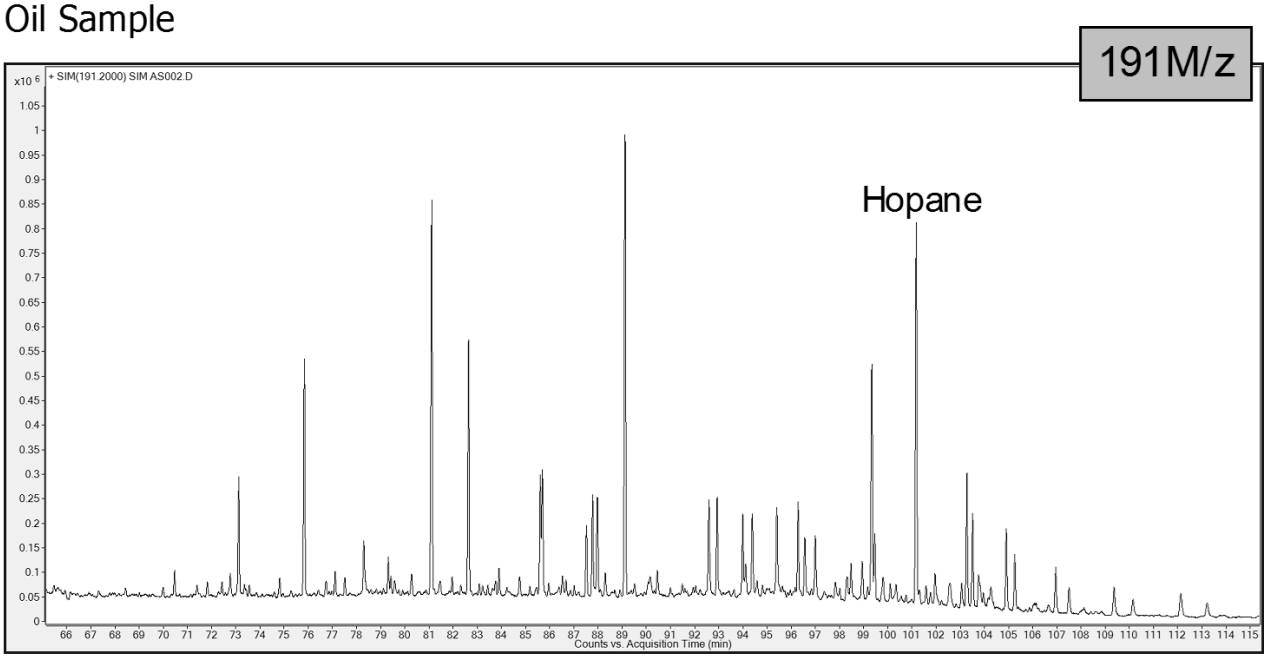

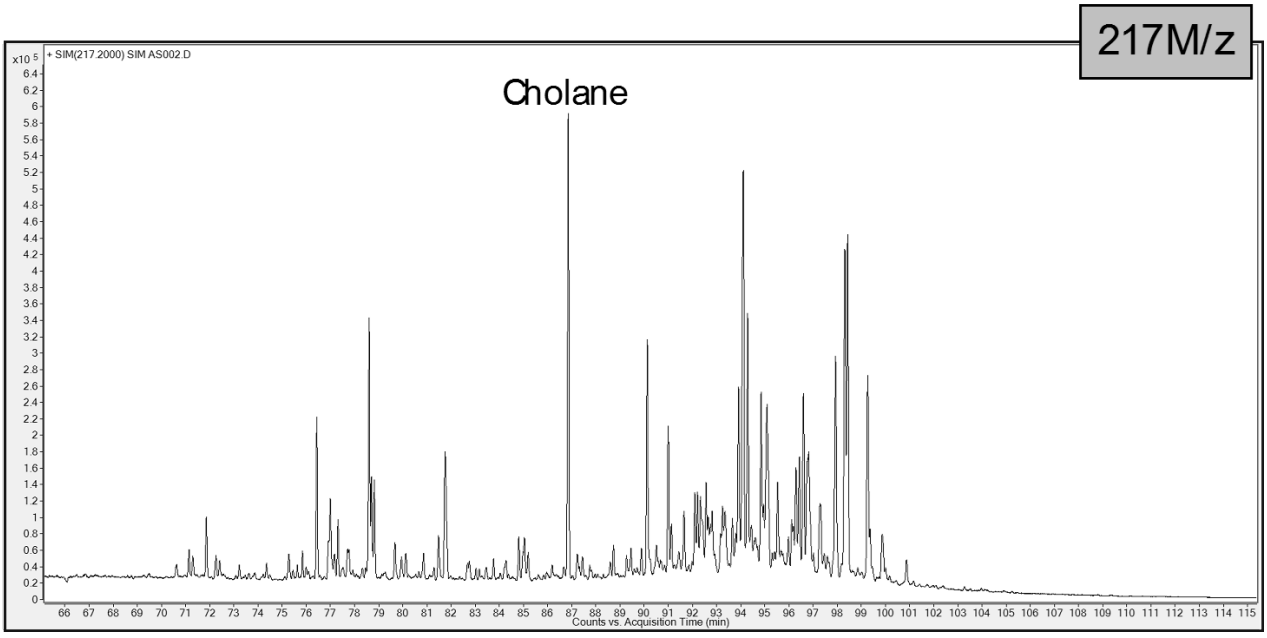

Figure 4. Continued.

Sample: Me-Py-1
Oil Sample

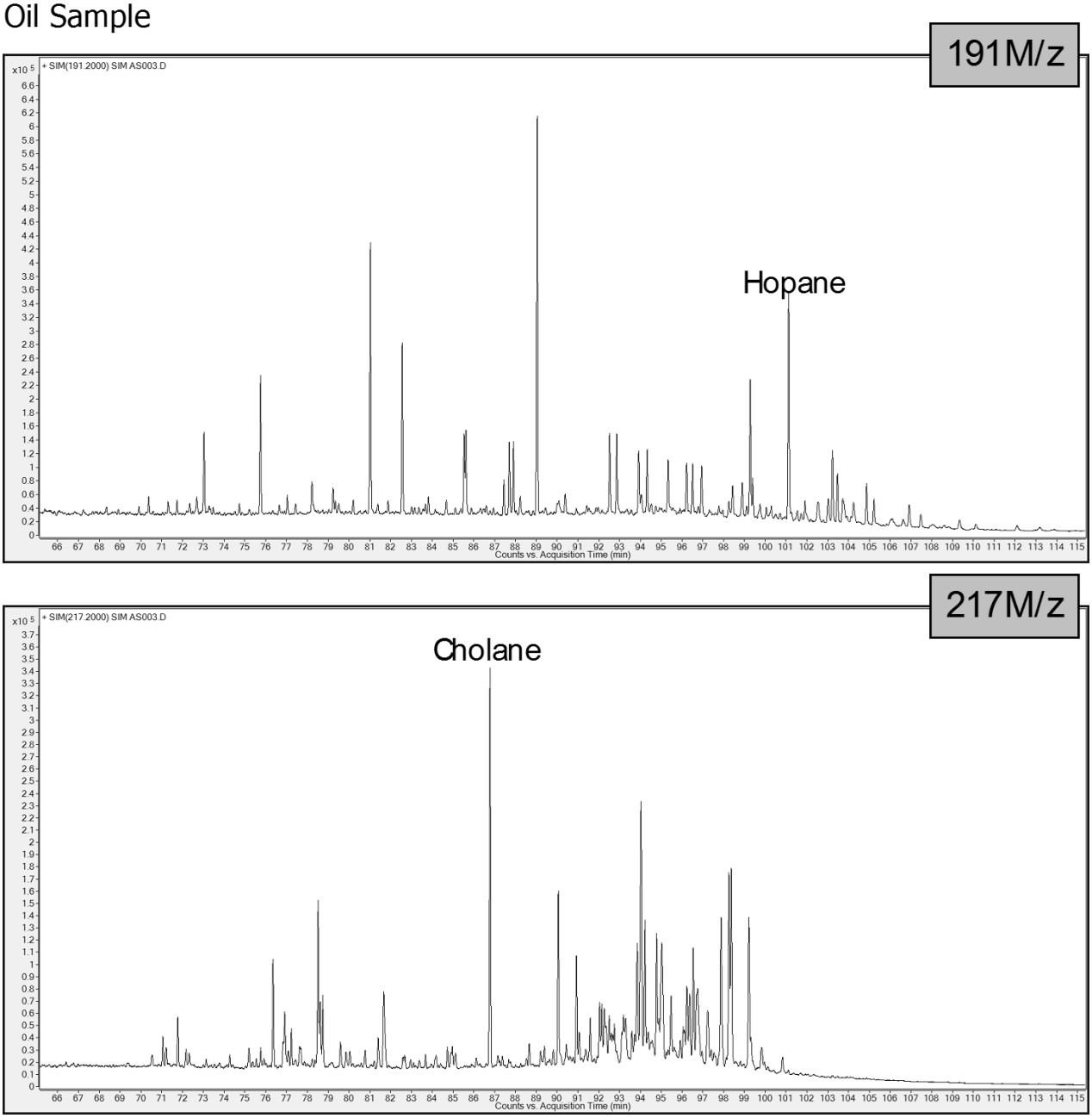

Figure 4. Continued.

Sample: To-Py-1
Oil Sample

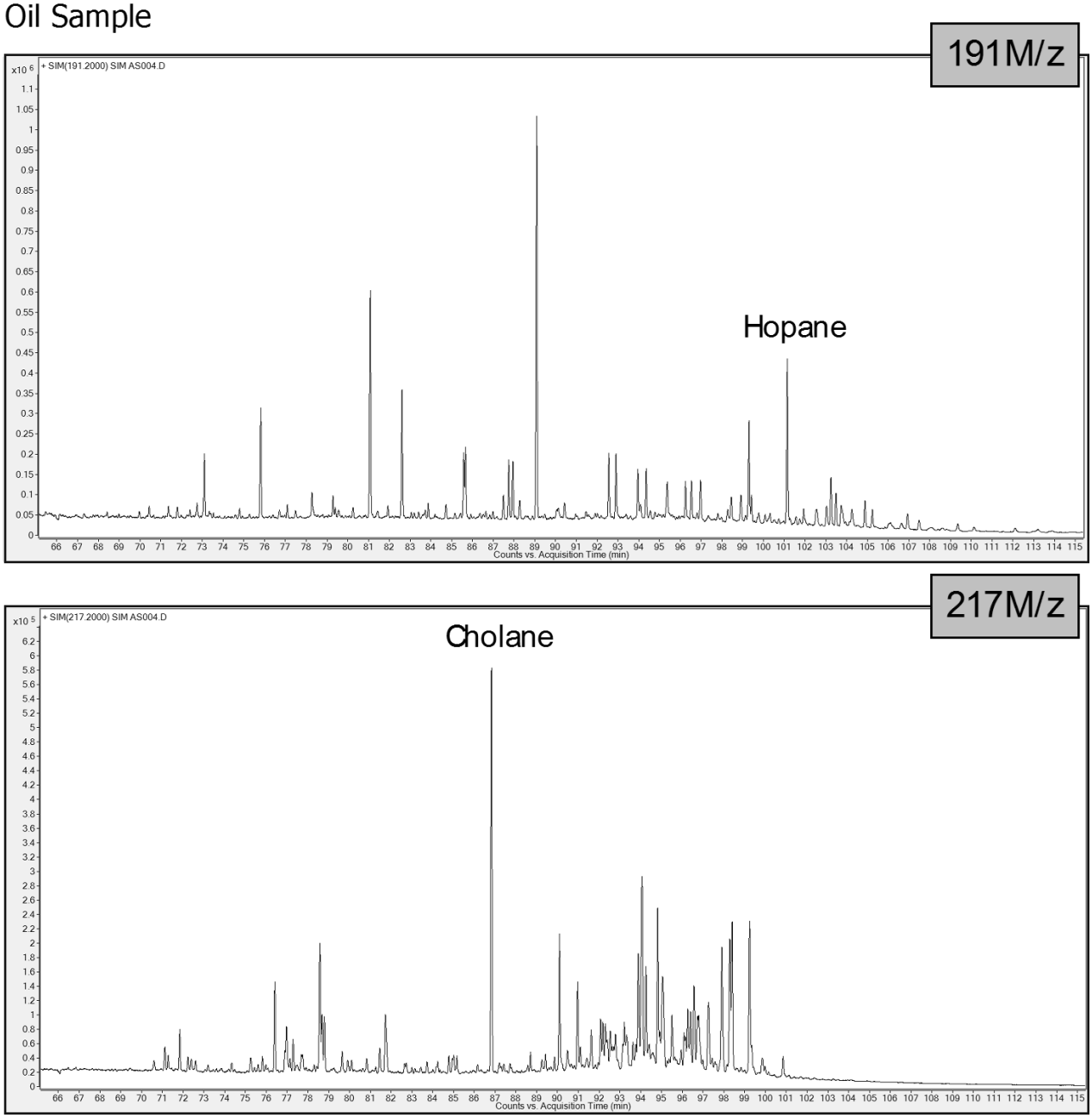

Figure 4. Continued.

Sample: Wh-Lo-1
Oil Sample

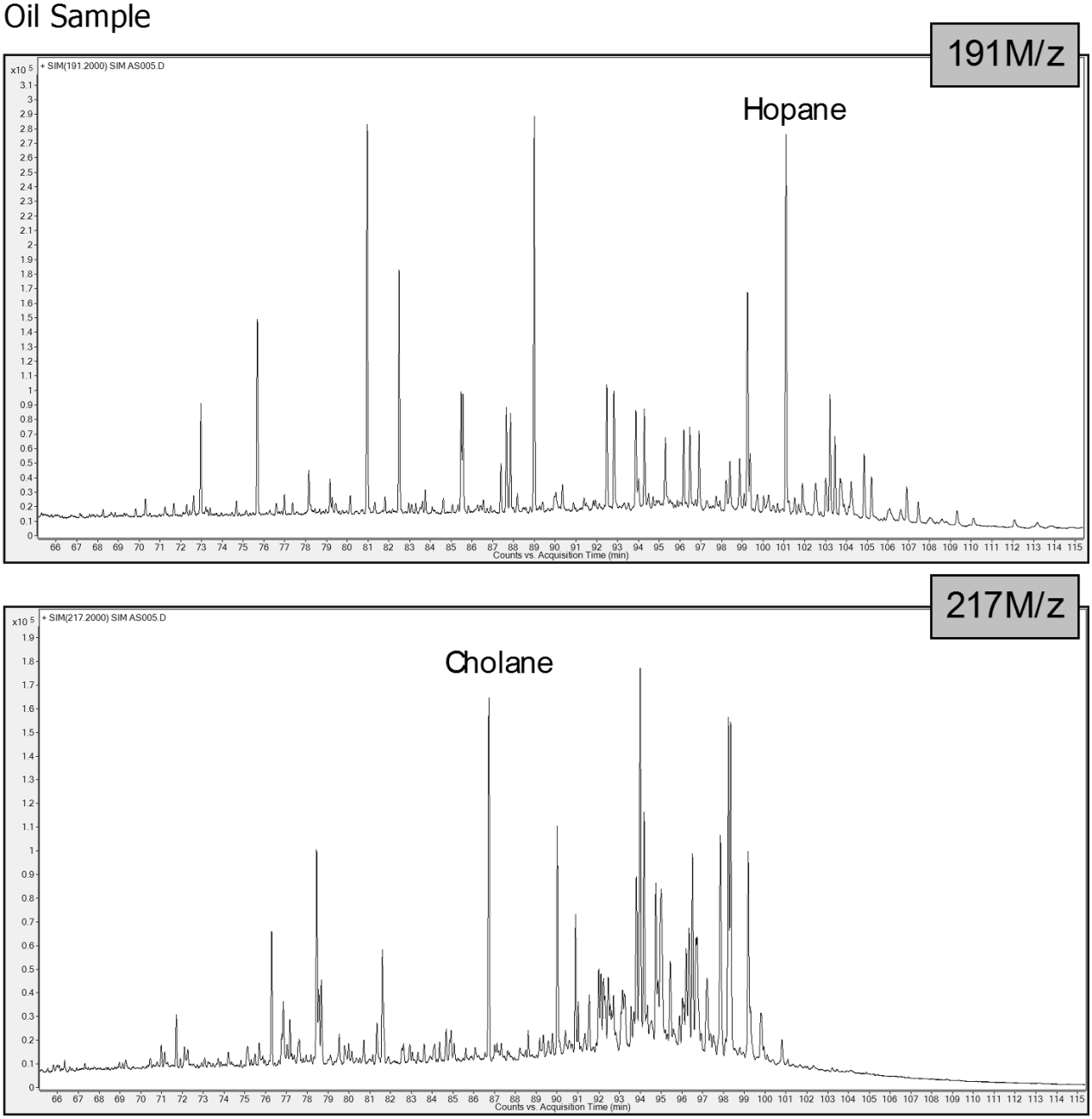

Figure 4. Continued.

Sample: Ka-Al-1
Oil Sample

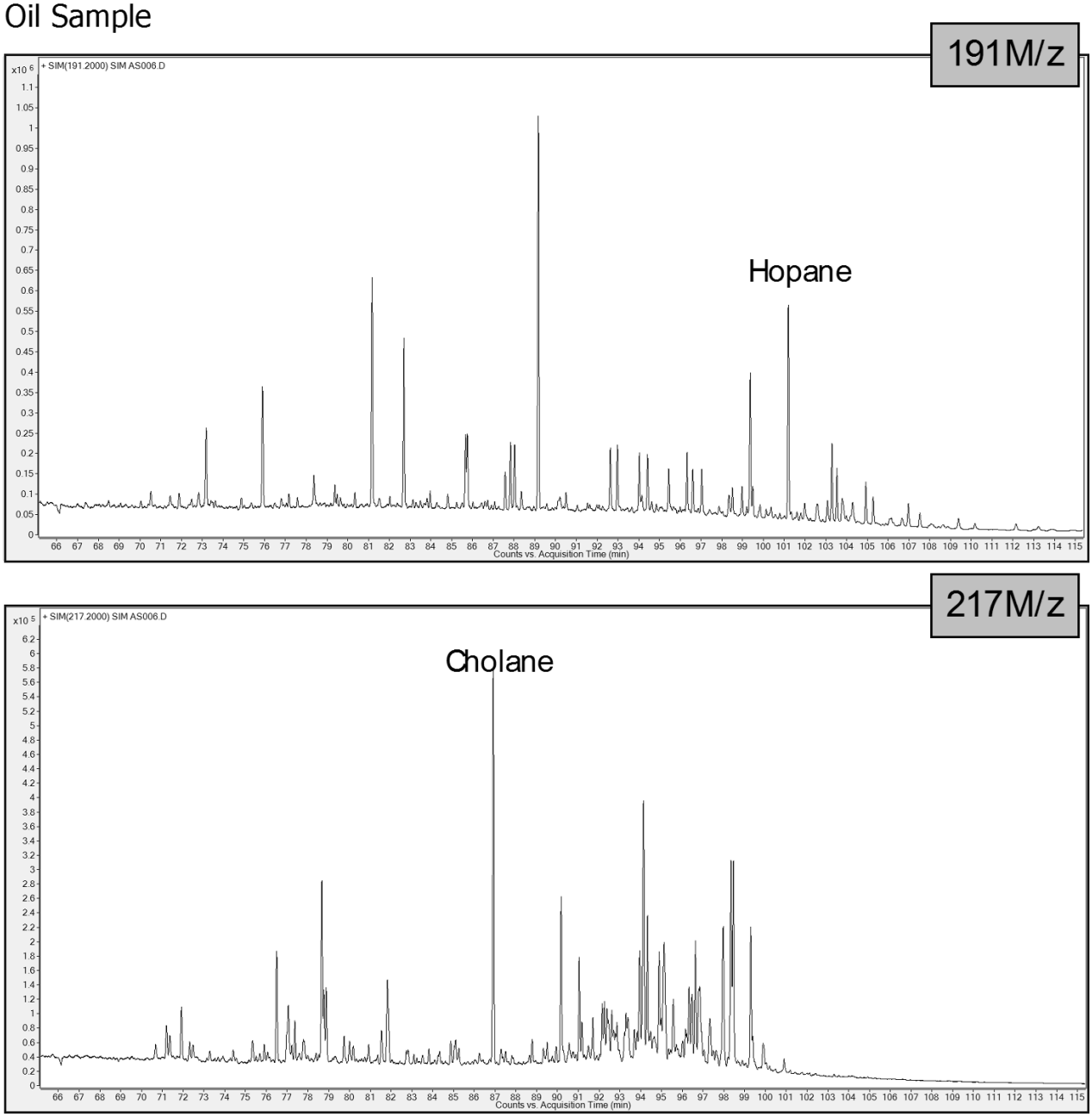

Figure 4. Continued.

Sample: Ri-Wo-1
Oil Sample

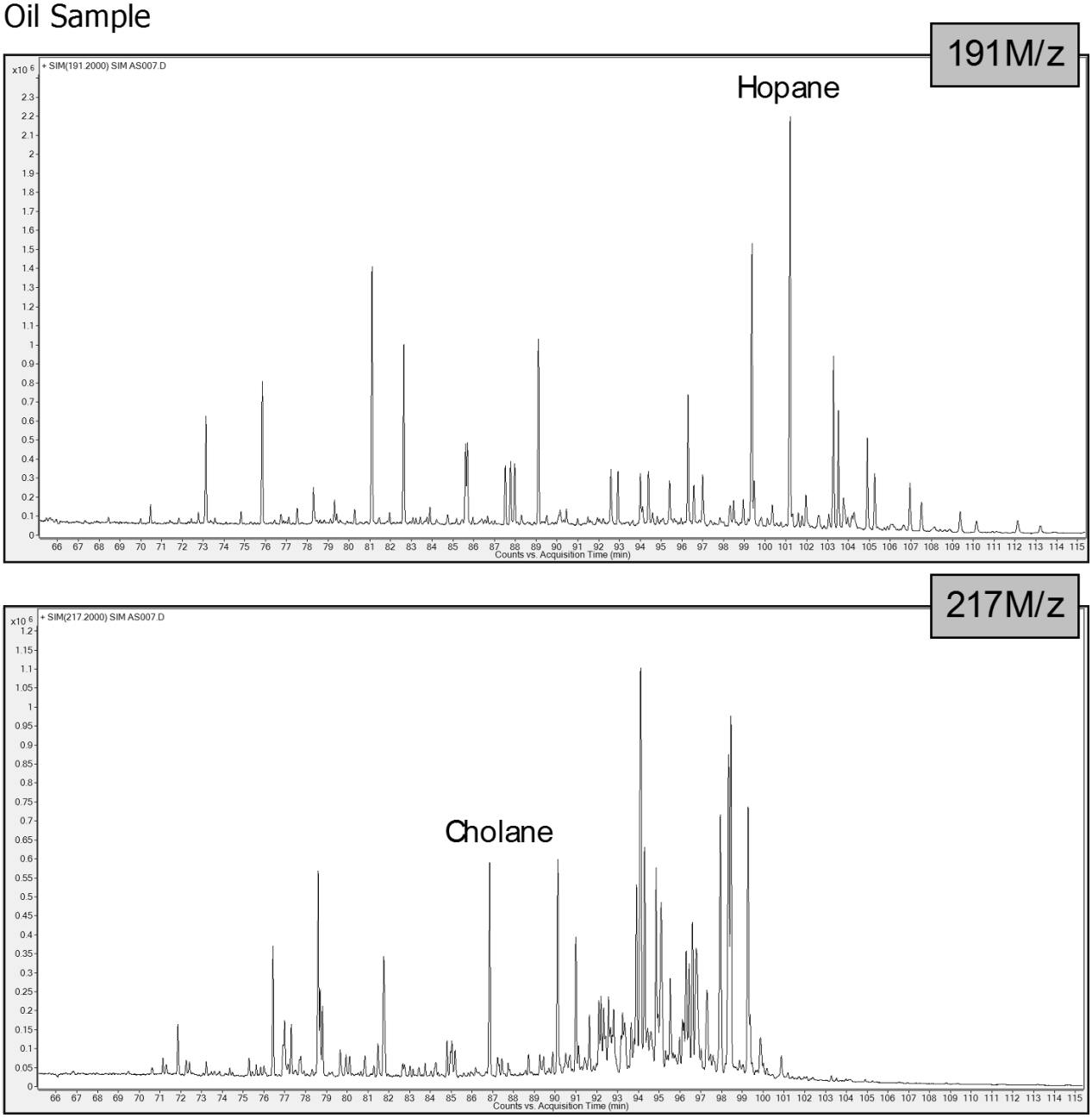

Figure 4. Continued.

Sample: Da-Wo-1
Oil Sample

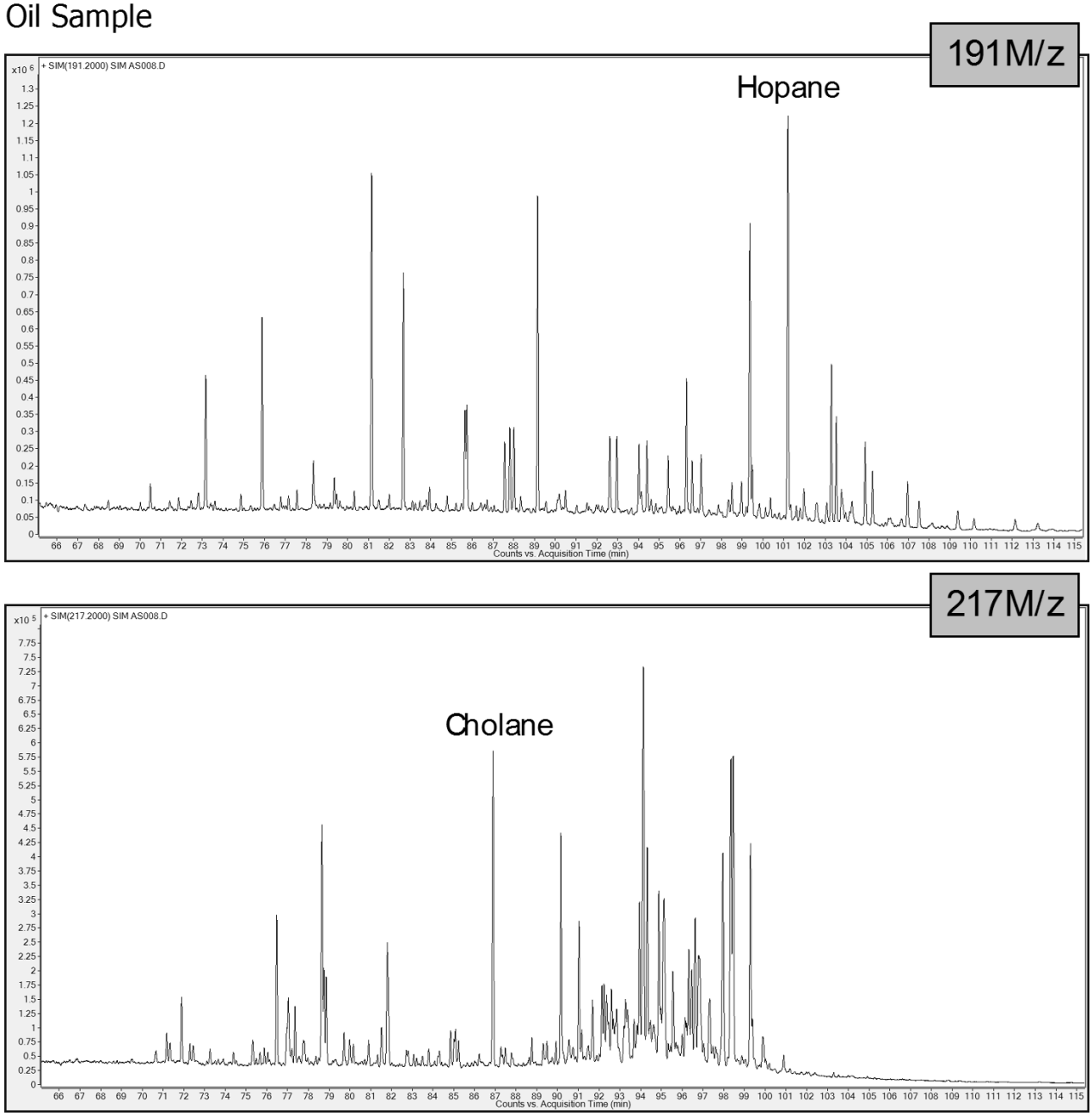

Figure 4. Continued.

Sample: Wh-Lo-2
Oil Sample

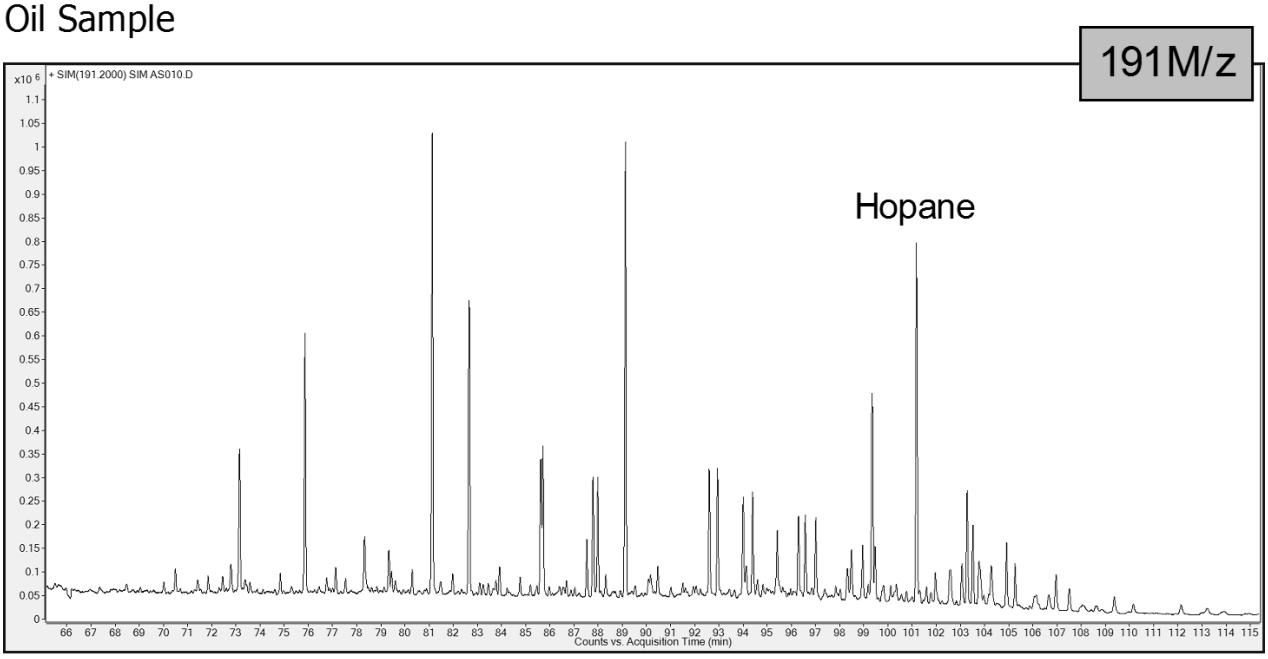

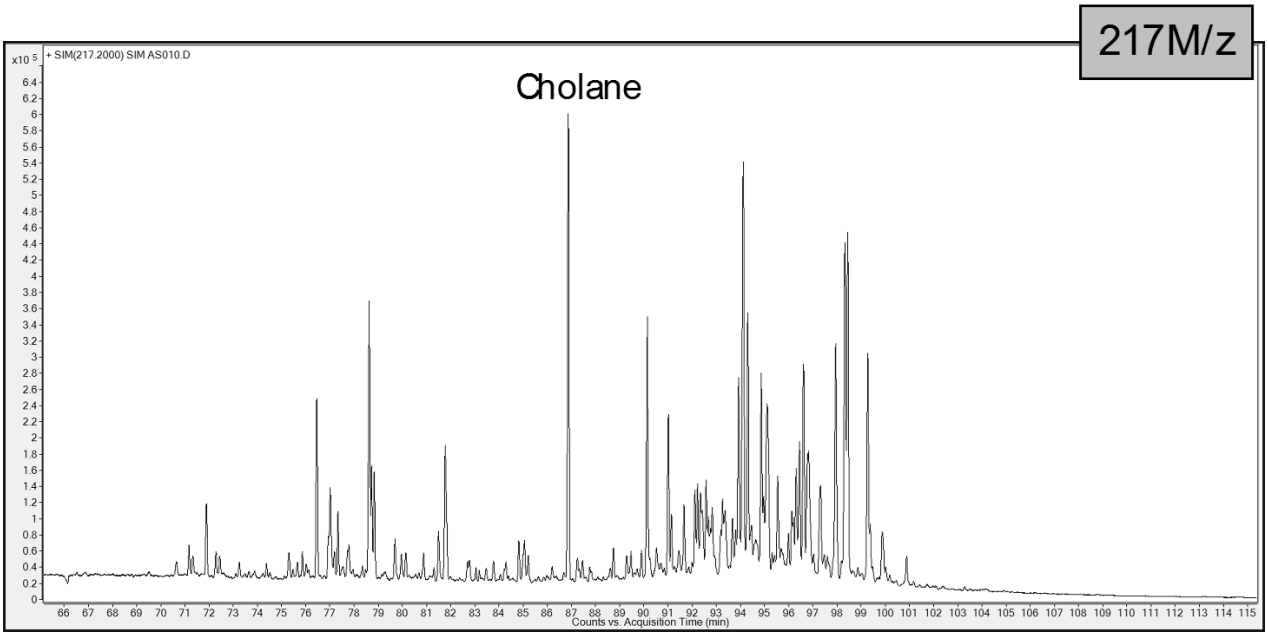

Figure 4. Continued.

Sample: Je-Py-1
Oil Sample

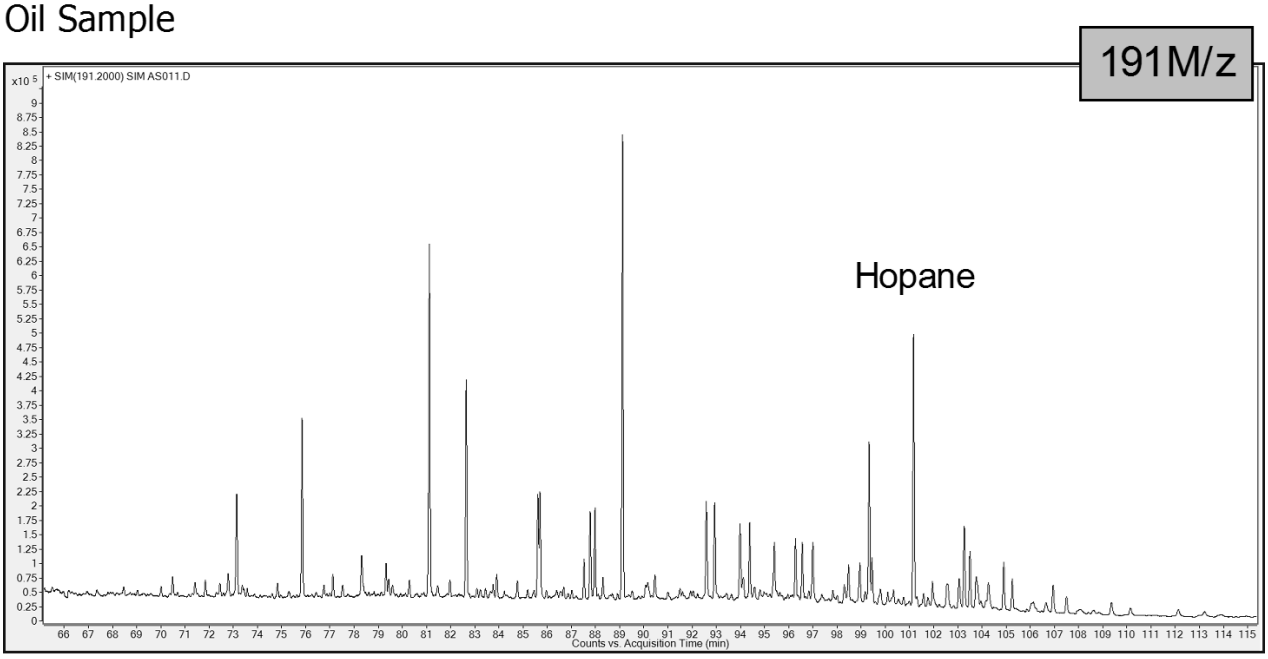

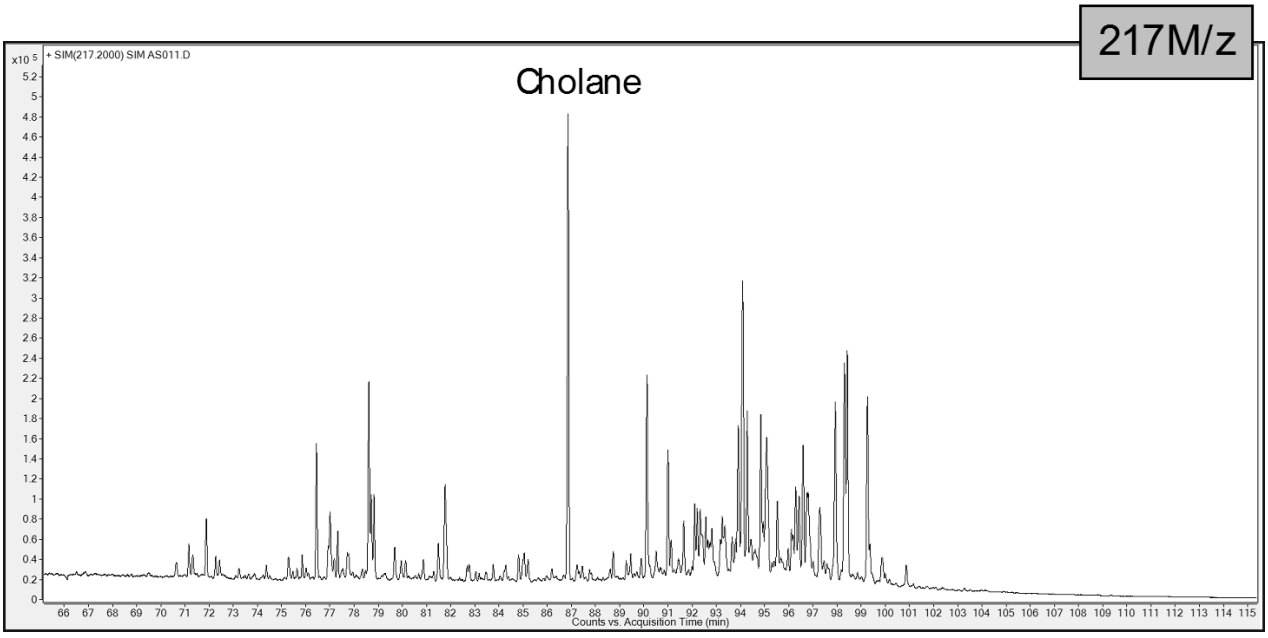

Figure 4. Continued.

Sample: Wi-Py-6
Oil Sample

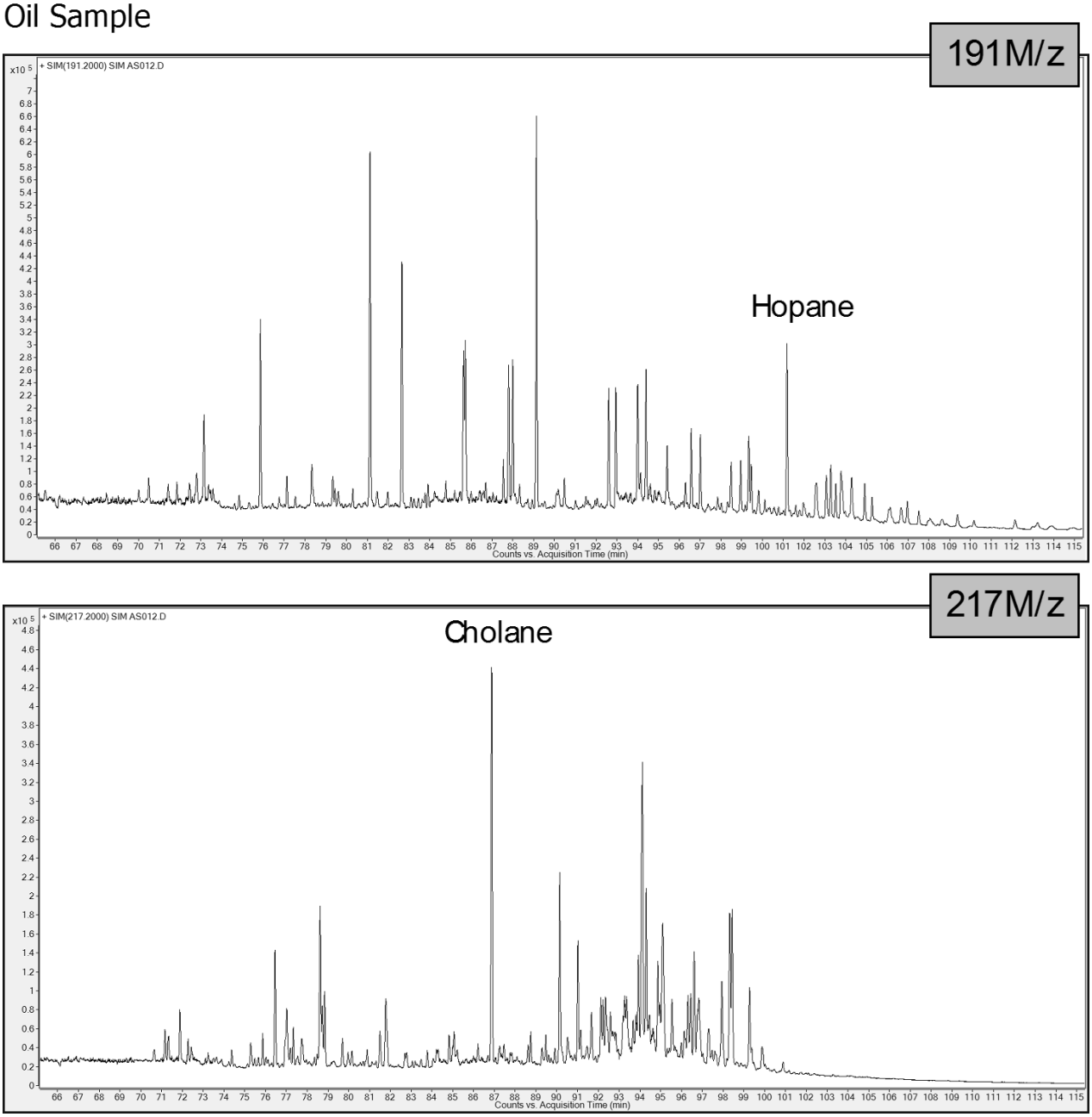

Figure 4. Continued.

Sample: El-Py-3
Oil Sample

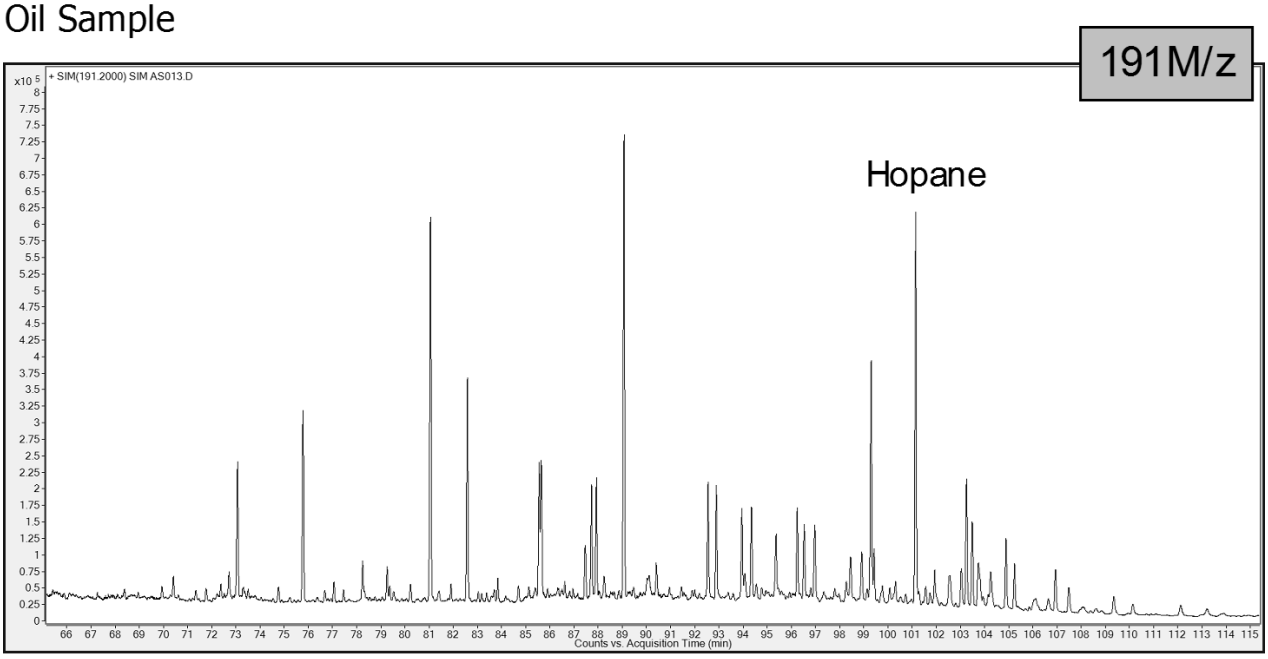

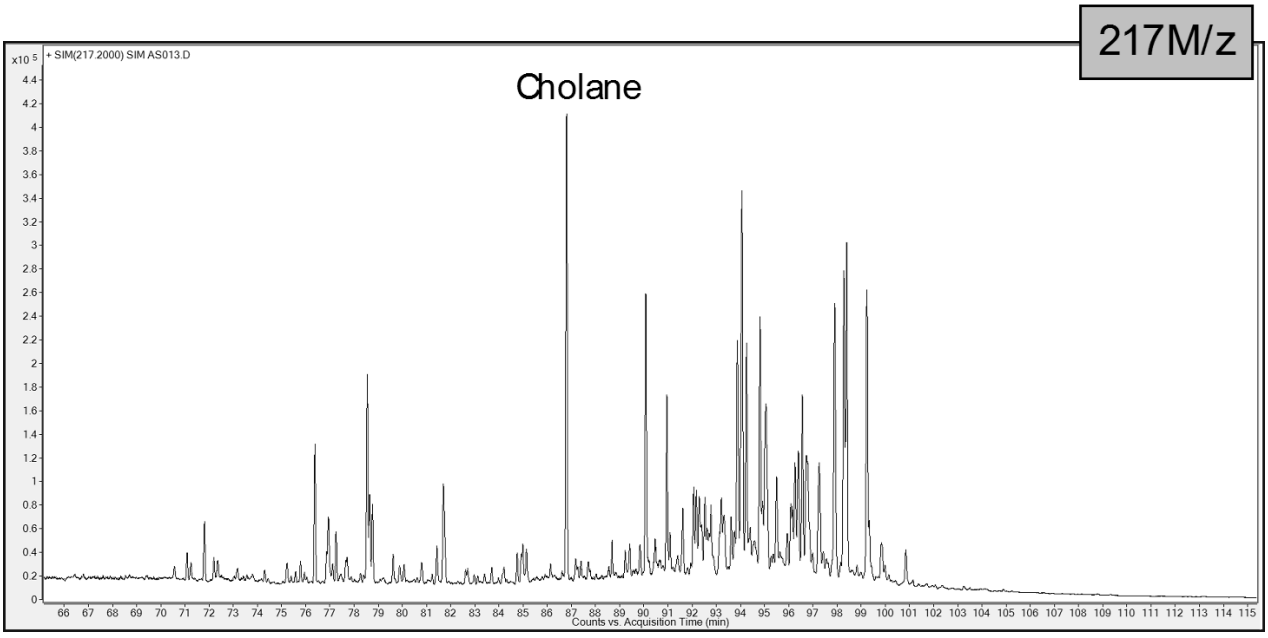

Figure 4. Continued.

GC-MS-MS Chromatograms

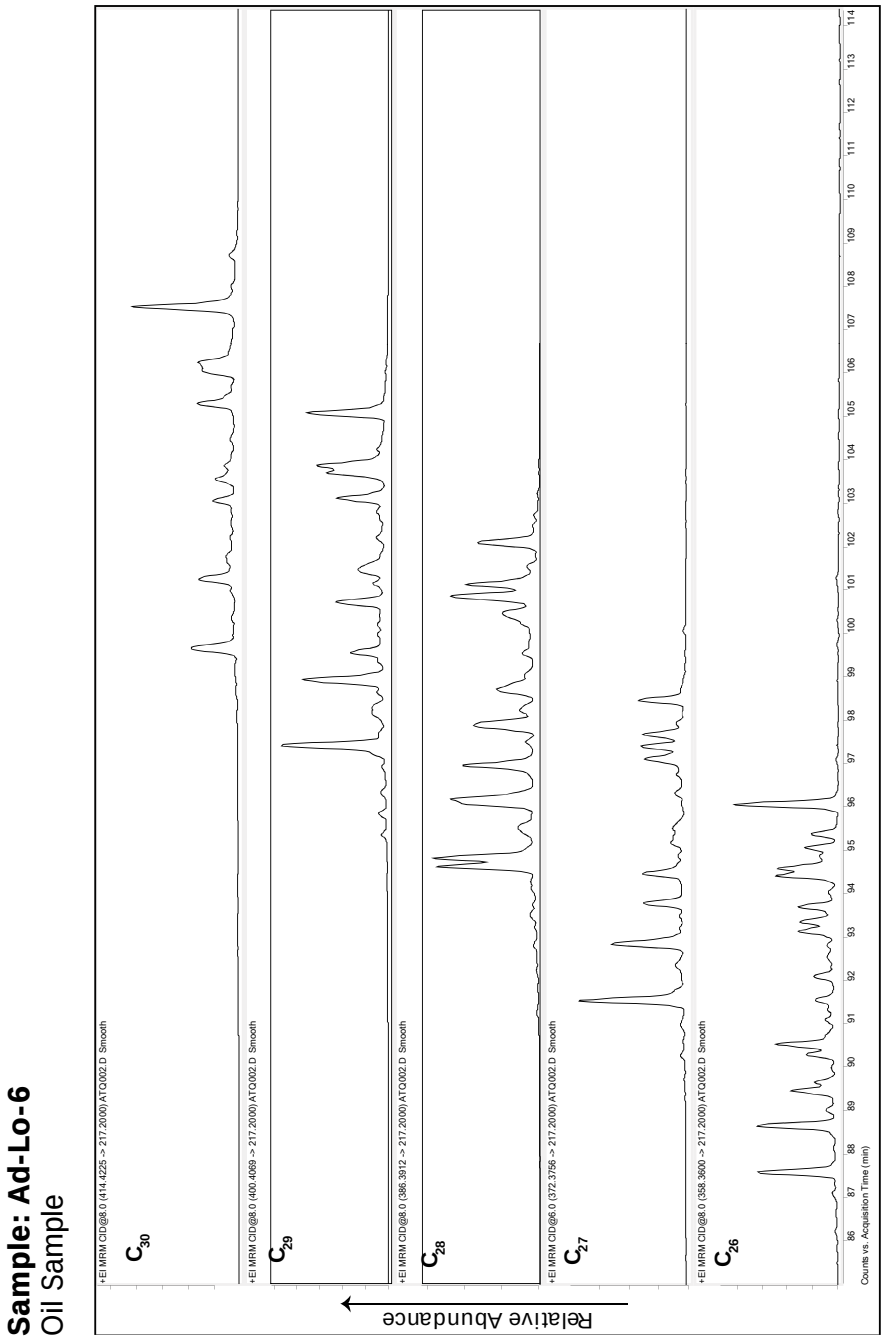

Figure 5. GC-MSMS of C_{27}-C_{30} steranes biomarkers.

Sample: St-Al-1
Oil Sample

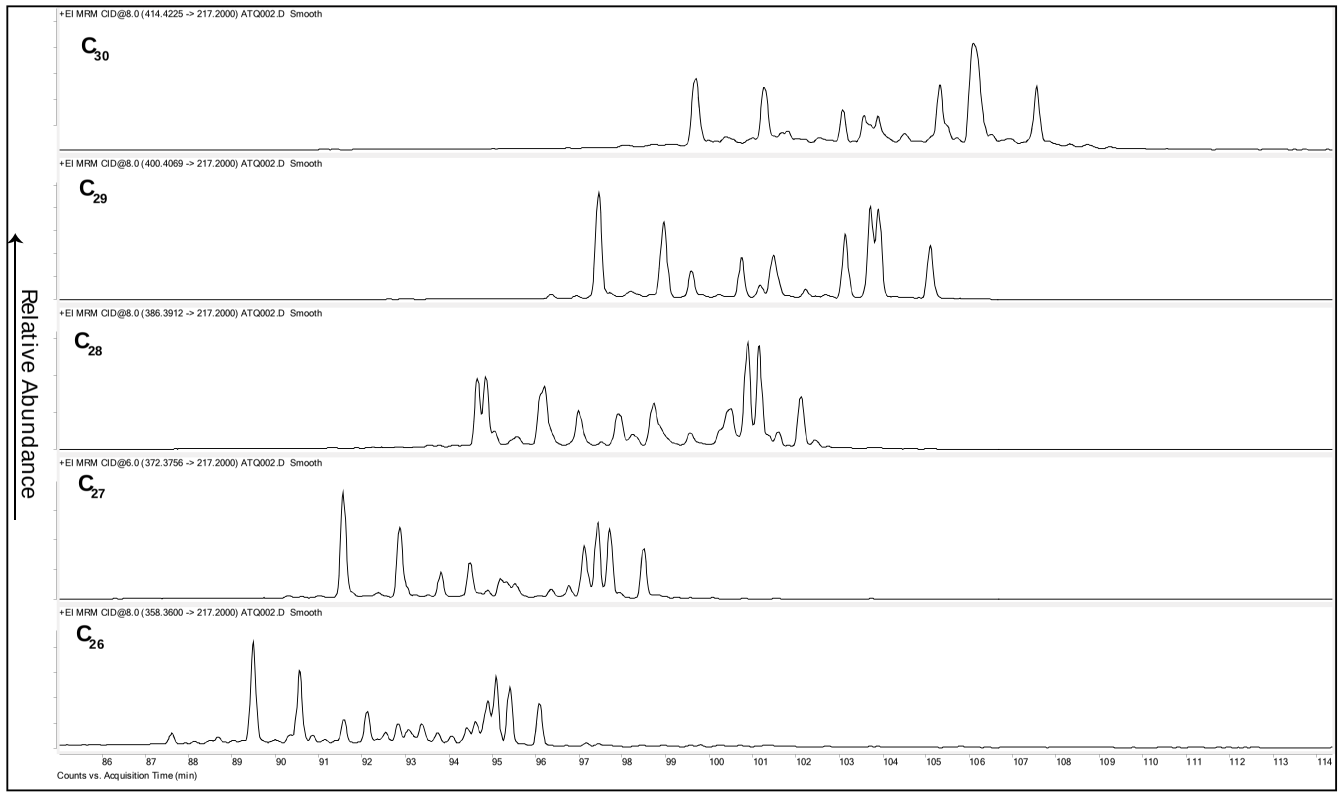

Figure 5. Continued.

Sample: Me-Py-6
Oil Sample

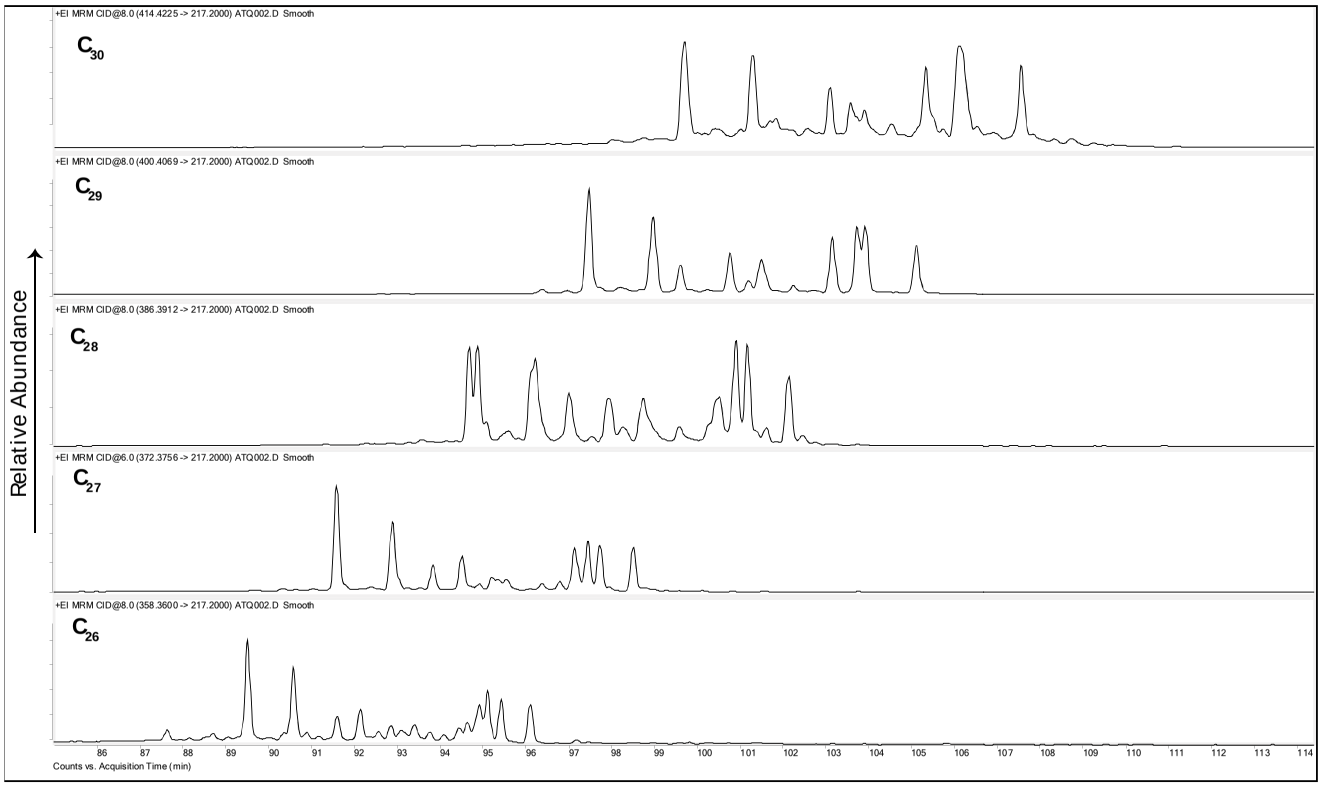

Figure 5. Continued.

Sample: To-Py-1
Oil Sample

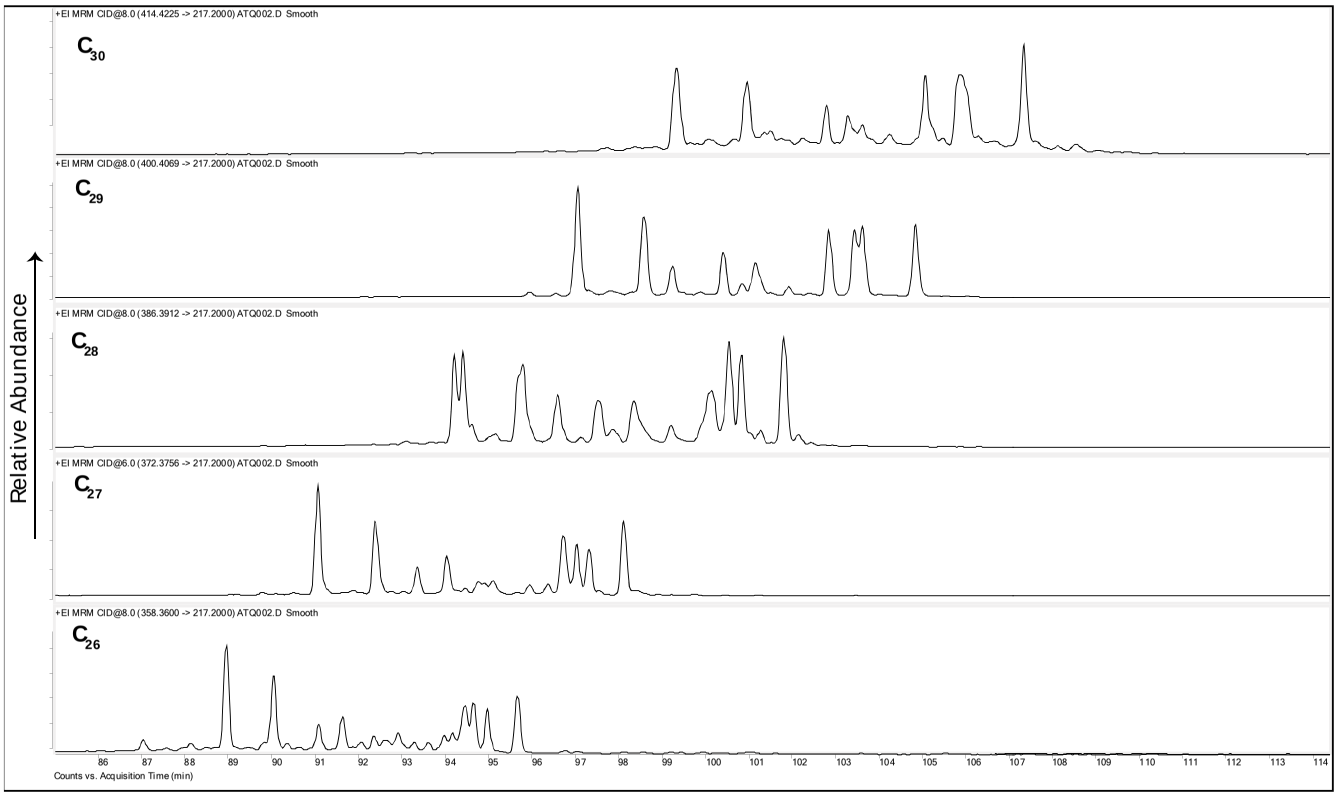

Figure 5. Continued.

Sample: Wh-Lo-1
Oil Sample

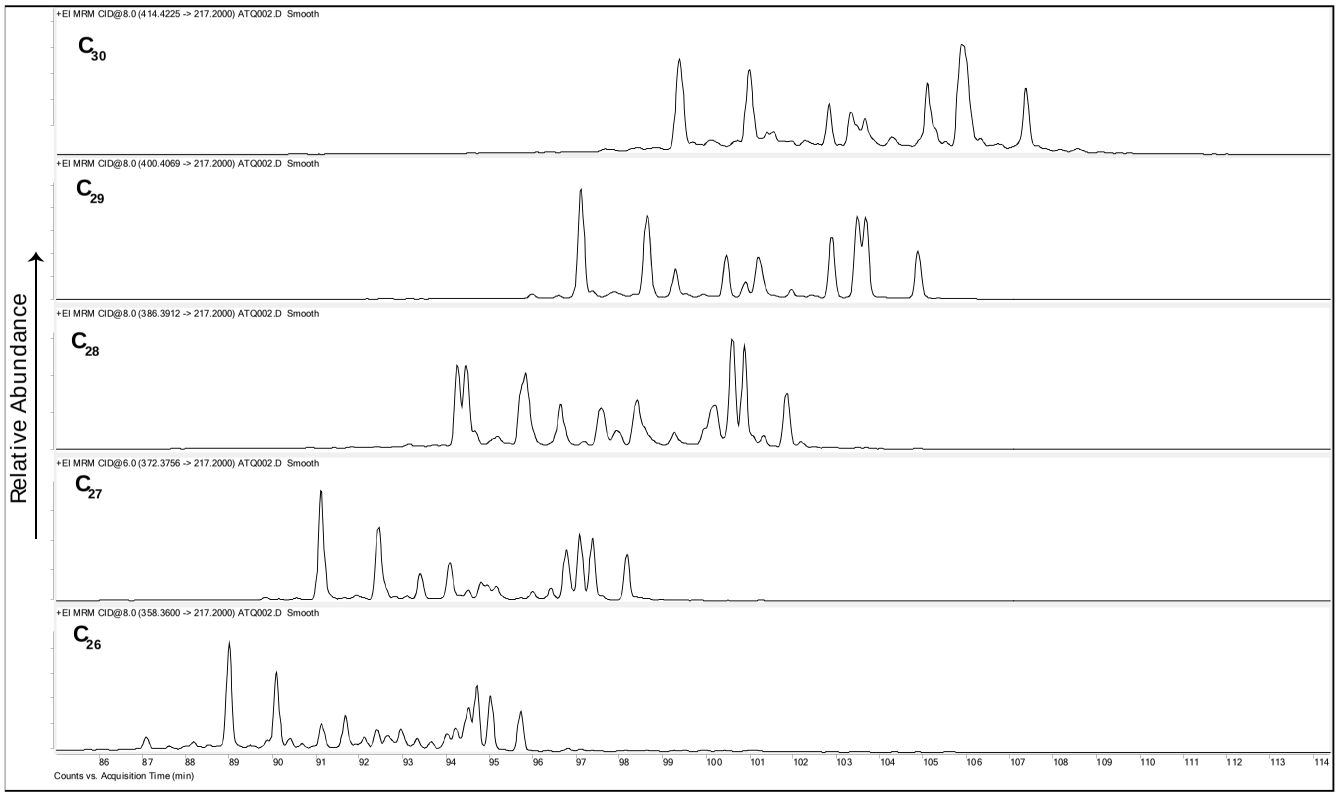

Figure 5. Continued.

Sample: Ka-Al-1
Oil Sample

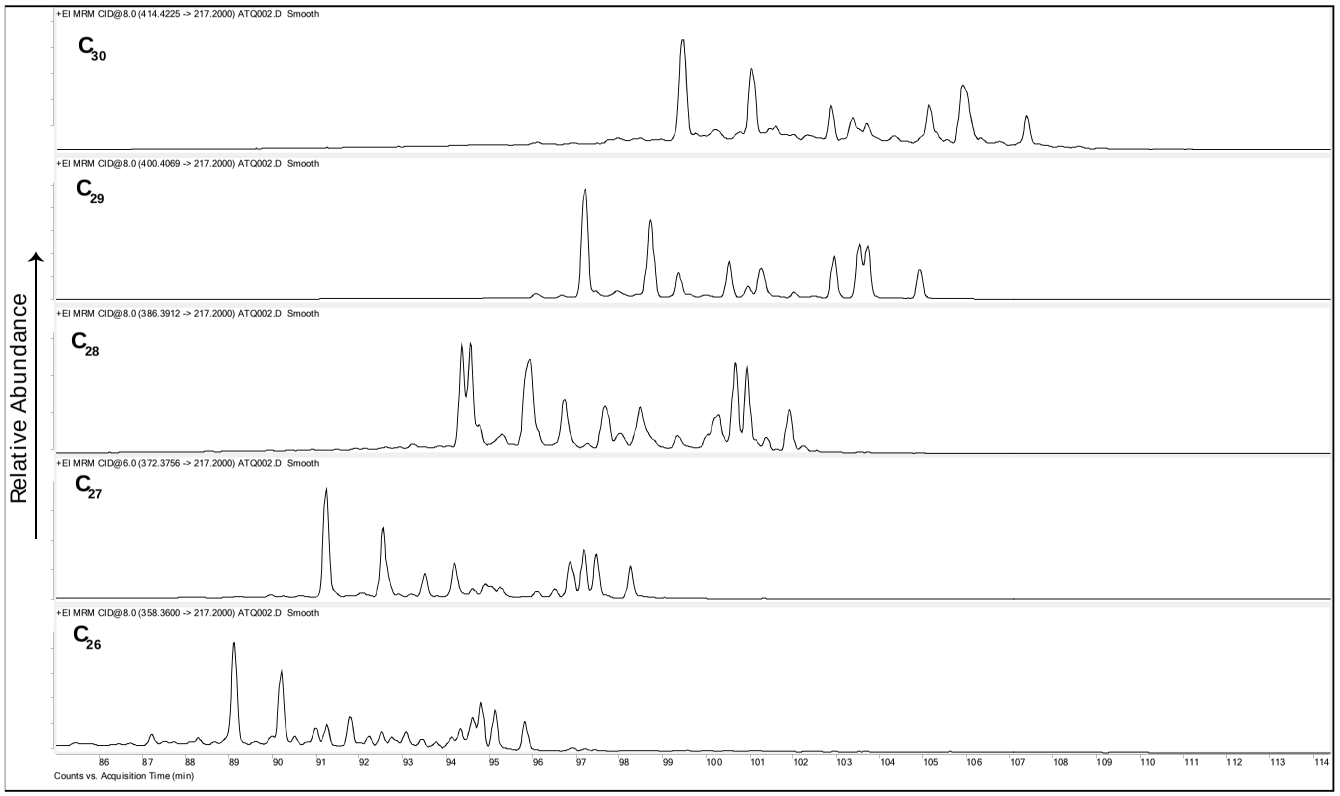

Figure 5. Continued.

Sample: Ri-Wo-1
Oil Sample

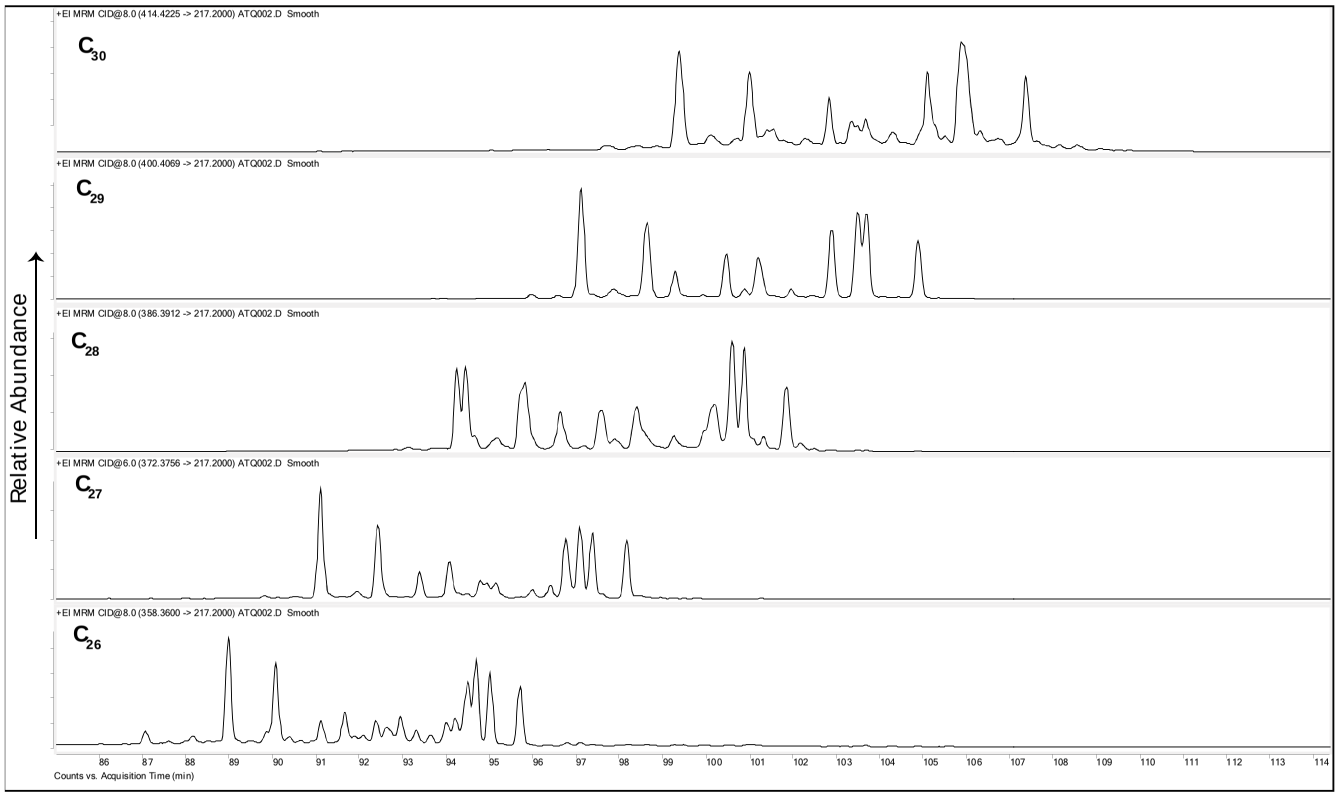

Figure 5. Continued.

Sample: Da-Wo-1
Oil Sample

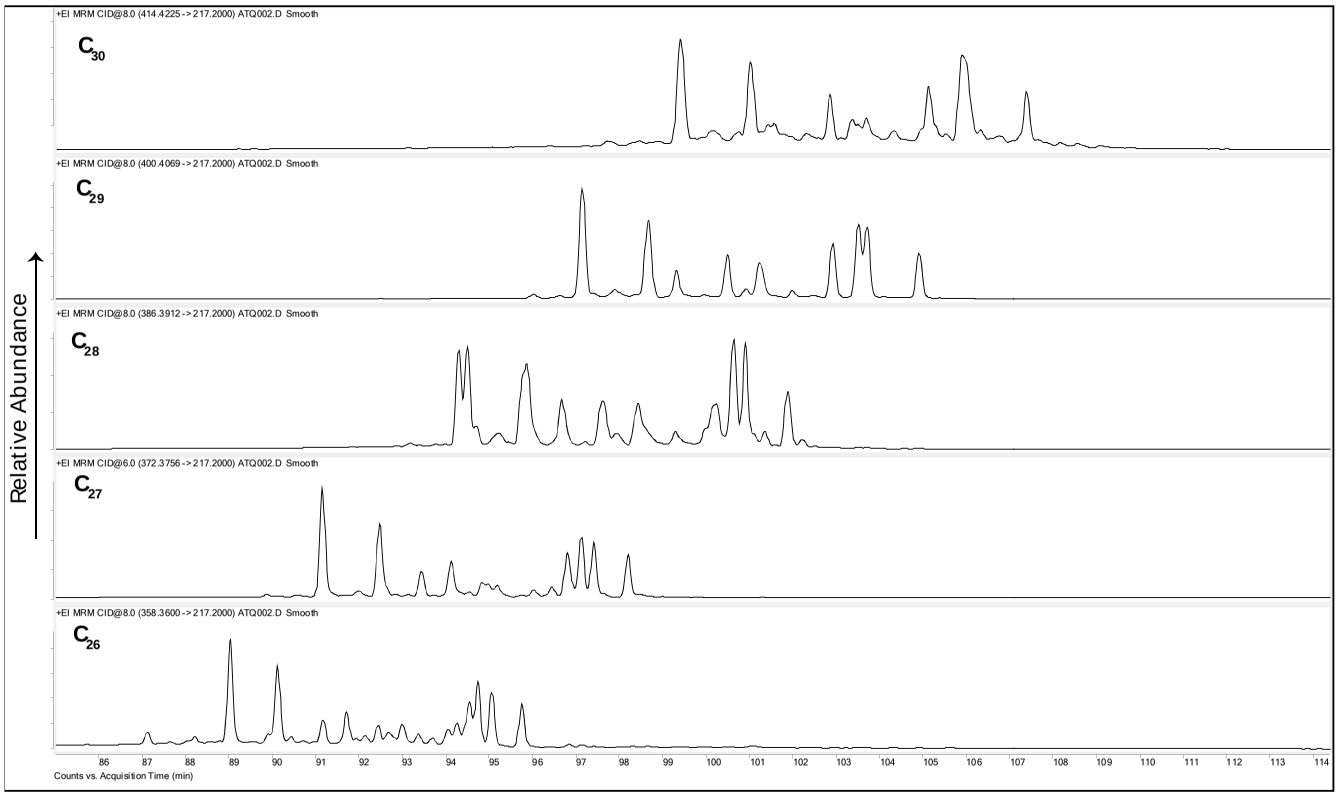

Figure 5. Continued.

Sample: Wh-Lo-2
Oil Sample

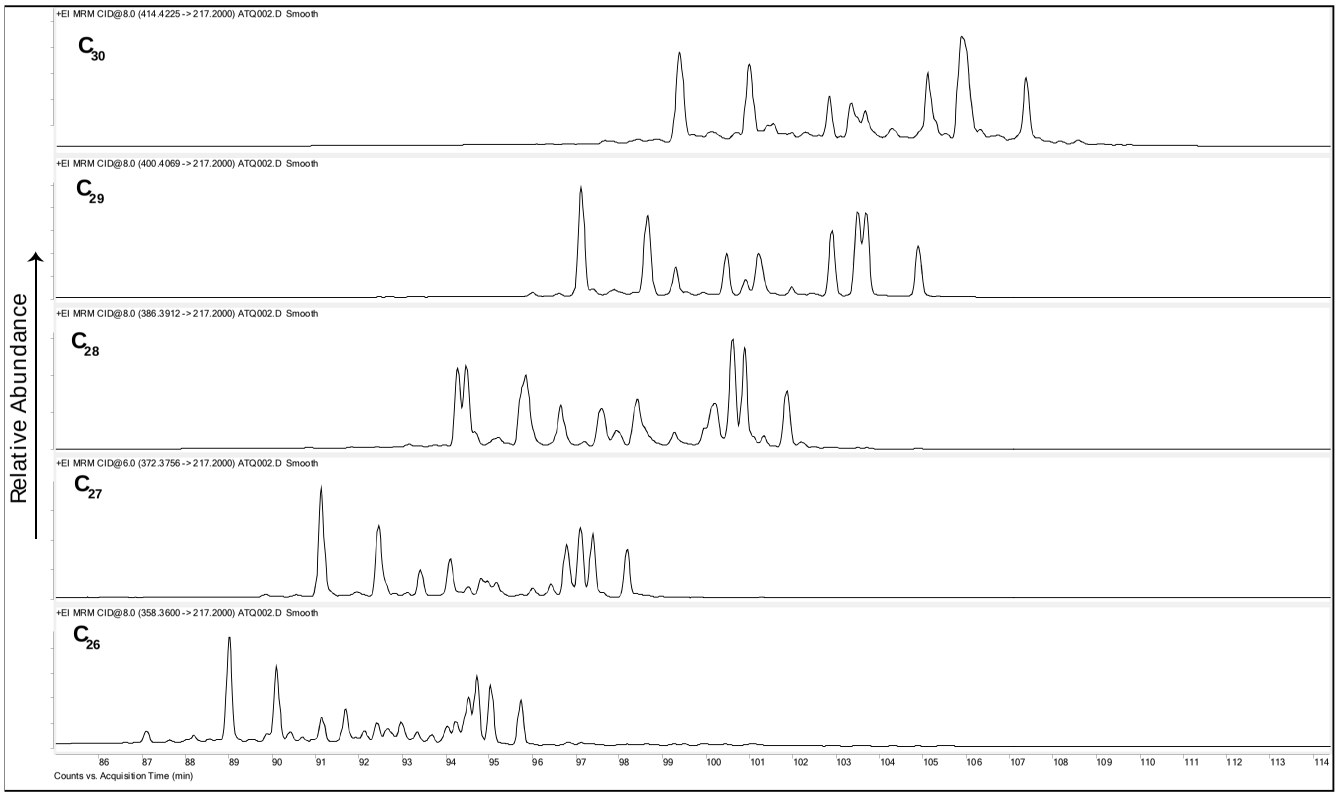

Figure 5. Continued.

Sample: Je-Py-1
Oil Sample

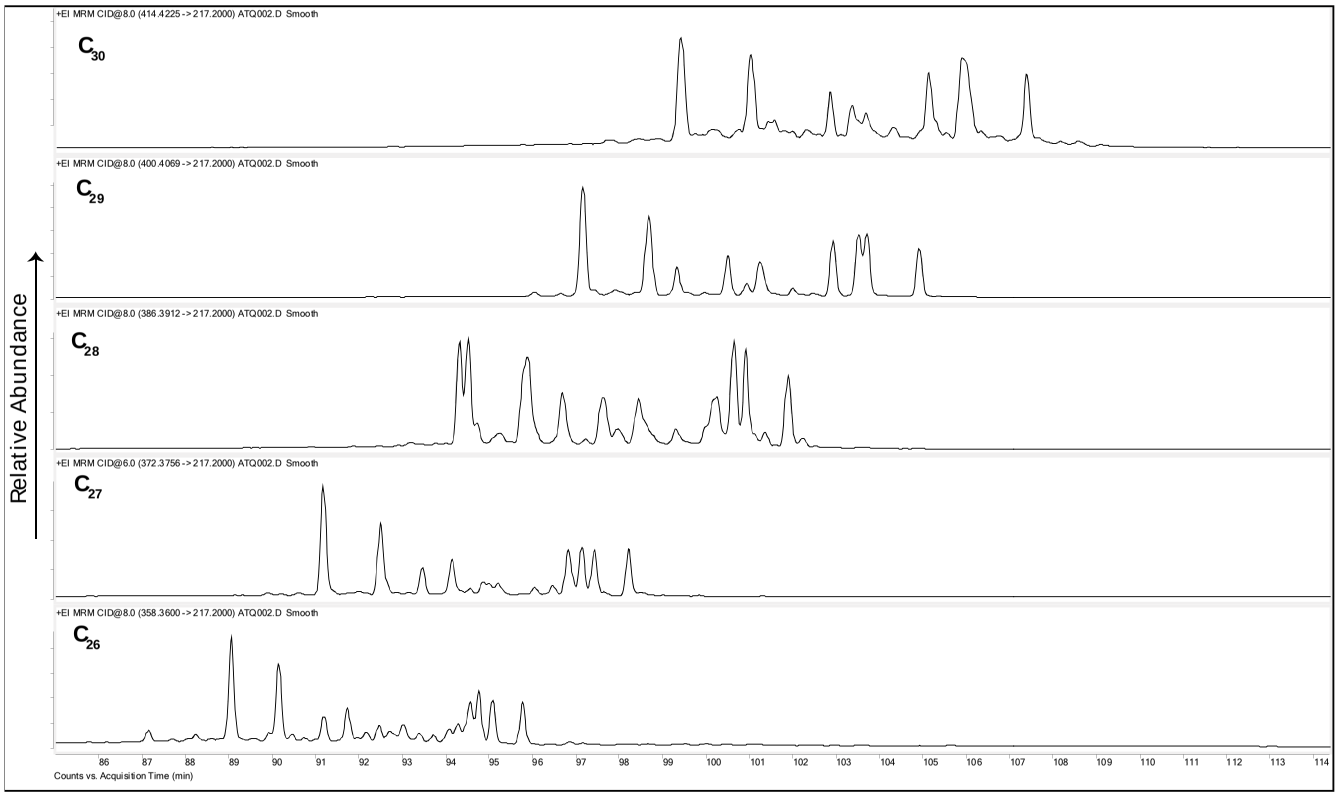

Figure 5. Continued.

Sample: Wi-Py-6
Oil Sample

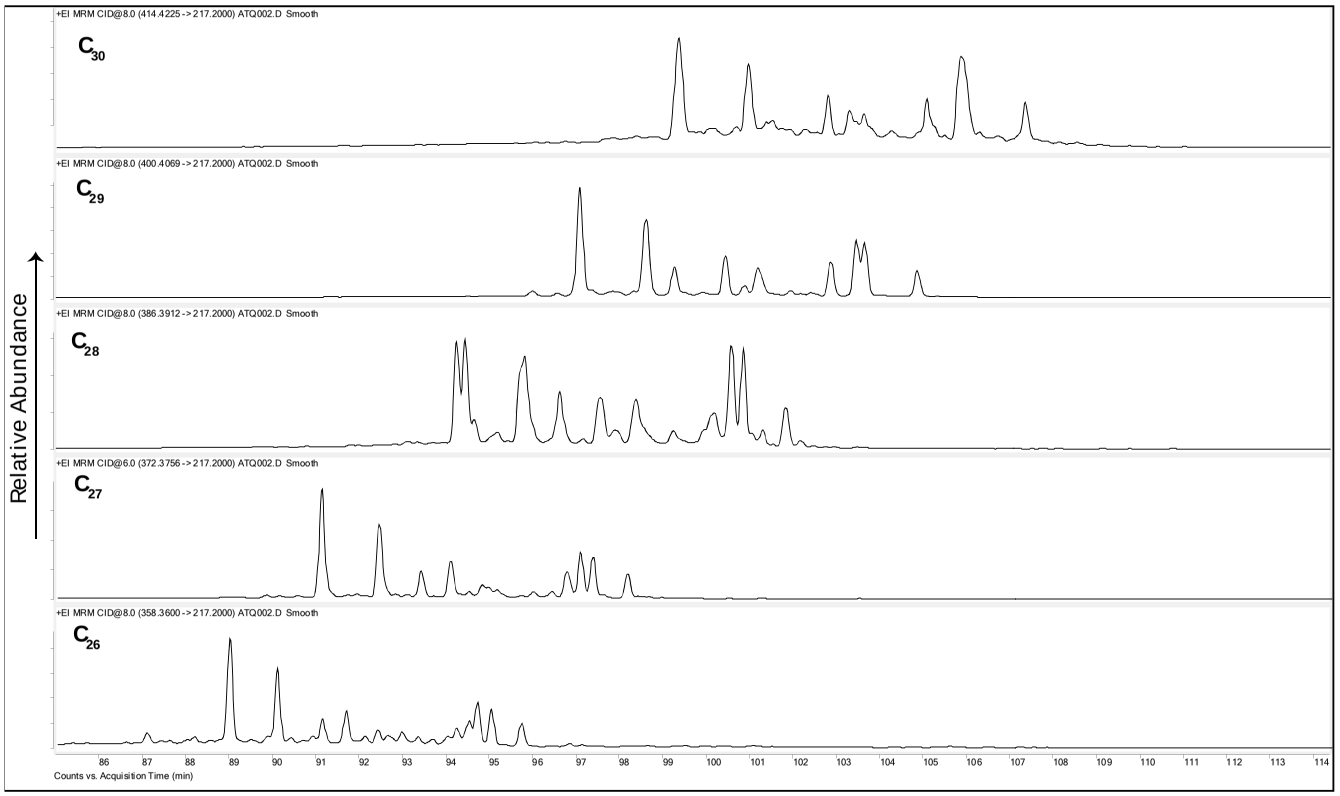

Figure 5. Continued.

Sample: El-Py-3
Oil Sample

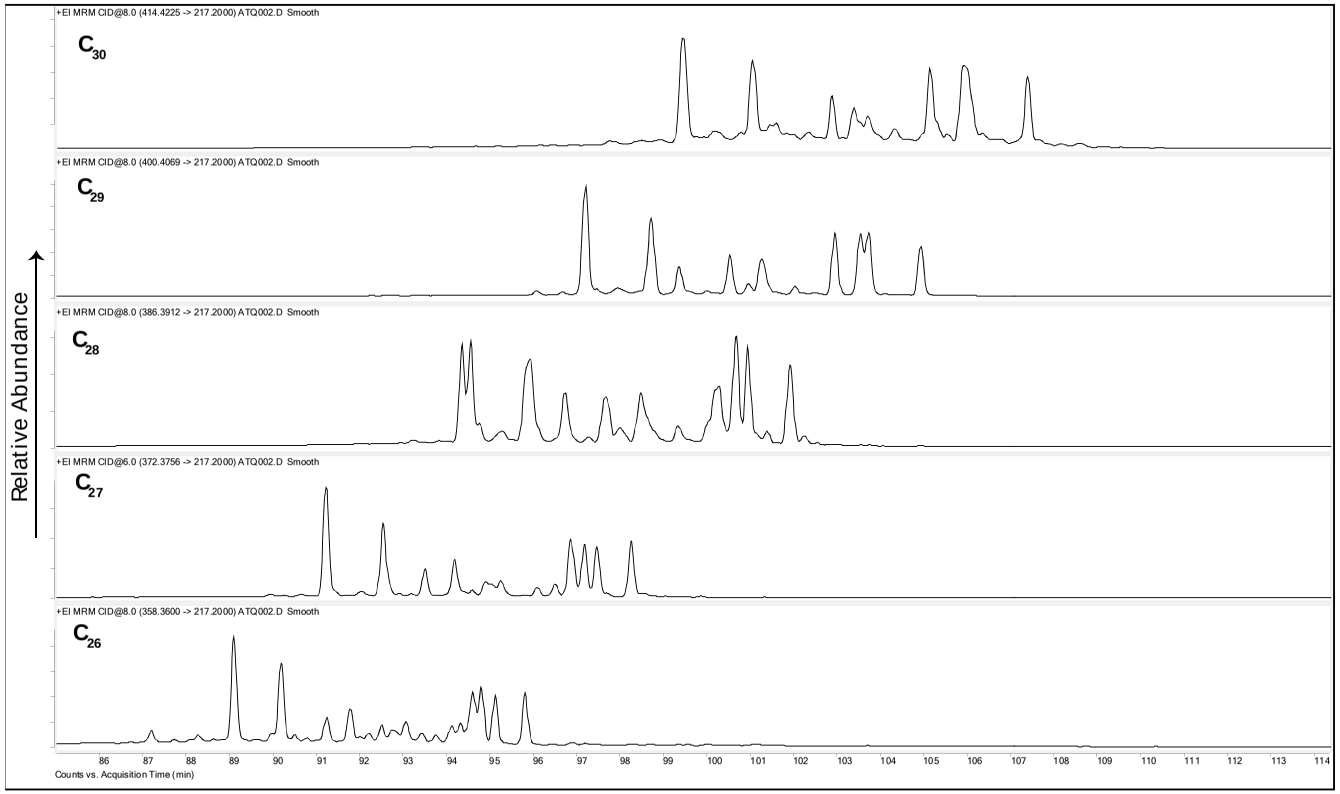

Figure 5. Continued.

VITA

Ibrahim Zayed Al Atwah

Candidate for the Degree of

Master of Science

Thesis: ORGANIC GEOCHEMISTRY AND CRUDE OIL SOURCE ROCK CORRELATION OF THE DEVONIAN-MISSISSIPPIAN PETROLEUM SYSTEMS NORTHERN OKLAHOMA

Major Field: PETROLEUM GEOCHEMISTRY

Biographical:

Education:

Completed the requirements for the Master of Science in Geology at Oklahoma State University, Stillwater, Oklahoma in May, 2015.

Completed the requirements for the Bachelor of Science in Geology at University of Tulsa, Tulsa, Oklahoma in May 2011.

Experience: Saudi Aramco (2011-2013):

Organic geochemical assessment of source rock and oil, Geochemistry, Geology Technology Team, Upstream Advance Research Center, 2013

Regional resource assessment and play-based analysis, Exploration Resource Assessment Department, 2012

Geosteering: utilize real- time logging data for optimal well placement, Reservoir Characterization Department, 2012

Development of calibration tool for absolute maturity, Geology Technology Team, Upstream Advance Research Center, 2011

Professional Memberships: American Association of Petroleum Geologists, Society of Petroleum Engineers, Oklahoma State University Geological Society, The Honor Society of Phi Kappa Phi.